Interactions of the DNA Repair Protein Rad23 in the Yeast Two-Hybrid System

by

Robert Daniel Kirkpatrick

Submitted to the Faculty of Graduate Studies in Partial Fulfillment of the requirements
of
Degree of Master of Science

Department of Human Genetics
University of Manitoba
Winnipeg, Manitoba
Fall, 1999

THE UNIVERSITY OF MANITOBA

FACULTY OF GRADUATE STUDIES

*****

COPYRIGHT PERMISSION PAGE

Interactions of the DNA Repair Protein Rad23 in the Yeast Two-Hybrid System

BY

Robert Daniel Kirkpatrick

A Practicum submitted to the Faculty of Graduate Studies of The University of Manitoba in partial fulfillment of the requirements of the degree of

MASTER OF SCIENCE

ACKNOWLEDGMENTS

First and foremost, I want to thank my family for being there for support when I faltered and the encouragement you always gave me. Without all of you, this chapter of my life may have turned out drastically different.

To my friends and colleagues, each one of you has added a spice to my University experience which has made for a potent concoction. From all the hypothetical to outright ridiculous discussions about science and everything in between, I really felt like part of the giant think-tank that is a University. Many of you have taught me invaluable lessons in science and even a few in life.

To my supervisor, Dr. Gietz, you taught me a lot about science and gave me a chance to develop strong molecular skills. I will always appreciate that you took me on as a student and will likely always regret that things did not turn out better between us.

I count my blessings that I'm around to write these words and hope that I can return the good fortune that was given so freely to me.

Table of Contents

List of Tables

List of Figures

Abbreviations

aa	amino acid(s)
APS	ammonium persulfate
BEB	band elution buffer
β-ME	β -mercaptoethanol
bp	base pair(s)
BSA	bovine serum albumin
CIP	calf intestinal alkaline phosphatase
CPDs	cyclobutane pyrimidine dimers
cpm	counts per minute
ddH_2O	sterile distilled and deionized water
dsDNA	double-stranded DNA
DMF	dimethyl formamide
dNTP	deoxy nucleotide triphosphate
DMSO	dimethyl sulfoxide
DTT	dithiothreitol
EDTA	ethylene diamintetraacidic acid
EtBr	ethidium bromide
EtOH	ethanol
GGR	Global genome repair
HEPES	N-[2-Hydroxyethyl]piperazine-N'-2-ethanesulfonic acid
NaOH	sodium hydroxide
nt	nucleotide
ONPG	*ortho*-nitrophenyl galactoside
PAGE	polyacrylamide gel electrophoresis
PEG	polyethylene glycol
PMSF	phenylmethylsulfonyl fluoride
SC	synthetic complete
SDS	sodium dodecyl sulphate
ssDNA	single-stranded DNA
TCA	trichloroacetic acid
TCR	Transcription-coupled repair
TEMED	*N,N,N',N'*-tetramethylethylene
TFIIH	transcription factor IIH
TRCF	transcription-repair coupling factor
UV	ultraviolet radiation
X-gal	5-bromo-4-chloro-3-indolyl-β-D-galactoside

Abstract

DNA damage represents a threat to the livelihood of a cell or organism. This damage must be dealt with in an efficient manner to prevent cell death, or in higher organisms, neoplasia. The study of DNA repair in yeast has been greatly aided by the discovery of radiation-sensitive mutants and their corresponding *RAD* genes. A loss of function of these *RAD* or related genes compromises the cell's ability to repair DNA damage. One of the most effective pathways for repairing DNA damage is nucleotide excision repair. Within this pathway, the *RAD23* gene product plays a crucial, albeit poorly understood role. In this study, three Rad23p-interacting proteins were investigated in order to better understand the role of Rad23p itself. Two of the three proteins investigated were found to be important to cell viability while the remaining protein appeared to be functionally disposable. None of the proteins were found to play a role in DNA repair using the methods in this thesis, suggesting that their interaction with Rad23p is not biologically significant. Alternatively, these genes may be involved with *RAD23* in cellular processes unrelated to DNA repair.

1. INTRODUCTION

Genetic material, such as DNA, must be able to transmit information from one generation to the next with a high degree of accuracy in order to assure the continuation of the species. It was discovered, however, that DNA is susceptible to mutation from faulty replication and environmental insults which threaten this stability. Although the effects of specific mutations on an individual can be devastating, this very instability is essential for species' evolution. To ensure the survival of individuals, evolution has bestowed upon virtually every species a powerful collection of proteins designed to preserve, maintain and restore the integrity of the genetic material. Collectively these proteins are referred to as DNA repair proteins and are capable of repairing a multitude of DNA damage types.

1.1 DNA Repair

The existence of DNA repair mechanisms was demonstrated with the discovery of radiation-sensitive mutants. The first radiation-sensitive mutant was isolated in *E. coli* (Hill, 1958) and nine years later, the observation of radiation sensitivity was extended to yeast (Nakai and Matsumoto, 1967). The failure of cells to repair DNA was soon found to be associated with the radiation-sensitive human disease xeroderma pigmentosum and provided the first evidence of the true importance of DNA repair (Cleaver, 1968).

Mutagenic damage can be caused by a variety of physical and chemical agents, both endogenous and environmental in origin, which alter the structure of DNA. The most prominent physical agents which pose a threat to DNA are ionizing and ultraviolet radiation. These can break the chemical bonds found in DNA to induce single- or double-

stranded breaks or cause cross-linking of adjacent or opposing nucleotides. Physical agents can also cause the formation of free radicals within a cell which can then act on DNA to cause mutation. Chemical agents act on DNA in many ways. Some chemicals attach to and alter the structure of nucleotides which alters the normal base pairing properties of the nucleotides. Other chemicals which resemble normal nucleotides, called analogues, can be incorporated into DNA. These analogues have different base pairing properties than the nucleotide they resemble and can produce mutations in subsequent replication. Another common source of mutation is attributable to polymerase infidelity. In the absence of environmental insults, the cell normally deals with mismatched bases in DNA caused by the insertion of improper nucleotides during replication. Nucleotides in DNA can also undergo spontaneous rearrangement of their chemical bonds resulting in loss of portions of the nucleotide or altered base pairing.

The conservation of DNA repair mechanisms from yeast to humans allows findings in one system to aid discoveries in the other (Botstein *et al.*, 1997). This co-operative effect makes yeast a very useful organism for the study of DNA repair.

Multiple mechanisms for dealing with DNA damage exist in prokaryotes and eukaryotes. These mechanisms can be roughly categorized into six groupings as follows:

i) damage reversal. The simplest method of dealing with damage is to reverse it. Two model mechanisms for damage reversal are exemplified by the photolyase enzymes and the methyltransferases. The former class of proteins deals with the most common form of damage induced by UV irradiation - the pyrimidine dimer. The covalent linkage of adjacent pyrimidine molecules through their double bonds to form a pyrimidine dimer disrupts normal base pairing. Photoreactivation is the process by which photolyase enzymes specifically interact with such lesions and utilize the energy from visible light to catalyze the

disruption of the inappropriate linkage, thus restoring the normal pyrimidine structure (reviewed in Sancar, 1996b). The second class of damage reversal proteins deals with monofunctional alkylation of DNA such as inappropriate methylation. The mutagenic O^6-methylguanine represents a prime example of this type of damage. Demethylation occurs by the transfer of the inappropriate methyl group to the active site of a methyltransferase to restore the normal chemical structure, and thus base-pairing, of guanine (reviewed in Mitra and Kaina, 1993). The range of substrates for damage reversal is limited by the highly specific nature of these enzymes.

ii) post-replication repair. Some DNA damage can impeded the progress of the replication proteins and prevent full or proper duplication of the genome. Post replication repair is better termed DNA tolerance rather than repair since it allows replication proteins to ignore certain forms of DNA damage and to leave them to be dealt with by a true repair process at a later time. Cells utilize two methods of damage tolerance, both of which are employed during the process of replication of DNA. In the first, the polymerase steps over the damage and resumes replication at a point after the damage, leaving a gap in the newly synthesized strand. The second hypothesized mechanism for damage tolerance predicts that the polymerase replicates through the damage (reviewed in Walker, 1995). Regardless of which form of damage tolerance the cell has employed, the damage still persists and must be eventually dealt with by one of the other damage repair mechanisms.

iii) mismatch repair. The inherent error rate of DNA polymerases allows for the occasional insertion of an inappropriate nucleotide into DNA during the process of replication. Mismatch repair acts to increase the fidelity of replication by correcting the mistakes and also acts to repair certain forms of chemical or spontaneous damage (reviewed in Kolodner,

1995). The mechanism has been studied in detail in bacteria and homologous systems have been found in yeast and humans. Various mechanisms are thought to be employed to ensure that the proper strand is repaired, not all of which are understood. In the *E. coli* system, newly synthesized DNA exists briefly in a state in which the template strand is methylated while the new strand is not. The mismatch repair proteins are able to recognize the methylation status of the DNA strands and direct repair to the new strand which is most likely to contain the error (reviewed in Modrich and Lahue, 1996).

iv) recombinational repair. High energy ionizing radiation can physically break the sugar-phosphate DNA backbone to produce double strand breaks (DSBs). Recombination repair proteins act to restore the normal continuity of such broken chromosomes and can also fill in gaps created by one of the post-replication repair schemes (reviewed in Shinohara and Ogawa, 1995). This repair pathway requires the presence of two homologous DNA molecules.

v) base excision repair. Damage to single bases can be dealt with by the efficient process of base excision repair. The various types of damage repaired by this pathway are specifically recognized by DNA glycosylase enzymes. These enzymes act to cleave the glycosidic bond and release the damaged base, creating an apyrimidinic/apurinic (AP) site. The AP site further serves as a substrate for repair by AP endonucleases which cleave the backbone portion of the AP site to leave a one base gap. This gap is then filled in by a DNA polymerase and sealed by a DNA ligase. AP endonuclease and DNA glycosylase activity can exist in the same molecule or be separate proteins (reviewed in Lindahl *et al.*, 1997).

vi) nucleotide excision repair (NER). This DNA repair process can to deal with a wide range of structurally unrelated lesions and is often described as the most versatile DNA repair mechanism. NER is the primary defense mechanism against so-called 'bulky' DNA damage which results in distortion of the DNA helix and the broad substrate spectrum of this process marks it as one of the most important repair pathways. The study of NER was initiated early during investigation into DNA repair and has since received a lot of attention. Recent biochemical analysis has allowed for fine-structure understanding of the NER complex assembly and incision reactions, which has greatly aided the understanding of the phenotypes of NER defects in humans.

1.2 Nucleotide Excision Repair (NER)

I shall discuss this specific category of repair in more detail as it is the focus of my thesis. A simplified diagram showing the main features of NER for prokaryote and eukaryote systems is shown in Figure 1. Many types of DNA damage can serve as substrates for NER: cyclobutane pyrimidine dimers (CPDs), pyrimidine-pyrimidone (6-4) photoproducts, psoralen adducts, cisplatin adducts and other "bulky" base damage (reviewed in Friedberg, 1985). The basic mechanism of NER involves five steps. 1) The damage is recognized and bound. 2) The two strands of DNA in the vicinity of the damage are locally disassociated or "melted" by helicase action. 3) Endonucleases cleave the damage-containing strand of DNA on either side of the damage. 4) The damage-containing oligomer is removed and a DNA polymerase synthesizes a new strand using the opposite, intact strand as a template. 5) A DNA ligase seals the remaining nick. As we will see, the bacterial system represents a rather simple view of NER while the eukaryote system is

Figure 1 General NER Steps

The basic steps of NER from either prokaryote or eukaryote systems are shown here. The repair proteins are omitted for simplicity.

A. DNA damage is detected and initial binding by the damage recognition proteins occurs.

B. The action of helicase and/or other proteins acts to unwind the DNA duplex in the immediate area of the damage.

C. Incisions on either side of the damage are made in the DNA strand containing the damage.

D. A polymerase synthesizes the new portion of DNA using the opposite, intact strand as a template

E. The remaining single-stranded nick is sealed by a ligase to complete the repair process.

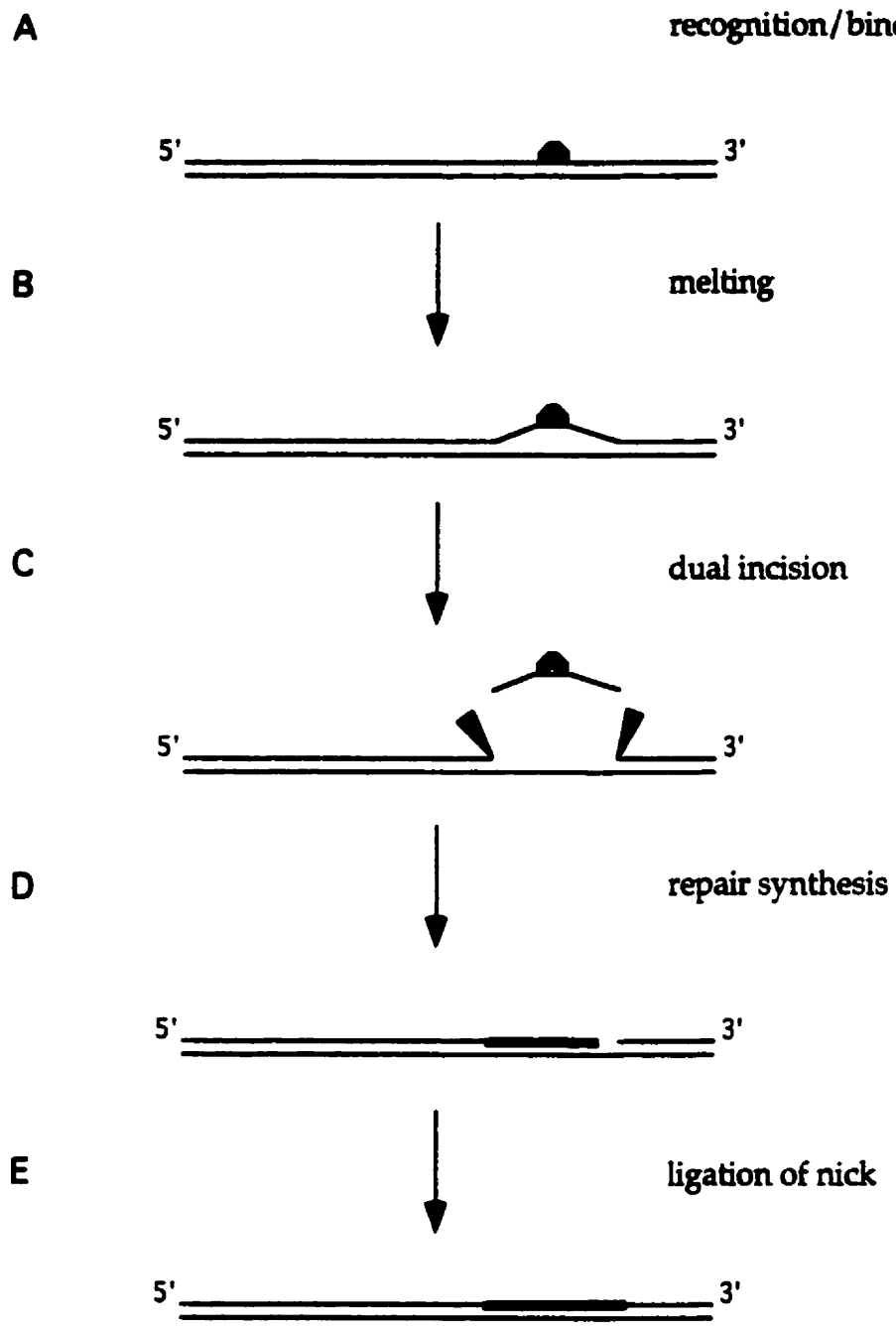
A
recognition/binding
5'
3'
B
melting
5'
3'
C
dual incision
5'
3'
D
repair synthesis
5'
3'
E
ligation of nick
5'
3'

more complex. The NER proteins are conserved among eukaryotes to such a degree that comparisons between yeast and human homologues are routine (Cleaver, 1994; Chu and Mayne, 1996; Lindahl *et al.*, 1997).

The rate at which DNA damage is repaired by NER is highly dependent on the rate of transcriptional activity in the region. It is known that the repair of active genes occurs at a much higher rate than the remainder of the genome. Furthermore, in transcriptionally active regions, there is a bias for rapid repair in the transcribed strand over the non-transcribed strand which is dependent on active transcription (reviewed in Drapkin *et al.*, 1994; Selby and Sancar, 1994). This preferential repair is termed transcription-coupled repair (TCR), while the slower repair of the remainder of the genome is termed global genome repair (GGR). It is now known that GGR can act on DNA damage regardless of the strand or activity of the region while TCR acts exclusively on the transcribed strand of active genes (Bohr, 1991; Sancar, 1996a).

1.2.1 Transcription-Coupled Repair

The method of coupling repair to transcription was found to be due to the impediment of an elongating RNA polymerase at sites of damage. The stalled polymerase acts to signal the presence of damage and the subsequent assembly of the NER machinery at that site (Selby and Sancar, 1990; Selby and Sancar, 1993). The method by which TCR operates in prokaryotes and eukaryotes appears to be similar. In bacterial systems, the presence of a stalled RNA polymerase at sites of damage is a physical barrier to NER (Selby and Sancar, 1990). A transcription-repair coupling factor (TRCF), encoded by the *mfd* gene, displaces the stalled RNA polymerase to alleviate the barrier to repair, but also actively recruits the repair proteins (reviewed in Selby and Sancar, 1994). In eukaryotes, the TRCF plays a role in recruiting NER factors to sites of damage as in bacteria, however

it is unclear whether the TRCF causes the displacement of the stalled RNA polymerase. In yeast the TRCF is Rad26p (van Gool *et al.*, 1994) while in humans it is the products of the CSA and CSB genes, the latter being the homologue of Rad26p (Henning *et al.*, 1995; van Gool *et al.*, 1997).

Evidence that the eukaryote TRCF acts to recruit NER factors comes from several studies. It was determined that Rad26p is not required for TCR while TFIIH is still associated with the RNA polymerase complex and was thought to be crucial in the recruitment of TFIIH after it had dissociated from the elongating polymerase (Tijsterman *et al.*, 1997). CSB has been found in association with a complex containing RNA polymerase II and has also been found to interact with the exonuclease XPG (human homologue of Rad2p), providing a possible link to explain TCR (van Gool *et al.*, 1997). Interactions of CSA with CSB and a subunit of TFIIH also support this model (Henning *et al.*, 1995).

Although displacement of the RNA polymerase at sites of damage by the TRCF has not been demonstrated in eukaryotes, certain studies in the literature may have inadvertently discovered such a link. A study by Bregman *et al.* (1996) showed that RNA polymerase II is ubiquitinated in normal human cells after exposure to UV light. This activity was absent in cells derived from a patient with Cockayne syndrome but was complemented by introduction of the CSA or CSB genes. The ubiquitination appears to be an important part of the activity of these genes and may hint at a mechanism of displacement of RNA polymerase II.

1.2.2 Global Genome Repair

Global genome repair refers to the repair of lesions anywhere in the genome. It relies on a similar mechanism of uncovering DNA damage as that seen in TCR. Verhage *et al.* (1994) showed that yeast Rad7p and Rad16p were absolutely required for GGR. Recently, these proteins were found to exist as a complex with an ATP-dependent helicase activity that actively scanned DNA for lesions and was designated NEF-4 (Guzder *et al.*, 1998). A stalled NEF-4 appears to signal for the assembly of the NER complex, presumably in a similar fashion to TCR. It is not known how NEF-4 gains access to DNA in the higher order chromatin structure of untranscribed regions. There is evidence that Rad7p participates in the remodeling of chromatin, but the mechanism remains unknown (Paetkau *et al.*, 1994). The rate of damage recognition is likely greater in transcribed regions, compared to silent regions, thus explaining the discrepancy in apparent rate of repair between GGR and TCR. Once the damage is recognized by either TCR or GGR, the remainder of the NER process appears to proceed in the same fashion and at the same rate regardless of which pathway discovered the damage.

1.2.3 NER in Bacteria

Only six proteins are required for NER in *E. coli*: UvrA, UvrB, UvrC, UvrD, a DNA polymerase and a DNA ligase (reviewed in Sancar, 1996a). In an ATP-dependent series of steps, the damage is first recognized by a UvrA-UvrB complex in which UvrA "loads" UvrB onto the damage. UvrB then unwinds a local area around the damage and bends the DNA. This UvrB-DNA complex is then recognized by UvrC and dual incisions are made 12-13 bp apart in the damaged strand on either side of the lesion. A helicase

(UvrD) then unwinds the damaged oligomer from the opposite strand allowing DNA polymerase I to fill in the gap. The nick is then ligated to finish the repair process.

1.2.4 NER in Eukaryotes

At least 19 proteins are required for eukaryote NER *in vitro* including the DNA polymerase and DNA ligase proteins. Table 1 lists the proteins required for NER and also shows the homologous comparisons between yeast and human systems. In eukaryotes, incision occurs roughly 22-24 bases 5' to the damage and 5 bases 3' to the damage to yield an oligomer of approximately 2-29 bp (Guzder *et al.*, 1995b; Huang *et al.*, 1994; Svoboda *et al.*, 1993). The biochemical analysis of NER has been pursued in yeast and humans using slightly different approaches. The information gathered in one organism is presumed applicable and complementary to the other so it is best to consider the details of NER in both yeast and humans at the same time.

1.2.4.1 Damage Recognition

The damage recognition step of NER has now been characterized in some detail. Although the damage appears to be recognized initially by either the elongating polymerase or a NEF-4 like complex, the recognition step is historically defined as the binding of the DNA-damage specific proteins. In most cases, the DNA damage distorts the helix and acts as the signal for repair. The wide spectrum of NER damage substrates is thought to be a result of response to altered DNA structure rather than recognition of specific molecular types of damage (Gunz *et al.*, 1996). In yeast, the damage specific proteins consist of RPA (reviewed in Cleaver and States, 1997), Rad14p and Rad4p (Figure 2A). The human

counterparts for Rad14p and Rad4p are XPA and XPC. Most of our knowledge about the function of RPA comes from studies with the human complex and demonstrates that these proteins play a crucial structural role in assembly of the NER machinery. RPA has high affinity for ssDNA and binds a region of approximately 30 bp (Kim *et al.*, 1992). In *in vitro* experiments, it was found that RPA bound UV-damaged DNA with slightly higher affinity than undamaged DNA and that this preference was for 6-4 photoproducts, not pyrimidine dimers (Burns *et al.*, 1996). Rad14p and XPA also display a similar preference for DNA containing 6-4 photoproducts but again have little or no specificity for pyrimidine dimers (Guzder *et al.*, 1993; Jones and Wood, 1993). The interaction between RPA and XPA (Rad14) in humans imparts a cooperative binding to the complex so that it recognizes both 6-4 photoproducts and pyrimidine dimers in addition to multiple other forms of damage (He *et al.*, 1995). Rad4p is contained in a complex with Rad23p which is capable of recognizing multiple forms of damage and is absolutely required for NER (Jansen *et al.*, 1998; Guzder *et al.*, 1995b). In humans the equivalent complex, XPC-RAD23B is required only for global genome repair but is thought to play a key role in partial unwinding of the duplex DNA at sites of damage (Evans *et al.*, 1997). It has been proposed that the transcription bubble structure created by an elongating polymerase obviates the need for the XPC-RAD23B activity in mammalian transcription coupled repair (Mu and Sancar, 1997). Overall, the damage recognition proteins carry out two important processes. First, one or more of the proteins allows the duplex DNA to be separated slightly (GGR) or maintained in an open conformation (TCR). This altered conformation provides the structure necessary for binding by additional proteins. Second, the interactions between the damage recognition proteins and other NER factors localizes the latter to the damage site and provides the ordered scaffolding on which the NER complex is assembled

Figure 2 Proposed Model for NER Steps in Yeast
(Adapted from Habraken *et al.*, 1996)

The steps shown here are those common to both transcription-coupled and global genome repair up to and including the dual incision step. *RAD* genes are identified only by their numbers.

A. A complex containing the damage recognition protein Rad14p and the endonuclease complex Rad1p-Rad10p are localized to the site of damage along with the trimeric RPA complex and the Rad4p-Rad23p complex. These proteins provide the base on which the additional NER proteins are assembled in a highly ordered fashion.

B. The damage recognition proteins carry out or stabilize the slight unwinding of the duplex DNA around the damage. Through interactions with Rad14p, Rad23p and RPA, a complex containing TFIIH and Rad2p is recruited to the site of damage. Interactions between Rad2p and RPA may determine the 3' anchor site.

C. The helicase components of TFIIH (Rad3p and Rad25p) act in an ATP-dependent fashion to open the duplex DNA around damage to create a 25 nt bubble and provide the appropriate structure for the endonucleases.

D. Dual incision is made 3' by Rad2p and 5' by Rad1p-Rad10p.

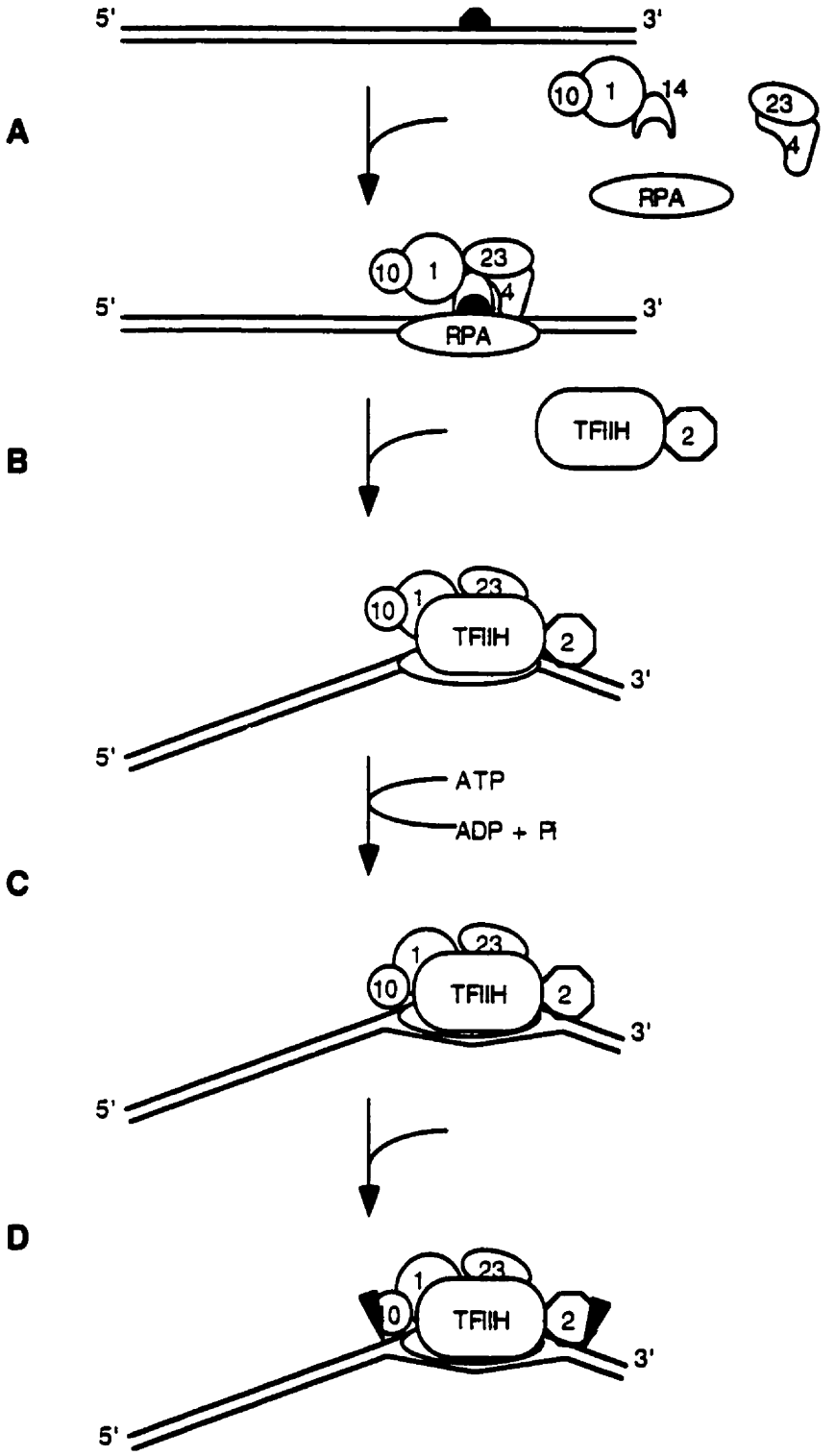
5'
3'
A
10
1
14
23
4
RPA
5'
3'
B
TFIIH
2
C
ATP
ADP + Pi
D

1.2.4.2 Incorporation of TFIIH and Duplex Melting

In order for the dual incisions to be made, the DNA around the site of damage must be in the correct conformation; this is achieved by the action of additional NER proteins. The damage recognition proteins present at the site of damage interact with other NER proteins to incorporate them into the complex. The TFIIH complex, which contains the helicase subunits Rad3p (XPD) and Rad25p (XPB) (Figure 2B) is an important component recruited to the NER complex. Rad3p and Rad25p act in an ATP-dependent manner to unwind the DNA strands in the region of damage to create a bubble structure of ~25 nucleotides (Evans *et al.*, 1997) (Figure 2C). TFIIH is known to interact directly with some damage recognition proteins, including XPA (He *et al.*, 1995); however efficient coupling of TFIIH to Rad14p (XPA) requires the activity of Rad23p (Guzder *et al.*, 1995a).

1.2.4.3 Dual Incision

The dsDNA-ssDNA boundaries at either end of the bubble structure are the target sites for the action of the endonuclease activities of Rad2p (XPG) and the Rad1p-Rad10p (XPF-ERCC1) complex. Rad2p performs the 3' incision which is immediately followed by the 5' incision carried out by the Rad1p-Rad10p complex (Mu *et al.*, 1996) (Figure 2D). The correct orientation of the incision complex relies on the positioning of the RPA protein which binds to the undamaged strand in a polar fashion and directs the assembly of subsequent proteins in a similarly polar fashion (de Laat *et al.*, 1998; Matsunaga *et al.*, 1996). It is thought that the interaction of RPA with XPG "anchors" the 3' incision site at a favorable location and that the 5' incision is then made at the set distance from the 3'

incision to create the ~30 nt incision product (de Laat *et al.*, 1998). In yeast the Rad1p-Rad10p proteins are complexed to Rad14p and are thought to localize to damage through that interaction (Guzder *et al.*, 1996). A similar situation exists in humans with XPA and the XPF-ERCC1 complex (Park and Sancar, 1994). Rad2p associates with TFIIH and is incorporated along with the TFIIH complex (Habraken *et al.*, 1996).

1.2.4.4 Repair Synthesis and Ligation

The final step in NER is the synthesis of a new strand of DNA to fill the gap and ligation of the remaining nick to restore the continuity of the DNA. RPA is known to play a role in this process again as well as the PCNA complex, RF-C and at least DNA polymerase ε (Aboussekhra *et al.*, 1995).

1.3 DNA Repair and Disease

The first observation of a DNA repair defect in human disease was found in the condition xeroderma pigmentosum (XP) (Cleaver, 1968). A detailed description of the condition and the XP complementation groups is given in Chu and Mayne (1996). The complementation groups XPA through XPG corresponded to the loss of function of one of the key repair proteins (see Table 1). XP patients have reduced or absent NER capacity and are extremely sensitive to the effects of sunlight (reviewed in Chu and Mayne, 1996). Patients with defects in TCR also show some degree of sun-sensitivity but display overriding neurological abnormalities. These patients have Cockayne syndrome (CS) and are defective in the activities of CSA or CSB (reviewed in Chu and Mayne, 1996). Trichothiodystrophy (TTD) is also classified as a DNA-repair deficiency syndrome and can

arise from mutations in XPB, XPD and TTDA (reviewed in Chu and Mayne, 1996). Mutations in certain genes, most notably XPB, can give rise to XP or a combination of XP with CS phenotypes (reviewed in Chu and Mayne, 1996).

Table 1 Components of NER Required for *in vitro* Incision
Adapted from Feaver *et al.* (1997)

Complex*	Components	NER Function	Human Homologue
NEF-1	Rad14p	Damage recognition	XPA
	Rad1p	Excision endonuclease with Rad10p	XPF
	Rad10p	Excision endonuclease with Rad1p	ERCC1
NEF-2	Rad4p	Damage recognition	XPC
	Rad23p	Complex assembly	RAD23A, RAD23B
NEF-3	Rad2p	Excision endonuclease	XPG
	Rad3p†	DNA helicase	XPD
	Rad25p†	DNA helicase	XPB
	Ssl1p†	?	BTF2p44
	Tfb1p†	?	BTF2p62
	Tfb2p†	?	BTF2p52
	Tfb3p†	?	MAT1
	Tfb4p†	?	BTF2p34
	Ccl1p†	?	Cyclin H
	Kin28p†	?	MO15/CDK7
RPA	Rfa1p	ssDNA binding/damage recognition	RPA1
	Rfa2p	?	RPA2
	Rfa3p	?	RPA3

* NEF = nucleotide excision repair factor (see Guzder *et al.*, 1996)
† subunit of TFIIH

1.4 *RAD23*

The *RAD23* gene was discovered during the analysis of a mutant strain overexpressing the yeast iso-2-cytochrome C protein (McKnight *et al.*, 1981). This mutant strain was found to contain a 5 kb deletion on Chromosome V and was UV sensitive. The

UV sensitivity of this strain was unlinked to any of the previously identified *rad* mutants, *rad1*Δ through *rad22*Δ, and was thus designated *rad23*. The region surrounding the *RAD23* locus contains the coding region for a gene involved in osmolarity sensitivity and the iso-cytochrome c gene. A similar three gene cluster exists on chromosome X which contains the DNA repair gene *RAD7*. Based on the conservation of gene functions in these regions, McKnight *et al.* (1981) suggested that the gene clusters, and thus the two *RAD* genes, shared a common ancestry and may carry out similar functions. Miller *et al.* (1982) showed that the *rad7*Δ and *rad23*Δ deletion mutants shared similar phenotypes with respect to removal of UV-induced pyrimidine dimers and psoralen intrastrand DNA crosslinks, strengthening the notion of gene relatedness. However, the genes did not complement each other (McKnight *et al.*, 1981), and the phenotype of a double mutant, *rad7*Δ *rad23*Δ, demonstrated an even greater sensitivity to both types of DNA damage (Miller *et al.*, 1982).

The DNA sequence of *RAD23* was determined independently by Melnick and Sherman (1993) and Watkins *et al.* (1993). The *RAD23* gene codes for a nuclear protein of 398 amino acids (aa) with a basic N-terminal region (pI = 9.71 for the first 81 aa), while the remainder of the protein is highly acidic (pI = 3.77). The N-terminal portion of the protein is intriguing because the amino acid residues 2-77 share 43% similarity (22% identity) to ubiquitin, a protein known to target other proteins for degradation (reviewed in Hilt and Wolf, 1996). This observation implied that Rad23p may be a target for regulated protein degradation. Removal of this ubiquitin-like domain caused UV sensitivity intermediate to that of *rad23*Δ and wild type, suggesting that this domain was required for *RAD23* function (Watkins *et al.*, 1993). Ubiquitin itself can functionally substitute for the N-terminal domain of Rad23p, as a chimeric ubiquitin-Rad23 protein, to provide wild-type levels of UV resistance (Watkins *et al.*, 1993). A small fraction (less than 0.1%) of cellular Rad23p was found to be conjugated to native ubiquitin, however the half-life of this protein

was greater than 6 hours, implying that the protein was highly stable *in vivo*. Schauber *et al.* (1998) identified *RAD23* as a suppressor of toxicity caused by overexpression of components of the protein degradation system, once again suggesting a proteolytic function for Rad23p. These authors demonstrated interactions between Rad23p and components of the protein degradation machinery and also demonstrated a proteolytic role for the ubiquitin-like domain of Rad23p.

Biochemical analysis revealed that Rad23p was responsible for effectively coupling the TFIIH complex and Rad14p (Guzder *et al.*, 1995a). This role for Rad23p is consistent with the *rad23Δ* partial UV sensitivity phenotype and the designation of Rad23p as an "accessory protein". Guzder *et al.* (1995b) went on to show that a Rad23p - Rad4p complex was required for the incision process of NER *in vitro*. He *et al.* (1996) found that the elimination of *RAD23* activity did not abolish NER in cell-free extracts of yeast, but did affect the efficiency of the process. Although this observation appears to contradict the findings of Guzder *et al.* (1995b), the two systems differed significantly such that the observations are not mutually exclusive. Wang *et al.* (1997) carried out similar experiments and arrived at the same conclusion for *RAD23*. These studies looked specifically at transcription-independent repair. Mueller and Smerdon (1996) showed that a functional *RAD23* allele was required for efficient repair in both the transcription-coupled and global genome repair pathways but that both pathways had residual activity in the absence of *RAD23*. Rad23p also interacts with Rad4p *in vitro* (Guzder *et al.*, 1995a) and in the two-hybrid system (Wang *et al.*, 1997).

The ubiquitin-like portion of Rad23p places it in a unique class of proteins bearing such a domain. Another such ubiquitin-like gene, *DSK2*, confers temperature-sensitive growth defects when mutated in combination with *RAD23* (Biggins *et al.*, 1996). *DSK2* is involved in spindle pole body duplication, suggesting that *RAD23* may also function in

cell-cycle progression. An additional domain is found twice in *RAD23* which is referred to as the UBA domain (for ubiquitin-associated) (Hofman and Bucher, 1996). This domain is common in other proteins involved in the ubiquitination pathways.

Two human counterparts for *RAD23* were discovered in 1994 (Masutani *et al.*, 1994) and found to encode highly similar proteins, including the conserved N-terminal ubiquitin-like domain. At least one of the homologues, *RAD23B*, interacts with XPC, the human equivalent of *RAD4* (Masutani *et al.*, 1994). The *RAD23B* product was shown to stimulate XPC activity in an *in vitro* repair system (Sugasawa *et al.*, 1996). Overexpression of *RAD23A*, the second human homologue of *RAD23*, was recently shown to prevent the cell cycle arrest caused by the HIV-1 viral protein Vpr (Withers-Ward *et al.*, 1997). Homologues of *RAD23* have also been found in mouse (van der Spek *et al.*, 1996), rice (Schultz and Quatrano, 1997) and *Arabidopsis* (Sturm and Lienhard, 1998). Despite the apparent importance and conservation of *RAD23* no human diseases have been associated with this gene. To date the evidence still seems to point to Rad23p as an accessory factor in the efficiency of NER.

1.5 The Two-Hybrid System

The Two-Hybrid System (THS) was first reported by Fields and Song in 1989 (see Figure 3). The system takes advantage of the modular nature of the Gal4p transcription factor. This protein can be divided into distinct and functional domains which carry out one of the two key functions of the transcription factor - DNA binding and transcriptional activation. Reconstitution of the two domains allows for them to act in concert as with the native protein. In the two-hybrid system, the two domains are independently fused to proteins of interest to create two hybrid proteins. If the fused proteins are capable of

Figure 3 Diagrammatic Representation of the Two-Hybrid System

(Adapted from Gietz *et al.*, 1997)

A simplified illustration of the two-hybrid system is shown here using Rad23p as the "bait". The *TRP1* or *LEU2* plasmids contain gene fusions which allow the production of hybrid proteins. The two domains of the Gal4p transcription factor are shown with a speckled pattern. The protein product of Rad23p is shown with a hatched pattern and those of Sap1p, Hmo1p or Byh1p are shown with filled patterns. The Gal4p binding domain (BD) localizes the BD:Rad23 hybrid to the promoter region of a reporter gene. Interaction between Rad23p and Sap1p, Hmo1p or Byh1p allows the AD:LibraryDNA fusion protein to be in position to activate the reporter gene through the Gal4p activating domain (AD). Interactions are detected by assaying for *lacZ* activity and/or histidine auxotrophy.

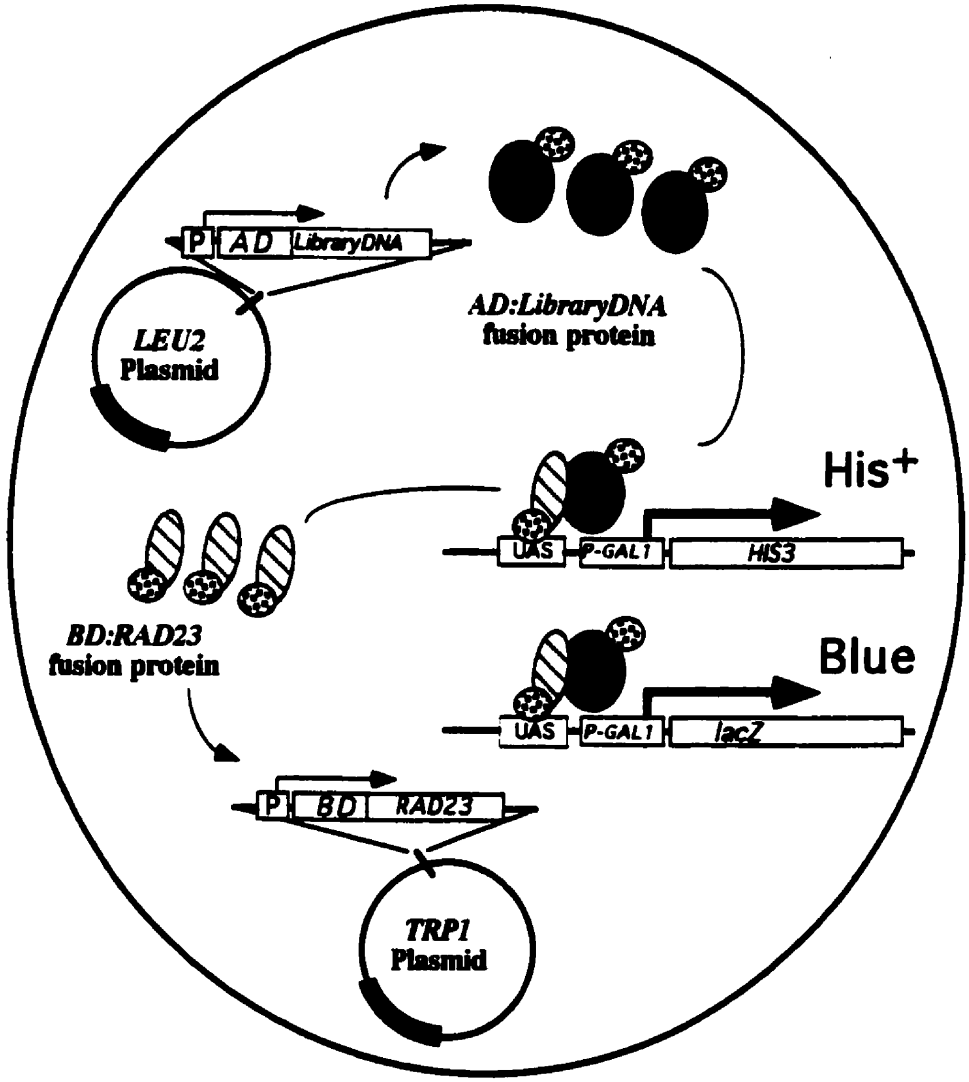
P
AD
LibraryDNA
LEU2
Plasmid
AD:LibraryDNA
fusion protein
His+
UAS
P-GAL1
HIS3
BD:RAD23
fusion protein
Blue
UAS
P-GAL1
lacZ
P
BD
RAD23
TRP1
Plasmid

interacting with one another, the transcription factor will be reconstituted and allow activation of a specific reporter gene. By assaying for the activity of the reporter gene (usually a nutritional marker or enzyme such as *lacZ*), it can be determined if two fusion proteins interact. One of the most versatile adaptations of this system is the two-hybrid screen in which a protein of interest is fused to a DNA binding domain such as the $Gal4_{BD}$ or the *lex*A protein and tested against a library of fusion proteins to identify interacting partners. Not only does this system allow the interaction to occur *in vivo*, but the process of identification is rapid and serendipitously results in the cloning of the novel gene(s). By performing multiple two-hybrid screens, it may be possible to create a "proteome map" for a given cellular process linking each protein to its partners. In this way it is possible to extend the knowledge of interactions within a given pathway but also to link one pathway with another.

Prior to my arrival in the lab, the THS was used by Sharon Simon to identify novel Rad23p interacting proteins. It was anticipated that the nature of the interacting proteins would clarify the role of Rad23p in DNA repair. Three novel Rad23p interacting proteins were identified, however, the function of these proteins is not fully understood and therefore not immediately informative.

1.6 Thesis Objectives

I investigated the protein-protein interactions that were identified by the Rad23p two-hybrid screen to determine if these Rad23p interacting proteins were involved in DNA repair and what was the significance of their association with Rad23p. To accomplish this I tested the interactions *in vivo* and *in vitro* and examined the phenotypes of null mutants for DNA repair phenotypes.

2. MATERIALS AND METHODS

2.1 Bacteriophage Lambda Clones

The bacteriophage lambda strain MG14 (American Type Culture Collection (ATCC)) was used for all preparations of lambda DNA. Lambda clones were obtained from ATCC as freeze-dried, bacteria-free lysates. These lysates were reconstituted in 0.5 ml SM media and stored at 4°C for general use. Bacteriophage lysate solutions were preserved in 7% DMSO (v/v) at -80°C.

2.2 Bacterial Strains

The *E. coli* strains used in this study are listed in Table 2. All bacterial stocks were maintained in 20% glycerol at -80°C.

Table 2 Bacterial Strains

Strain	Genotype	Source	Reference
DH5α	F⁻ f80d*lacZ*ΔM15Δ(*lacZYA-argF*)U169 *deoR recA1 endA1 phoA hsdR17*(r_K^-, m_K^+) *supE44 thi-1 gyrA96 relA1* λ⁻	R.D. Gietz	Gibco BRL
GM2163	F⁻ *ara-14 leuB6 thi-1 fhuA31 lacY1 tsx-78 galK2 galT22 supE44 hisG4 rpsL136* (Str^r) *xyl-5 mtl-1 dam13*::Tn*9* (Cam^r) *dcm-6 mcrB1 hsdR2* (r_K^- m_K^+) *mcrA* λ⁻	R.D. Gietz	NEB
C600	F⁻ *thi-1 thr-1 leuB6 lacY1 tonA21 supE44* λ⁻	R. Hodgetts	NEB

2.3 Yeast Strains

The yeast strains used in this study are listed in Table 3. CTY10-5d was used for all two-hybrid system analysis. MKP° and RSY185 were used for all genetic manipulations. MKP° and the isogenic strain MKP° *rad23Δ* were used as controls for UV irradiation experiments. All yeast stocks were maintained in 20% glycerol at -80°C.

Table 3 Yeast Strains

Strain	Genotype	Source	Reference
CTY10-5d	*MATa ade2 gal4 gal80 his3Δ200 leu2-3,112 trp1-Δ901 ura3-52 URA3::lexAopGAL1-lacZ*	S. Fields	Bartel *et al.*, 1993
MKP°	*MATα can1-100° ade2-1° lys2-1° ura3-52 leu2-3,112 his3-Δ200 trp1Δ901*	B. Kunz	Pierce *et al.* 1987
MKP° *rad23Δ*	*MATα can1-100° ade2-1° lys2-1° ura3-52 leu2-3,112 his3-Δ200 trp1Δ901 rad23ΔhisG*	R.D. Gietz	
MKP° *rad6Δ*	*MATα can1-100° ade2-1° lys2-1° ura3-52 leu2-3,112 his3-Δ200 trp1Δ901 rad6ΔLEU2*	R.D. Gietz	
RSY185	*MATa/MATα leu2-3,112/leu2-3,112 ura3-52/ura3-52 his1-1/his1-7 can1^s/can1^r TRP2/trp2 HOM3/hom3-10*	R. Schiestl	

2.4 Plasmids

Plasmid vectors used but not constructed for this study are listed in Table 4. All plasmid samples were maintained in 1 x TE at 4°C or less.

Table 4 Plasmids

Plasmid	Genes	Source	Reference
pUC18	Ap^R	R.D. Gietz	Norrander *et al.*, 1983
pUC19	Ap^R	R.D. Gietz	Yanisch-Perron *et al.*, 1985
pKM1310	Ap^R, *TRP1*, HA-tag	K. Madura	
pGAD424	Ap^R, *LEU2*, $GAL4_{AD}$	R.D. Gietz	Bartel *et. al.*, 1993
pBS(KS+)	Ap^R	R.D. Gietz	Stratagene
pBTM116	Ap^R, *TRP1*, $lexA_{BD}$	R.D. Gietz	Bartel *et. al.*, 1993
pDG317	Ap^R, *LEU2*	R.D. Gietz	Gietz and Sugino, 1988
pRDG98	Ap^R, *URA3*	R.D. Gietz	
pDG328	Ap^R, *URA3*	R.D. Gietz	
pDG649	*TRP1*, Ap^R, $lexA_{BD}$-*RAD7*	R.D. Gietz	Paetkau *et al.*, 1994
pJR3	*LEU2*, ApR, $GAL4_{AD}$-*SIR3*	R.D. Gietz	Paetkau *et al.*, 1994
pUb-Met-lacZ	Ap^R, Ub-Met-*lacZ*	K. Madura	Bachmair *et al.*, 1986
pUb-Arg-lacZ	Ap^R, Ub-Arg-*lacZ*	K. Madura	Bachmair *et al.*, 1986
pKG86	Ap^R	R.D. Gietz	

2.5 Media and Solutions

Media and solutions were made essentially as in Sambrook *et al.* (1989). Solid medium was prepared by adding 10 g Difco Agar per 600 ml liquid before autoclaving. Autoclaving was carried out for 20 min. at 121°C.

2.5.1 Bacterial Media

2.5.1.1 LB (Luria-Bertani) Broth

Difco Bacto-yeast extract	3.0 g
Difco Bacto-tryptone	6.0 g
NaCl	6.0 g
ddH_2O	to 600 ml
pH 7.0	

LB+carbenicillin and LB+Mg^{++} were prepared as for LB media. After autoclaving, the media was allowed to cool to ~55°C. Carbenicillin was then added to a final concentration of 20 mg/l to make LB+carbenicillin and $MgSO_4$ was added to a final concentration of 10 mM to make LB+Mg^{++}. LB+Mg^{++} top agar was prepared as for LB+Mg^{++} except that only 7 g of Difco Bacto-agar per 1000 ml volume was added.

For selection of recombinant plasmids involving the disruption of the *lacZ* gene of pUC18, pUC19 or pBS(KS+), 60-75 μl of a solution containing X-gal (25 mg/ml in DMF) was spread on the surface of LB+carbenicillin plates. This allowed the differentiation between bacterial colonies containing plasmids with or without cloned DNA inserts (white and blue colour colonies respectively).

2.5.1.2 SOC

Difco Bacto-yeast extract	12.0 g
Difco Bacto-tryptone	6.0 g
NaCl	0.36 g
KCl	0.108 g (or 600 μl of 2.5 M KCl)
Dextrose	1.2 g
ddH_2O	to 600 ml

Before use, a 2 M solution of magnesium salts (1 M $MgCl_2$, 1M $MgSO_4$) was added to a final concentration of 0.5%.

2.5.2 Yeast Media

2.5.2.1 YPA Dextrose (YPAD)

Difco Bacto-yeast extract	6.0 g
Difco Bacto-peptone	12.0 g
Dextrose	12.0 g
Adenine Hemisulfate	48.0 mg (solid medium) 24.0 mg (liquid medium)
ddH_2O	to 600 ml

2.5.2.2 Synthetic Complete (SC) Dropout medium

Bacto-yeast nitrogen base w/o $(NH_4)_2SO_4$ or amino acids	1.0 g
Ammonium sulfate	3.0 g
Dropout mix	350.0 mg
Dextrose	12.0 g
ddH_2O	to 600 ml
pH 5.6	

2.5.2.3 Dropout Mix for Synthetic Medium

The appropriate ingredient was omitted to make SC-dropout media.

	Amount	Final Concentration
Adenine sulfate	4 g	46 mg/l
Arginine HCl	2 g	23 mg/l
Aspartic acid	2 g	23 mg/l
Glutamic acid HCl	2 g	23 mg/l
Histidine HCl	2 g	23 mg/l
Homoserine	6 g	70 mg/l
Isoleucine	2 g	23 mg/l
Leucine	2 g	23 mg/l
Lysine HCl	2 g	23 mg/l
Methionine	2 g	23 mg/l
myo-Inositol	2 g	23 mg/l
p-aminobenzoic acid (PABA)	0.2 g	2 mg/l
Phenylalanine	3 g	35 mg/l
Serine	2 g	23 mg/l
Threonine	2 g	23 mg/l
Tryptophan	2 g	23 mg/l
Tyrosine	2 g	23 mg/l
Uracil	2 g	23 mg/l
Valine	9 g	105 mg/l

2.5.2.4 Galactose Media

Media containing galactose was made as above except that galactose was substituted for dextrose at a final concentration of 2%.

2.5.3 Preparation of *E. coli* C600 for Lambda Infection

The *E. coli* strain C600 was grown in LB medium containing maltose to induce the expression of the bacteriophage lambda receptor. A single colony was inoculated into 50 ml of 37°C pre-warmed liquid LB medium supplemented with 0.2% maltose and incubated

overnight with shaking at 37°C. The culture was harvested by centrifugation at 3000 *g* for 10 minutes (room temperature) using an IEC Centra® MP4 desktop centrifuge (International Equipment Company). The supernatant was decanted and the bacterial pellet was resuspended in 10 mM $MgSO_4$ to a final volume of 0.4 x the original volume of culture (i.e. 20 ml) and stored at 4°C. These cells were used up to three days after preparation after which time they were discarded.

2.5.4 Bacteriophage Lambda Plating

High titer bacteriophage lysates were first produced on solid media. Bacteriophage lysates (0.1 ml) were mixed with an equal volume of C600 bacteria in a 5 ml polystyrene capped tube (VWR). These tubes were incubated in a 37°C water bath for 20 minutes to allow adsorbtion of the bacteriophage to the bacterial surface. LB+Mg^{++} top agar was melted in the microwave then maintained in a liquid state in a 47°C waterbath. Top agar (3.0 ml) was added to the tubes and mixed by inversion. The tube contents were immediately poured onto LB+Mg^{++} plates (preheated to 37°C) and gently swirled to evenly distribute the liquid across the surface of the media. The plates were left at room temperature for 10 minutes to allow the top agar to solidify then inverted and incubated at 37°C overnight.

2.5.4.1 Isolation of Lambda Clones

Visible plaques in the bacterial lawn were isolated by using a Pasteur pipette to remove an agar plug containing a single lambda plaque. The 'plug' was then dispensed

into 1.0 ml of SM media and incubated for at least one hour at room temperature to allow diffusion of the bacteriophage particles into the SM media.

2.5.4.2 Lambda Plate Lysate Cultures

Plates displaying confluent lambda lysis were flooded with 5 ml of SM media and incubated at 4°C for a minimum of 4 hours to harvest the bacteriophage particles and establish high titer plate lysates. The liquid was then removed and transferred to a 15 ml capped polypropylene centrifuge tube. The culture was cleared of bacterial debris by centrifugation for 10 minutes at 4°C at 5488 *g* in a Sorval® Superspeed RC2-B centrifuge and the supernatant was transferred to a fresh centrifuge tube. The centrifugation was repeated and the supernatant was decanted to a new polypropylene tube. Chloroform (15 μl) was added to prevent further bacterial growth and lysates were stored at 4°C.

Lysates were titered using 10-fold serial dilutions in SM media. The dilutions were used to infect C600 and plated as previously described. The number of visible plaques produced on the bacterial lawn was counted for each dilution and the titer determined as number of plaque forming units per/ml (PFU/ml).

2.5.5 Liquid Lambda Lysate Cultures

Plate lysate cultures were used to produce high titer lysates in liquid cultures. Fresh plating bacteria (0.1 ml, ~$1x10^8$ cells) were mixed with an appropriate volume of diluted lambda lysate culture to obtain the desired multiplicity of infection and incubated at 37°C for 20 minutes to allow the bacteriophage to adsorb to the bacterial cells. LB liquid medium (10 ml), pre-warmed to 37°C, was added and the culture incubated with vigorous shaking

at 37°C for 6 - 12 hours until good lysis had occurred as indicated by the appearance of bacterial debris precipitate. Chloroform was then added to 1% (v/v) followed by the addition of DNAseI and RNAseA to 1 μg/ml and the tubes were incubated at 37°C with shaking for an additional 20-30 minutes.

Each culture was decanted into a 50 ml polypropylene centrifuge tube and the bacterial debris was cleared by a 3000 *g* centrifugation for 10 minutes at room temperature using an IEC Centra® MP4 desktop centrifuge. The supernatant was transferred to a fresh 50 ml polypropylene centrifuge tube and centrifugation was repeated. Finally, the supernatant was transferred to a 30 ml polypropylene Oak Ridge centrifuge tube with sealing cap (Nalgene) and stored at 4°C.

2.5.6 Isolation of Bacteriophage DNA

Bacteriophage λ particles were concentrated from liquid lysates in preparation for DNA isolation. Solid sodium chloride and PEG 8000 were added to each lysate to final concentrations of 0.5 M and 10% (w/v), respectively. The NaCl/PEG treated lysates were then incubated on ice for at least one hour to allow the precipitation of the bacteriophage particles. The bacteriophage particles were harvested by centrifugation for 10 minutes at 12100 *g* and 4°C using a JA20 rotor in a Beckman model J2-21 centrifuge. The supernatant was discarded and the pellet was drained at 4°C for 30 minutes. The remaining supernatant was carefully removed with a Kimwipes® tissue and the bacteriophage pellet was resuspended in 500 μl SM media, by repeated pipetting of the SM media over the bacteriophage pellet until the pellet appeared fully resuspended. The resulting bacteriophage preparations were transferred to separate 1.5 ml microfuge tubes and stored at 4°C.

DNA was released from bacteriophage particles by proteolytic digestion of the bacteriophage capsid. Proteinase K (50 μg/ml final concentration), SDS (0.5% final concentration) and EDTA (20 mM final concentration) were added to the resuspended bacteriophage particles and the tubes incubated in a 42°C waterbath for 1 hour. The samples were extracted in succession with one volume (500 μl) of buffer-saturated phenol, one volume of phenol/chloroform (1:1) and one volume of chloroform. The phases were separated by centrifugation at room temperature for 5 minutes at 15000 *g* and the aqueous phase was transferred to a fresh 1.5 ml microfuge tube for each successive extraction. The λ DNA was then precipitated by the addition of 1/10 volume sodium acetate (3 M, pH 6.0) and 2.5 volumes of absolute ethanol then incubated at -20°C for at least one hour. The precipitated DNA was pelleted at 15000 *g* for 5 minutes (4°C) and washed with 70% ethanol. The pellets were briefly air dried then dissolved in 100 μl TE by incubation at 37°C for 30 minutes.

2.6 Preparation of Electrocompetent Bacteria

2.6.1 DH5α

Electrocompetent *E. coli* DH5α were prepared by a modified version of the method of Dower *et al.* (1988). A 50 ml volume of LB broth media was inoculated with a single colony of DH5α and grown overnight at 37°C with agitation in a 250 ml Erlenmeyer flask. The following day, 5 ml aliquots were inoculated into four 500 ml volumes of LB broth in 2 L Erlenmeyer flasks and incubated at 37°C with agitation until the OD_{600} reading was approximately 0.7. The 500 ml cultures were transferred to four 500 ml wide-mouth

polypropylene centrifuge bottles (Nalgene). The cells were harvested by centrifugation at 8670 *g* for 10 minutes (4°C) in a Beckman model J2-21 centrifuge using a pre-chilled JA10 rotor. The cells were then washed in one volume of sterile ice cold ddH_2O and harvested again. A 100 ml volume of ice cold ddH_2O was added to each tube to resuspend the pellet and the cells were combined into two cultures. The volume of these remaining two cultures was brought up to 500 ml using ice cold ddH_2O then harvested as above. Both bacterial pellets were resuspended in 20 ml of ice cold ddH_2O and transferred to 30 ml polypropylene Oak Ridge centrifuge tubes with sealing caps (Nalgene). The cells were harvested by centrifugation at 4400 *g* for 10 minutes at 4°C in a Beckman model J2-21 centrifuge using a pre-chilled JA20 rotor and resuspended in a final volume of 20 ml with sterile 10% glycerol. The cells were harvested again at 3000 *g* for 10 minutes (4°C), resuspended in 1 ml of sterile 10% glycerol and allocated in 25-50 μl samples to 0.5 ml centrifuge tubes pre-chilled on ice. The dispensed cultures were then flash-frozen in liquid nitrogen and stored at -80°C.

2.6.2 GM2163

Electrocompetent *E. coli* GM2163 was rapidly prepared immediately before using. A toothpick was used to scrape an approximate 50 μl volume of bacterial cells from solid media which were then resuspended in 1 ml of ice-cold ddH_2O in a 1.5 ml centrifuge tube. The cells were pelleted at 15000 *g* for 30 seconds and the liquid was removed. The cells were washed twice with 1 ml of ice-cold ddH_2O then resuspended in one volume (50 μl) of ice-cold ddH_2O and stored on ice until use.

2.7 Electroporation of Electrocompetent Bacteria

Plasmid DNA was electroporated into bacterial cells by electroporation based on the method of Dower *et al* (1988). Gene Pulser® electroporation cuvettes (BioRad) and plasmid DNA samples or ligation reactions were cooled on ice. Samples of electrocompetent cells were equilibrated on ice prior to electroporation. After the addition of plasmid DNA the cells were placed into an electroporation cuvette (0.1 cm electrode gap). The electroporation cuvette was immediately placed in the safety chamber slide of a GenePulser™ apparatus (BioRad) and pulsed at 1.25 kV with the capacitance set to 25 μFD and the resistance set to 400 ohms in parallel to the sample. After electroporation, 500 μl of SOC or LB media was immediately added to the electroporation chamber to resuspend the cells. The cell suspensions were pipetted into 1.5 ml centrifuge tubes and incubated in a 37°C waterbath for 30 minutes. Samples of 10 μl and 100 μl of this culture were plated separately on LB+carbenicillin media and incubated for 12-20 hours at 37°C until colonies were visible.

2.8 Isolation of Bacterial Plasmid DNA

A modified version of the alkaline lysis miniprep procedure of Birnboim and Doly (1979) was used to extract plasmid DNA from small scale cultures of bacteria. Single isolated bacteria colonies were inoculated into 2 ml of LB media supplemented with ampicillin to a final concentration of 50 μg/ml. Cultures were grown to stationary phase at 37°C with agitation. Approximately 1.5 ml of culture was then decanted into 1.5 ml polypropylene centrifuge tubes pre-chilled on ice and pelleted at 15000 *g* for 30 seconds and the supernatant was removed by aspiration. The cells were fully resuspended in 100 μl of resuspension solution then lysed by the addition and mixing of 200 μl of lysis solution.

Bacterial debris was precipitated out of solution by adding 150 μl of potassium acetate solution and briefly mixing by vortex. All tubes were allowed to stand on ice for a maximum of five minutes following the addition of potassium acetate. The supernatant was cleared of bacterial debris by centrifugation at 15000 *g* for 5 minutes (4°C) and transferred to a new pre-chilled 1.5 ml polypropylene centrifuge tube. DNA samples were cleared of residual protein and other cellular debris by phenol:chloroform extraction and precipitated by the addition of 2.5 volumes absolute ethanol and 1/10 volume 3M Na Acetate (pH 6.0). The nucleic acid was pelleted by centrifugation at 15000 *g* for five minutes (4°C). The ethanol was removed and the pellet was washed with 100 μl of 70% ethanol then air dried for five minutes. Samples were resuspended in 50 μl of 1 x TE.

2.9 Restriction Endonuclease Digestion of DNA

Restriction enzyme digestion was used to determine the identity of plasmid and lambda DNA samples. Approximately 0.4 μg of DNA (2 μl) was digested by the addition of 19 μl ddH_2O, 2.5 μl of the recommended 10 x reaction buffer, 1 μl RNAseA (1 mg/ml) and 0.5 μl enzyme (2.5-10 units). Prior to electrophoresis, the DNA was concentrated by ethanol precipitation and resuspended in 16 μl of 1 x TE.

DNA samples required for plasmid or strain construction were digested with restriction enzymes in a similar fashion to that above. Approximately 10 μg of plasmid or lambda DNA was mixed with 390 μl ddH_2O, 50 μl of 10x reaction buffer, 5 μl RNAseA (1 mg/ml) and 5 μl enzyme (25-100 units) for a final volume of 500 μl. The DNA was digested to completion, extracted with phenol/chloroform, concentrated by ethanol precipitation and resuspended in 20-50 μl 1 x TE. DNA samples requiring digestion with methylation sensitive enzymes were purified from the dam$^-$ bacterial strain GM2163.

2.10 Agarose Gel Electrophoresis of DNA

Restriction enzyme digested DNA was analyzed by agarose gel electrophoresis. UltraPure™ agarose (Gibco BRL) was dissolved in 1 x TAE to a final concentration of 0.75% (w/v) by boiling. EtBr was added to a final concentration of 0.5 μg/ml and the gel was then cast in a plastic mold tray with a comb in place to create the loading wells. When the gel solidified, the comb was removed and the gel was placed in a horizontal electrophoresis apparatus. TAE buffer (1 x) was poured into the apparatus to cover the gel to a depth of approximately 3-5 mm. Samples were loaded into the loading wells and electrophoresed at 200 volts for 15 minutes except where otherwise noted. Lambda DNA was heated to 65°C for 5 minutes before loading into the agarose gel wells. Migration of the DNA was noted by the addition of loading dye to the samples at a final concentration of 10%. DNA molecular weight markers (1 kb ladder) were electrophoresed alongside samples to allow estimation of fragment sizes. Gels were illuminated with short wave UV light using a Spectroline TR254 transilluminator and photographed using a Polaroid MP4 land camera (f8, 10 second exposure), Polaroid type 667 film and a Kodak #9 Wratten filter.

2.11 Purification of DNA From Agarose Gels

DNA was isolated from agarose gels following the procedure of Girvitz *et al.* (1980). DNA samples were brought up to a final volume of approximately 95 μl using ddH_2O and 7 μl of loading dye was added. The samples were then loaded into two contiguous wells (50 μl each well) on a 0.75% agarose gel. The samples were electrophoresed at 200 volts for 5-10 minutes to allow the fragments to exit the loading wells and enter the gel matrix. The voltage was then reduced to 100 volts until fragments

were separated. Any fragments migrating slower than the fragment of interest were removed by cutting away the upper part of the gel. A slit was then cut into the gel perpendicular to the direction of fragment migration, immediately in front of the fragment(s) of interest. A piece of 3 MM Whatman® paper (Rose Scientific) backed by a piece of dialysis tubing was pre-wet in 1 x TAE and placed in the slit with the Whatman® facing the direction of the DNA to be isolated. The samples were then electrophoresed for 15 minutes at 150 volts to allow the fragments to enter the barrier. The barrier combination was then carefully removed and placed in a catch-tube combination. This combination consisted of a decapitated 0.5 ml microfuge tube, punctured through the bottom, which was then placed inside a decapitated 1.5 ml microfuge tube. A 101 μl volume of BEB was pipetted over the surface of the Whatman® paper and tubes were centrifuged at 354 g for 10 seconds. The liquid which collected in the decapitated 1.5 ml tube was transferred to a fresh 1.5 ml tube. The BEB was added and collected twice more and combined with the previous collected sample. The tube containing the Whatman® paper and dialysis tubing was centrifuged at 15000 g for 30 seconds and the final volume of liquid was collected. The combined eluates were extracted with one volume of phenol/chloroform, ethanol precipitated and resuspended in 20 μl 1 x TE.

2.12 Ligation

2.12.1 Polyethylene Glycol (PEG) Purification of DNA

Large molecular weight DNA was isolated from digested RNA or small DNA oligomers by the addition of 0.6 volumes of a PEG/NaCl solution (20% PEG 8000 w/v, 2.5 M NaCl) to the DNA samples. The sample was mixed briefly and placed in an ice-

water bath for one hour then collected by centrifugation at 15000 *g* for 10 minutes (4°C). The ethanol was removed and the pellet was washed with 70% EtOH, dried and resuspended in 50 μl of 1 x TE unless otherwise stated.

2.12.2 Dephosphorylation of Linearized Plasmid DNA

Linearized plasmid DNA which was purified by PEG precipitation was treated with CIP to remove 5' phosphate groups. Dephosphorylation buffer was added to 1 x final volume along with 2 units of CIP (Boehringer Manheim) and samples were incubated at 37°C. For DNA with 5' overhang ends, the reaction was carried out for 30 minutes while DNA with flush ends and 3' overhang ends were incubated for up to one hour. Samples were then brought up to at least 100 μl with 1 x TE and extracted with one volume of phenol/chloroform and ethanol precipitated. The DNA pellet was collected as before, washed with 70% EtOH and resuspended in 50 μl.

2.12.3 Ligation Reactions

To estimate the concentration of the vector and insert DNA to be used in a ligation reaction, samples were electrophoresed side-by-side on an agarose gel and compared for intensity and size. These approximations were used to estimate the volume of each DNA sample needed to obtain the target ratio of insert:vector DNA for ligation purposes.

2.12.3.1 Sticky-End Ligations

Ligations involving DNA fragments with compatible 5' or 3' overhangs were set up to achieve an approximate 3:1 ratio of insert:vector DNA molecules. The appropriate amounts of vector and insert DNA were mixed in a 0.5 ml microfuge tube with 2 μl of 10 x T4 DNA ligase buffer and brought up to 20 μl with ddH_2O. T4 DNA ligase (0.625 Weiss units) (Boehringer Manheim) was mixed gently into the reaction which was then incubated at 12°C overnight. The ligations were then ethanol precipitated and resuspended in 20 μl of 1 x TE.

2.12.3.2 Blunt-End Ligations

For reactions involving DNA fragments with incompatible 5' overhangs, the ends were treated with Klenow polymerase and dNTPs. Vector and insert DNA were mixed in a 0.5 ml microfuge to achieve an approximate ratio of 5:1 insert:vector molecules. To this was added 2 μl of 10 x blunt-end ligation buffer, 1 μl dNTP solution, 1 μl Klenow (5 units) and the reaction was brought to 19 μl with ddH_2O. The reaction was incubated at room temperature for 30 minutes after which 0.5 μl of ATP (50 mM), 0.5 μl DTT (250 mM) and 1 μl (5 Weiss units) of T4 DNA ligase were added and the reaction was incubated at 12°C overnight. The ligations were ethanol precipitated, washed with 70% EtOH and brought to a final volume of 20 μl with 1 x TE.

2.13 Isolation of DNA From Yeast

DNA was isolated from yeast by a modification of the method of Hoffman and Winston (1987). Yeast cultures from 2 ml YPAD or SC dropout liquid medium were transferred to a 1.5 ml tube and pelleted by centrifugation at 15000 *g* for 30 seconds. The liquid was removed by aspiration and the cells were gently resuspended in 200 μl of yeast lysis buffer. To this was added approximately 300 mg of acid washed glass beads (Sigma - 425-600 microns) and 200 μl of phenol/chloroform. Samples were mixed by vortex three times for 30 seconds while being maintained on ice for at least 30 seconds between successive mixings. Tubes were centrifuged for 2 minutes at 15000 *g* to separate the aqueous and organic layers and the aqueous layer was removed to a new 1.5 ml centrifuge tube and ethanol precipitated. After collecting the DNA by centrifugation, the pellet was washed with 70% EtOH and dissolved in 50 μl of 1 x TE.

2.14 Sequencing of Plasmid DNA

All DNA sequencing was carried out by the dideoxy chain termination method (Sanger *et al.*, 1977) using the T7 Sequenase™ version 2.0 DNA sequencing kit (Amersham). [^{35}S]-dATP labeled nucleotides (NEN® Life Science Products) were used for radioactively labeling fragments. Plasmid DNA samples (~10 μg in 50 μl) were treated with 2 μl of RNAseA (1 mg/ml) for 30 minutes at 37°C, purified by PEG precipitation and resuspended in 20 μl of 1 x TE. For some experiments the DNA sample was brought up to a 100 μl volume after PEG precipitation using 1 x TE and extracted with phenol/chloroform before ethanol precipitation. A 2 μl volume of 10 N NaOH was dispensed into a 0.5 ml centrifuge tube and 18 μl of the plasmid DNA was mixed with the NaOH. The samples were denatured for five minutes at room temperature then precipitated by the addition of 8

μl of 5 M NH_4Ac and 100 μl absolute ethanol. The DNA samples were placed at -20°C for at least one hour then pelleted by centrifugation at 15000 *g* for 5 minutes (4°C). The supernatant was removed and the pellets were allowed to dry at room temperature. The DNA pellet was resuspended in 7 μl ddH_2O, mixed with 6 ng of primer, 2 μl of Sequenase Reaction Buffer and then heated to 65°C for five minutes. The samples were allowed to cool to 37°C. A 2.5 μl volume of each dideoxy nucleotide was separately dispensed into 0.5 ml centrifuge tubes and kept on ice while the (5 x) Labeling Mix was diluted to 1 x using ddH_2O and maintained on ice. Sequenase enzyme was diluted using the supplied Enzyme Diluent Buffer immediately before use and kept on ice. Once the DNA/primer solution had cooled to 37°C, the tubes were centrifuged for 2 seconds and 1 μl DTT (0.1 M), 2 μl of the diluted Labeling Mix and 0.5 μl of ^{35}S-dNTP (~6.25 μCi) was added to the samples. The tubes were equilibrated in a 37°C waterbath and 2 μl of diluted Sequenase enzyme was added to the samples to initiate the labeling reaction. After 2.5 minutes, 3.5 μl samples were withdrawn from the labeling reaction and added to each of the four dideoxy nucleotide samples in 15 second intervals to initiate the termination reactions. Termination reactions were allowed to incubate at 37°C for five minutes after which time 4 μl of the Stop Solution was added in 15 second intervals as before. The tubes were chilled on ice then maintained at -20°C.

2.15 Separation of Sequencing Reaction Products

Sequencing reaction products were electrophoresed on a 6% denaturing polyacrylamide gel (1:19 bis:acrylamide, 7 M urea, 90 mM Tris-borate, 1 mM EDTA) in 1 x TBE buffer. Reaction samples were heated to 85°C for 5 minutes, centrifuged for 2 seconds and briefly cooled on ice. Samples of 2.5 μl of each of the sequencing reactions

were electrophoresed at 60 watts for 1-2 hours as necessary maintaining a temperature of approximately 50°C. The gel was then transferred to 3 mm Whatman® paper and covered with plastic wrap then dried on a slab gel drier model SGD4050 (Savant) at 70°C for 1-2 hours. The plastic wrap was removed and a sheet of Kodak X-Omat™ AR film was placed over the dried gel in a film cassette and incubated at -80°C.

2.16 Developing Autoradiograph Films

All autoradiograph films were developed manually. Films were placed in developer solution for up to 5 minutes then transferred to stop solution for 2 minutes. The films were then transferred to fix solution for 2 minutes. The developed films were thoroughly washed with cold water and air dried at room temperature.

2.17 High Efficiency Yeast Transformation

Yeast transformation was carried out using a LiAc/PEG/ssDNA protocal similar to the method of Agatep *et al.* (1998). Briefly, an overnight liquid culture of yeast was used to inoculate 50 ml of YPAD or SC-dropout medium to a final concentration of 5×10^6 cells/ml in a 250 ml Erlenmeyer flask. This culture was grown at 30°C with agitation until the culture had reached a concentration of 2×10^7 cells/ml. The culture was then harvested by centrifugation at 3000 *g* for 5 minutes (room temperature) in 50 ml centrifuge tubes using an IEC Centra® MP4 (International Equipment Company) desktop centrifuge. The cells were washed once with 25 ml ddH_2O then resuspended in 1 ml of 100 mM LiAc and transferred to a 1.5 ml centrifuge tube. The cells were harvested by centrifugation for 30 seconds at 15000 *g* (room temperature) and resuspended in 100 mM LiAc to give a final

concentration of 2 x 10^9 cells/ml. Samples containing 1 x 10^8 cells (50 μl) were dispensed into new 1.5 ml centrifuge tubes for each transformation reaction and pelleted by centrifugation for 30 seconds at 15000 *g* (room temperature). To the cell pellet was added 240 μl of 50% (w/v) PEG 3350, 36 μl of 1 M LiAc, 25 μl of boiled single-stranded carrier DNA (from salmon sperm, 2 mg/ml) and DNA samples of 0.1-5 μg. The final volume was brought up to 360 μl with dH_2O and thoroughly mixed by vortex. The cells were incubated at 30°C for 30 minutes then subjected to a 20 minute heat shock at 42°C. The cells were harvested by centrifugation for 15 seconds at 8000 *g* (room temperature), the transformation mix was removed and the cells were resuspended in 1 ml of ddH_20. Samples up to 200 μl were plated on the appropriate media and incubated for 2-5 days at 30°C.

2.18 Assaying for β-galactosidase Activity

2.18.1 Yeast Colony Filter-Lift Assay

The β-galactosidase activity of yeast colonies was assayed according to the method of Breeden and Nasmyth (1985). Actively growing colonies were transferred to 70 mm diameter Whatman® #1 filter discs by placing the filter on the yeast colonies using sterile tongs or forceps. The filter was slowly removed and frozen in liquid nitrogen then thawed at room temperature. This cycle was repeated three times. Aliquots of 1.25 ml of Z buffer supplemented with β-ME (39 mM) and X-gal (420 μg/ml) were dispensed into petri plate dishes and a second filter paper was placed on the pool of liquid. The thawed filter paper was placed colony side up on the saturated filter paper and covered with the petri plate lid.

The plates were then incubated at 37°C in plastic bags to prevent desiccation and blue color development was monitored for up to 24 hours. The time required for strong blue colour development was noted.

2.18.2 Liquid Culture ONPG Assay

Individual colonies from SC-dropout plates were inoculated into 3 ml of SC-Trp-Leu liquid media in 13 ml polypropylene tubes and incubated overnight at 30°C with agitation. For each interaction to be tested, three colonies from each plate were used to inoculate separate overnight cultures. The cell concentration of each overnight culture was determined by reading the absorbence at OD_{600} of a 1:1 dilution. At the same time, 1.5 ml of overnight culture was transferred to 1.5 ml centrifuge tubes and harvested by centrifugation for 30 seconds at 15000 *g*. The cells were resuspended in 1 ml of Z buffer and harvested again. The cells were then resuspended in 200 μl of Z buffer and split into two 100 μl samples in 1.5 ml centrifuge tubes. The tubes were flash frozen in liquid nitrogen then thawed by immersion in a 42°C waterbath. The freeze-thaw cycle was repeated three times after which 700 μl of Z buffer containing β-ME (39 mM), 50 μl chloroform and 50 μl 0.1% SDS was added to the lysed cells and mixed by vortex for 30 seconds. A 100 μl volume of ONPG solution was added and the reactions were placed at 37°C for a maximum of 4 hours or until significant yellow color developed, whichever was less. Reactions were terminated by the addition of 400 μl of 1 M Na_2CO_3. The cultures were centrifuged for 10 minutes at 15000 *g* to clear the solution of debris, 1 ml samples were withdrawn to 1.5 ml polystyrene cuvettes (BioRad) and the absorbance A_{420} of the solution was determined.

2.19 Southern Blotting

2.19.1 Digestion, Separation and Transfer of DNA

Samples of 25 μl (~4 μg) of genomic DNA isolated by the glass bead method were digested with 10-40 units of enzyme in a final volume of 250 μl. Reaction components were scaled-down from the 500 μl reaction used for preparation of DNA for cloning purposes. The reaction proceeded for 16-20 hours then was concentrated by ethanol precipitation, washed with 70% EtOH and resuspended in 25 μl of TE. Loading dye was added to a final concentration of 10% and the DNA samples were loaded on a 10 cm x 14 cm 0.75% (w/v) agarose gel. Samples were electrophoresed for 400-450 volt-hours as necessary to achieve the desired separation of DNA fragments. The gel was stained for 30 minutes in 1 x TAE buffer containing 0.5 μg/ml EtBr then photographed under UV illumination as described above. The DNA was then transferred to Zetaprobe® membrane (BioRad) by alkaline transfer (Reed and Mann, 1985) for 1-2 hours with 0.4 N NaOH using the TurboBlotter™ apparatus (Schleicher and Schuell) assembled according to supplier's instructions. The membrane was neutralized by washing in 2 x SSC with agitation for five minutes then air dried.

2.19.2 Random Primed Klenow Labeling of DNA

The DNA fragment to be used as a probe was isolated from the plasmid by restriction enzyme digestion and band purification. The quantity of isolated fragment was estimated by comparison to the 1.6 kb fragment of the 1 kb ladder (Gibco BRL). The purified fragment was concentrated to yield approximately 100 ng of DNA in 5 μl of 1 x

TE. This was then mixed with 3 μl of pd$(N)_6$ random hexamer primers (3 μg) and the volume brought up to 14 μl with ddH_2O. This mixture was boiled for 3-5 minutes to denature the DNA then rapidly cooled on ice. The tubes were centrifuged briefly then 2.5 μl of dNTP mix, 2.5 μl of 10 x Klenow buffer, 5 μl (50 μCi) [α-^{32}P]-dCTP or [α-^{32}P]-dATP (3000 Ci/mmol, 10 mCi/ml) (NEN® Life Science Products) and 1 μl of Klenow (5 units) were added and allowed to incubate at room temperature for two hours. The reaction was stopped by the addition of 1 μl of EDTA (0.5 M, pH 8.0) and the labeled DNA was purified by passing through a Sephadex® G-50 DNA Grade Nick™ Column that was equilibrated with buffer (1 x SSC, 0.1% SDS) according to the manufacturer's directions. The specific activity of the purified probe was determined by measuring the counts per minute (cpm) of 1 μl of the labeled probe eluate in 1 ml of EcoLume™ scintillation fluid (ICN) using a Beckman scintillation counter (Model LS1800).

2.19.3 Membrane Hybridization

The Zetaprobe® membranes with the transferred DNA were prewet in 2 x SSC and placed in a glass tube. A 5 ml volume of Westneat hybridization buffer containing 500 μg of boiled single stranded salmon testis carrier DNA was added to the glass tubes and the membranes were incubated for a minimum of 30 minutes at 65°C in a Robbins Scientific hybridization oven. Approximately 1 x 10^7 cpm of labeled probe was boiled for 10 minutes then added to the pooled Westneat solution, avoiding the membrane surface until the probe was sufficiently mixed in the Westneat solution. The membranes were hybridized with the labeled probe overnight for a minimum of 16 hours. The labeled probe solution was discarded and the membranes were rinsed three times in the glass tubes using 30 ml of 2 x SSC. The membranes were then transferred to a glass dish and washed with

increasingly stringent conditions. The membranes were first washed in 2 x SSC at room temperature followed by solutions of 2 x SSC with 0.5% SDS at 50°C, 1 x SSC with 0.5% SDS at 65°C, and 0.1 x SSC with 0.5% SDS at 65°C until a localized reading of approximately 200 cpm was noted using a Model PUG 1AB Geiger counter (Technical Associates). If necessary, a final wash step was carried out using a solution of 0.1 x SSC, 0.1% SDS at 65°C. Each wash was carried out for up to 20 minutes in a 250 ml volume of buffer using a shaking waterbath set to the necessary temperature. The membranes were blotted dry with a paper towel to absorb any excess liquid then wrapped in plastic wrap and placed in a film cassette. A piece of Kodak X-Omat™ AR film was placed over the membrane and exposed for various times at -80°C then developed as above.

2.20 Determination of Sensitivity to UV Damage

The dose response of a yeast strain to UV light was determined by noting the survival levels after irradiation at 254 nm. A single yeast colony was inoculated into 5 ml of liquid YPAD media in a 20 ml capped glass culture tube and grown overnight at 30°C with agitation. The titre of the overnight culture was determined using a haemocytometer. Duplicate samples were plated on YPAD medium and exposed to increasing doses of UV light at a rate of 2 $J/m^2/sec$. After irradiation the plates were wrapped in a double layer of tinfoil and incubated for 2-3 days at 30°C. The number of colonies on each plate was counted and compared to unirradiated controls.

2.21 *in vitro* Transcription and Translation

Production of recombinant proteins in vitro was achieved using the TNT™ SP6 Coupled Reticulocyte Lysate System (Promega). Plasmid DNA samples (~10 μg) were prepared by treatment with RNAseA for 30 minutes at 37°C and purified by PEG precipitation. Samples were then extracted with phenol/chloroform and resuspended in 50 μl of 1 x TE. Rabbit reticulocyte lysate was allocated to 0.5 ml centrifuge tubes in 12.5 μl volumes. For each coupled transcription and translation reaction, 1.0 μl TNT™ Reaction Buffer, 0.5 μl Amino Acid Mixture Minus Methionine (1mM), 0.5 μl RNasin® Ribonuclease Inhibitor (40 U/μl), 2.0 μl translation grade L-[^{35}-S]-methionine (1000 Ci/mmol) (NEN® Life Science Products) at 10 mCi/ml and approximately 0.5 μg DNA template were added to the reticulocyte lysate. Sterile ddH_2O was added to bring the volume up to 24.5 μl and 0.5 μl of SP6 Polymerase was added to initiate transcription. The reaction was incubated at 30°C for 2 hours then transferred to 1.5 ml conical screw cap centrifuge tubes with O-rings (VWR). Proteins were concentrated by the addition of 25 μl of 4 M NH_4SO_4, placed on ice for 20 minutes, then pelleted by centrifugation at 15000 *g* for 10 minutes (4°C). The supernatant was discarded and the pellet was washed with 50 μl of ice cold 2 M NH_4SO_4 supplemented with 2 mM DTT (final concentration). As much supernatant was removed as possible and 100 μl of prechilled Buffer B was added to resuspend the proteins.

The level of incorporated label was assayed by spotting 2.5 μl of the protein solution onto 1 cm^2 pieces of 3 mm Whatman® filter and air dried for 5-10 minutes. The filters were then placed in 50 ml of 5% (w/v) TCA in a 250 ml Erlenmeyer flask which was then placed in a boiling water bath for 10 minutes. The TCA solution was discarded, 50 ml of fresh 5% (w/v) TCA was added, and the tubes were allowed to stand at room temperature for 10 minutes. The TCA solution was replaced by 50 ml of 95% EtOH and

incubated at room temperature for 2 minutes. The EtOH was discarded and the filters were allowed to air dry completely then placed in 1 ml of EcoLume™ scintillation fluid (ICN). Incorporated radioactivity was measured using a Beckman scintillation counter (Model LS1800). Protein samples were mixed 1:1 with SDS sample buffer for analysis by SDS-PAGE. All samples were stored at -80°C.

2.22 Immunoprecipitation

Protein samples were mixed with 1 μl of 12CA5 (BAbCo) antibody raw ascites fluid giving a 1:100 dilution. The tubes were placed on a Thermolyne Speci-Mix rocker pad (Sybron) and incubated with rocking overnight at 4°C. A 25 μl volume of a 50% slurry of proteinA-Sepharose beads in PBS was added to the tubes and mixed briefly by flicking the tube. Tubes were replaced on the rocker pad and further incubated at 4°C for 2 hours. The beads were pelleted by centrifugation at 350 *g* for 30 seconds and the supernatant was removed. The beads were resuspended in 0.5 ml of ice cold BufferB then pelleted again by centrifugation at 350 *g* for 30 seconds. The supernatant was removed and the wash step was repeated a third time. After the third wash, as much supernatant was removed as possible, 25 μl of SDS sample buffer was added and the beads were mixed thoroughly.

2.23 Denaturing Polyacrylamide Gel Electrophoresis (SDS-PAGE)

Proteins were analyzed by SDS-PAGE using the BioRad Mini-Protean® II Cell electrophoresis unit. Samples were mixed with SDS sample buffer as stated and placed in a boiling water bath for 3 minutes before loading on an SDS-PAGE gel consisting of a

upper stacking gel (4.4% 1:29 bis:acrylamide, 12.5 mM Tris-HCl, 0.1% SDS) and a lower separating gel (10% 1:29 bis:acrylamide, 37.5 mM Tris-HCl, 0.1% SDS). Proteins were electrophoresed in 1 x SDS running buffer at 33 mA for approximately 30 minutes until the bromophenol blue had migrated to the bottom of the gel. The gels were then submersed in 20 volumes of 10% acetic acid for 1 hour then washed twice with agitation for 15 minutes in 20 volumes of ddH_2O at room temperature. Gels were placed in 20 volumes of 1.0 M sodium salicylate (Chamberlain, 1979) for 30 minutes then transferred to a piece of 3 mm Whatman® paper and dried on a slab gel drier at 60°C for 1-2 hours. A sheet of Kodak X-Omat™ Blue XB-1 film was placed over the dried gel in a film cassette and stored at -80°C for 1-5 days. The film was developed as described in section 2.16.

3. RESULTS

3.1 The Rad23p Interacting Proteins

The two-hybrid screen identified three previously uncharacterized Rad23p interacting proteins. These proteins correspond to the open reading frames designated YDR174w, YER047c and YHL010c. During this study, the BLAST algorithm (Altschul *et al.*, 1990, NCBI http://www.ncbi.nlm.nih.gov/BLAST/) revealed homologies of these proteins to distinct classes of proteins (see Appendix) but also revealed that each protein was reported in the literature. Lu *et al.* (1996) reported that YDR174w is a member of the high mobility group (HMG) class of proteins and was designated *HMO1* (see Table 5 and Appendix). The YER047c ORF was found to share homology to ATPase proteins such as those found in the 26S proteosome (see Table 5 and Appendix). This gene has recently been identified by Liberzon *et al.* (1996) and designated *SAP1* (*SIN1* associated protein), highlighting it's observed interaction with the chromatin protein *SIN1*. YHL010c has been partially characterized by Li *et al.* (1998) and shares significant homology to *BRAP2* and will be designated *BYH1* (*BRAP2* yeast homologue). *BRAP2* is a cytosolic human protein found to bind to the nuclear localization signals of *BRCA1* (see Table 5) potentially mediating it's retention in the cytoplasm (Li *et al.*, 1998). The full DNA sequence of each ORF was translated into protein sequence and compared to the PROSITE database (http://expasy.hcuge.ch/sprot/scnpsit1.html) to predict any notable protein domains or motifs. This analysis identified potential leucine zipper patterns in both *HMO1* and *BYH1* as well as an ATP/GTP binding site motif and an 'AAA' protein family signature in *SAP1*

(see Appendix). Li *et al.* (1998) also identified a putative zinc finger motif in *BYH1* that was not identified by PROSITE (see Appendix).

Table 5 Characteristics of *RAD23* Interacting Positives

NAME	CHR#	SIZE bp (aa)	λ	ATCC #	BLAST	PROSITE
YDR174w *HMO1*	IV	741 (246)	PM-2133	70352	HMG proteins	Leucine zipper
YER047c *SAP1*	V	2694 (897)	PM-6793	70795	26S regulatory subunits, AAA transcription factors	ATP/GTP binding motif A, 'AAA' signature
YHL010c *BYH1*	VIII	1758 (586)	PM-4992	70328	Homology to *BRAP2*	Leucine zipper, C2H2 zinc finger†

NAME = ORF name and *Gene Name* (if known)
CHR # = yeast chromosome containing ORF
SIZE bp/aa = size of ORF in base pairs (size of predicted protein in amino acid residues)
λ = designation of lambda clone containing ORF
ATCC # = reference number from American Type Culture Collection
BLAST = homologies revealed by BLAST search
PROSITE = protein features predicted by PROSITE comparison
† = reported in Li *et al.*, 1998

3.2 Cloning of Full Length *RAD23* Positives

The library fusion plasmids, isolated from CTY10-5d, contained only portions of the coding region of each gene as a result of the library construction. To proceed with analysis of these positives, the full length ORF for each gene was isolated from lambda clones containing yeast genomic DNA (ATCC). The full DNA sequence of these lambda clone inserts was known from the yeast genome sequencing project enabling us to determine the lambda clone containing each gene and the position of the gene in each clone.

The ORF for *SAP1* was determined to be contained within the lambda clone PM-6793 (ATCC # 70795), while the ORFs of *HMO1* and *BYH1* were determined to reside within lambda clones PM-2133 (ATCC # 70352) and PM-4992 (ATCC # 70328), respectively. The lambda clones containing each insert are listed in Table 5.

3.2.1 Isolation of Bacteriophage DNA

Lambda bacteriophage particles were amplified and harvested, as in Materials and Methods, for isolation of DNA containing the genes of interest. Lysates were created by infecting lawns of *E. coli* C600 previously grown in media containing maltose to induce expression of the lambda receptor. Two of the original bacteriophage lysates (PM-2133 and PM-4992) initially yielded two plaque phenotypes on bacterial lawns; the characteristic clear phenotype and a turbid plaque appearance. Isolated plaques of both appearances maintained the original phenotype through successive platings suggesting that this was not an artifact. DNA was isolated using lysates derived from clear plaque phenotypes and the nature of the turbid plaques was not investigated any further. Infection conditions were established over a range of MOI values from MOI = 0.05, 0.2, 0.5, 1.0 and 5.0. The bacteriophage particles were purified by precipitation in PEG 8000 and their DNA extracted by digesting the bacteriophage capsid with Proteinase K as in the Materials and Methods. Samples were then analyzed by agarose gel electrophoresis to ensure that sufficient quantity of DNA had been isolated and that the DNA visualized on the gel was of the appropriate molecular weight (see Figure 4). The properties of the isolated DNA were as expected (i.e. >12 Kb), however it was unfortunate that the appropriate molecular weight markers were not used to more accurately estimate size. The DNA samples appeared to be free of any other contaminating RNA or bacterial DNA.

Figure 4 Purified Lambda DNA

Purified lambda DNA was electrophoresed beside Gibco BRL 1 kb ladder on a 0.75% agarose gel containing 0.5 μg/ml EtBr. The upper band of the 1 kb ladder is 12 kb. For explanation of MOI values see Materials and Methods.

A. DNA from lambda strain PM-6793. Lanes A and B represent DNA isolation from two different MOI values. Lanes C and D represent two MOI values from a separate lambda lysate stock. The expected size of DNA isolated from PM-6793 is ~19 kb.

B. Lanes A-D represent various MOI values for DNA isolation from the lambda strain PM-2133. Lanes E-H represent various MOI values for DNA isolation from the lambda strain PM-4992. The expected size of DNA isolated from PM-2133 is ~15 kb. The expected size of DNA isolated from PM-2133 is ~17 kb.

A

A B C D

B

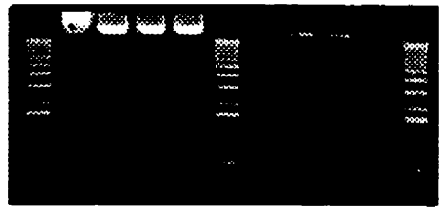

A B C D E F G H

3.2.2 Subcloning of ORFs From Bacteriophage DNA

Fragments containing each ORF were cloned into either pUC19 or pBS(KS+). The restriction enzymes used for each cloning were chosen based on the known DNA sequences available from ATCC to generate fragments containing the full ORF as well as some flanking DNA sequence. Purified DNA from lambda clone PM-6793 was digested with the enzyme *Pst*I. This enzyme was expected to cleave the insert DNA into five fragments which included a 3.2 kb fragment containing the *SAP1* ORF. This 3.2 kb fragment was isolated, ligated into *Pst*I digested pUC19, and electroporated into *E. coli* DH5α. Plasmid DNA was isolated from ampicillin resistant colonies and a plasmid containing the 3.2 kb fragment was identified by restriction enzyme digestion and designated pRK1. A restriction map of pRK1 is shown in Figure 5A. The purified DNA from lambda clone PM-2133 was digested with the enzyme *Hin*dIII and a 2.6 kb fragment containing the *HMO1* ORF was isolated and ligated into pBS(KS+) digested with *Hin*dIII. Plasmid DNA was isolated from ampicillin resistant colonies and a plasmid containing the 2.6 kb fragment was identified by restriction enzyme digestion and designated pRK7 (see Figure 5B). The purified DNA from lambda clone PM-4992 was digested with the enzyme *Cla*I. The 2.2 kb fragment containing the *BYH1* ORF was isolated and ligated into pBS(KS+) digested with *Cla*I. Plasmid DNA was isolated from ampicillin resistant colonies and a plasmid containing the 2.2 kb *Cla*I fragment was identified by restriction enzyme digestion and designated pRK9 (see Figure 5C).

Figure 5 Cloning of *SAP1*, *HMO1* and *BYH1*; Genes That Interact With *RAD23*

Restriction enzyme sites used in various cloning steps are indicated along with appropriate genes.

A. The 3.2 kb *Pst*I fragment from lambda PM-6793 containing the *SAP1* ORF was sticky-end ligated into pUC19 at the *Pst*I site to create pRK1.

B. The 2.6 kb *Hin*dIII fragment from lambda PM-2133 containing the *HMO1* ORF was sticky-end ligated into pBS(KS+) at the *Hin*dIII site to create pRK7.

C. The 2.2 kb *Cla*I fragment from lambda PM-4992 containing the *BYH1* ORF was sticky-end ligated into pBS(KS+) at the *Cla*I site to create pRK9.

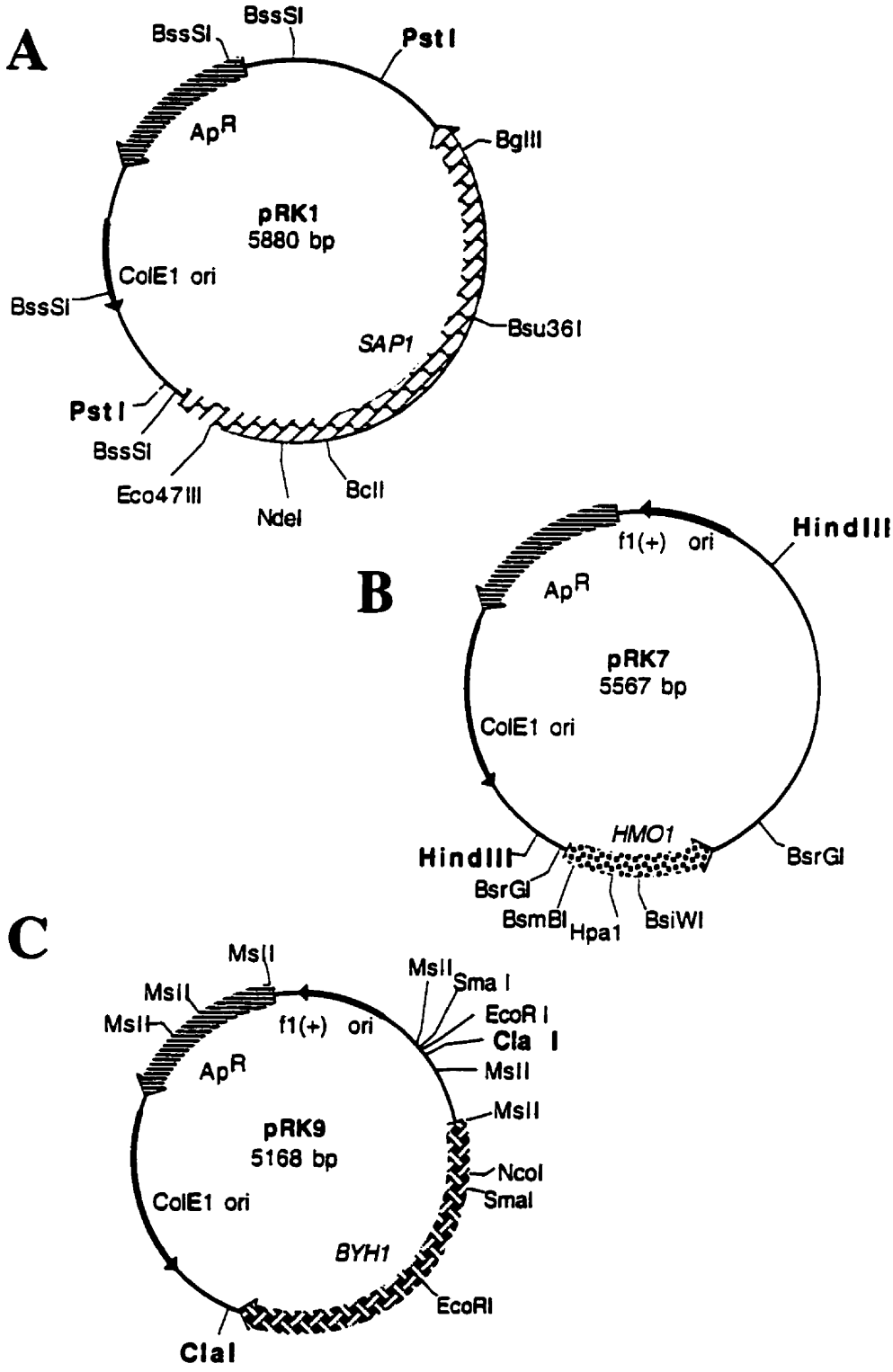
A
BssSI
BssSI
PstI
ApR
BglII
pRK1
5880 bp
ColE1 ori
BssSI
Bsu36I
SAP1
PstI
BssSI
Eco47III
NdeI
BclI
B
HindIII
f1(+) ori
ApR
pRK7
5567 bp
ColE1 ori
HMO1
HindIII
BsrGI
BsrGI
BsmBI
Hpa1
BsiWI
C
MslI
MslI
MslI
MslI
Sma I
EcoR I
f1(+) ori
Cla I
ApR
MslI
MslI
pRK9
5168 bp
NcoI
SmaI
ColE1 ori
BYH1
EcoRI
ClaI

3.2.3 Intermediate Cloning of ORFs

The construction of $GAL4_{AD}$ fusion genes required that in-frame stop codons preceding the first ATG of each ORF be excluded. Both *SAP1* and *BYH1* required an additional cloning step to produce a plasmid that could serve as a convenient source for fragments suitable for cloning into $GAL4_{AD}$ vectors. To accomplish this for the *SAP1* ORF, pRK1 was digested with *Bss*SI, which cleaves 43 bp upstream of the ATG and excludes any in frame stop codons. This enzyme also cleaved within the vector near the 3' end of the *Pst*I fragment, thus including a portion of the pUC19 MCS (see Figure 5A). This *Bss*SI fragment was blunt-end ligated into the *Sma*I site of pUC18 to create pRK16 (see Figure 6A). DNA sequencing revealed that the 5' 19 bp of the ORF had been deleted during cloning, likely the result of exonuclease contamination. The plasmid containing the *BYH1* ORF, pRK9, was digested with *Msl*I and *Cla*I to yield a 1.8 kb fragment containing no in frame stop codons 5' to the ATG. This fragment was blunt-end ligated into the *Hin*dIII site of pBS(KS+) to yield pRK24 (see Figure 6B).

3.2.4 *GAL4* Activating Domain Fusions

Each of the three ORFs was cloned into a two-hybrid system vector to create a gene fusion with the *GAL4* activating domain. The plasmid pRK16 (pUC18-*SAP1*) was digested with *Eco*RI to release the 3.2 kb *SAP1* fragment which was purified and ligated into the *Eco*RI site of pGAD424 to yield pRK26 (see Figure 7A). The *HMO1* ORF was released from pRK7 by digestion with *Bsr*GI which generates a fragment containing the entire *HMO1* ORF and no in-frame stop codons. This fragment was blunt-end ligated into the *Xma*I site of pGAD424 to produce pRK34 (see Figure 7B). The *BYH1* ORF was

Figure 6 Intermediate Cloning of *SAP1* and *BYH1* ORFs

A. A *Bss*SI fragment containing the *SAP1* ORF was isolated from pRK1 and blunt-end ligated into the *Sma*I site of pUC18 to create pRK16. This cloning allowed the *SAP1* ORF to be removed as an *Eco*RI fragment effectively eliminating in-frame stop codons preceding the initiator start codon. During isolation of the *Bss*SI fragment, a contaminating exonuclease had digested the ends of the DNA resulting in the loss of the first 6 codons.

B. An *Msl*I-*Cla*I fragment containing the *BYH1* ORF was isolated from pRK9 and blunt-end ligated into the *Hin*dIII site of pBS(KS+) to create pRK24. This cloning allowed the *BYH1* ORF to be removed as an *Eco*RV-*Cla*I fragment effectively eliminating in-frame stop codons preceding the initiator start codon.

A

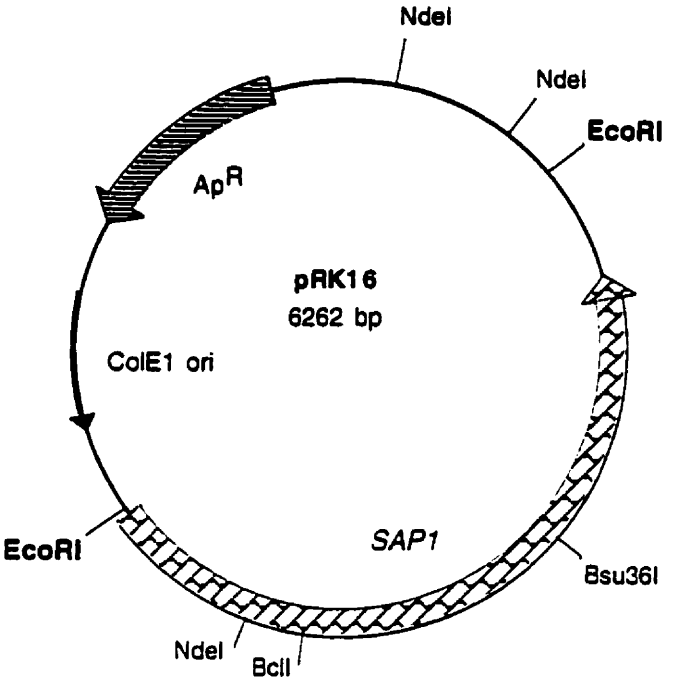
NdeI
NdeI
EcoRI
Ap^R
pRK16
6262 bp
ColE1 ori
EcoRI
SAP1
Bsu36I
NdeI
BclI

B

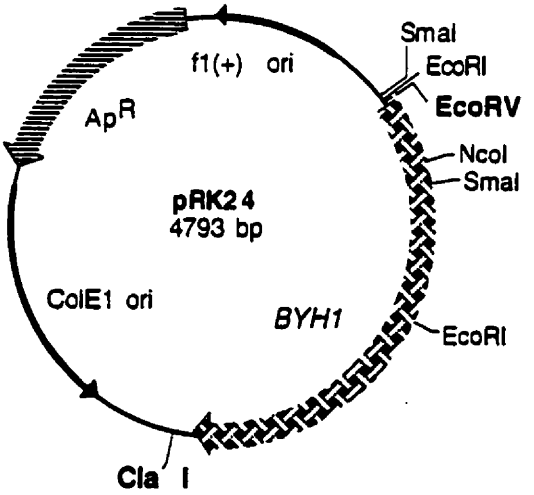
f1(+) ori
SmaI
EcoRI
EcoRV
Ap^R
NcoI
SmaI
pRK24
4793 bp
ColE1 ori
BYH1
EcoRI
Cla I

Figure 7 GAL4 Activating Domain Fusions for *SAP1*, *HMO1* and *BYH1*

A. The *Eco*RI fragment from pRK16 containing the *SAP1* ORF was sticky-end ligated into the *Eco*RI site of pGAD424 to create pRK26. This plasmid resulted in the fusion of amino acid residues 7-398 of Sap1p to the C-terminus of the GAL4 activating domain (amino acids 768-881).

B. The *Bsr*GI fragment from pRK7 containing the *HMO1* ORF was blunt-end ligated into the *Xma*I site of pGAD424 to create pRK34. This plasmid resulted in the fusion of amino acid residues 1-247 of Hmo1p to the C-terminus of the GAL4 activating domain.

C. The *Eco*RV-*Cla*I fragment from pRK24 containing the *BYH1* ORF was blunt-end ligated into the *Eco*RI site of pGAD424 to create pRK36. This plasmid resulted in the fusion of amino acid residues 1-586 of Byh1p to the C-terminus of the GAL4 activating domain.

Restriction sites used in deletion mapping are shown in bold. Note that for the *SAP1* deletion analysis, the 3' restriction site used in combination with the internal restriction sites is actually 2 *Sma*I sites. For each deletion, it was determined that the most 3' *Sma*I site, shown with an asterisk, was cleaved.

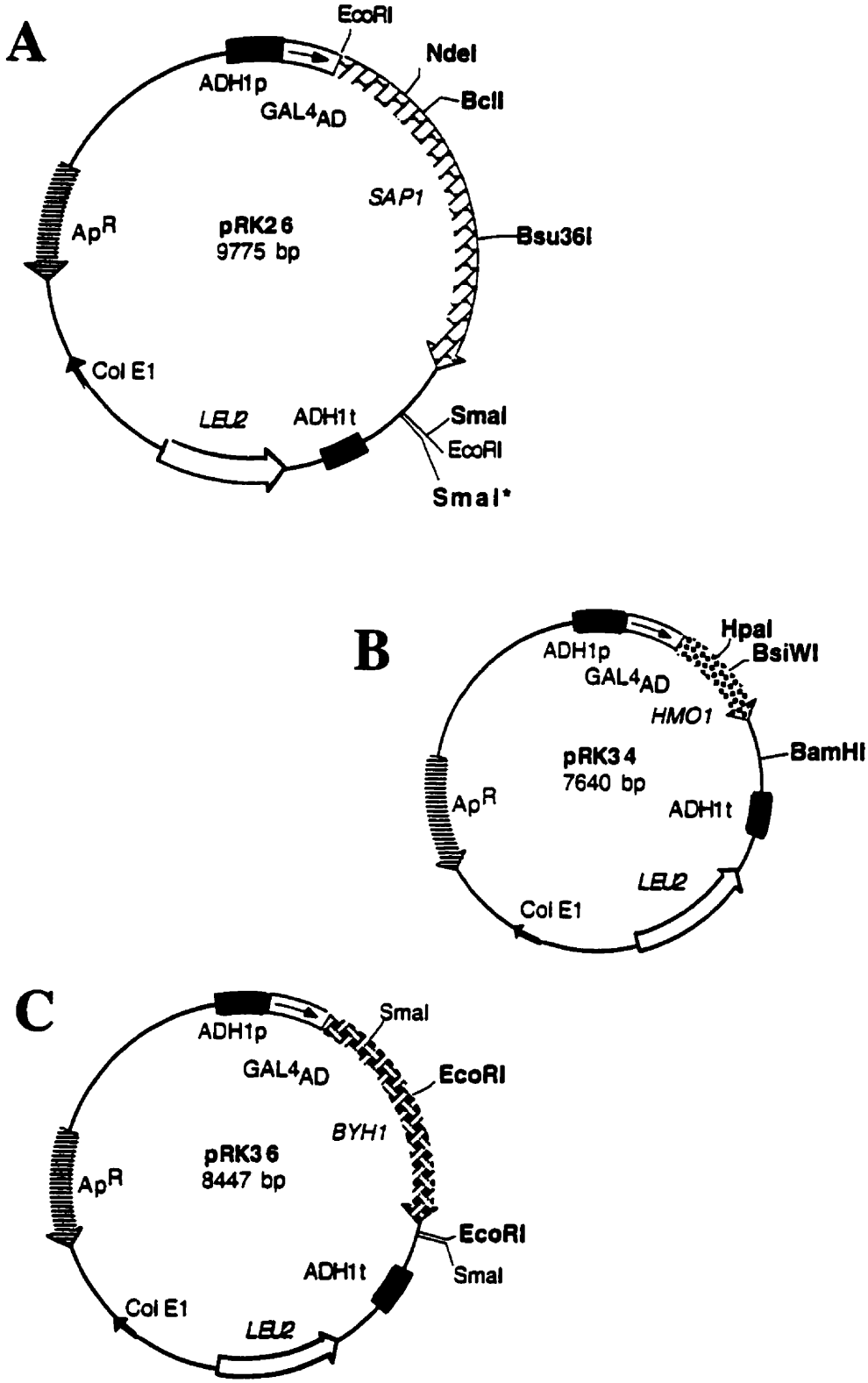
A
EcoRI
NdeI
BclI
ADH1p
GAL4AD
SAP1
Bsu36I
ApR
pRK26
9775 bp
Col E1
LEU2
ADH1t
SmaI
EcoRI
SmaI*
B
HpaI
BsiWI
ADH1p
GAL4AD
HMO1
BamHI
pRK34
7640 bp
ApR
ADH1t
LEU2
Col E1
C
SmaI
ADH1p
GAL4AD
EcoRI
BYH1
pRK36
8447 bp
ApR
EcoRI
ADH1t
SmaI
Col E1
LEU2

cleaved from the plasmid pRK24 by digestion with *Eco*RV and *Cla*I and ligated into the *Eco*RI site of pGAD424 to yield pRK36 (see Figure 7C). The fusion junction of each plasmid was sequenced to ensure that each ORF was fused in frame with the $GAL4_{AD}$ coding region.

3.3 Reconstruction of Two-Hybrid System Interactions

The $GAL4_{AD}$ fusion plasmids were tested for interaction with *RAD23* in the two-hybrid system. The original bait plasmid pDG840 (*lex*A-*RAD23*) was co-transformed into CTY10-5d with each of the plasmids pRK26 ($GAL4_{AD}$-*SAP1*), pRK34 ($GAL4_{AD}$-*HMO1*) and pRK36 ($GAL4_{AD}$-*BYH1*) and transformants were tested for activation of the *lacZ* reporter gene using the filter lift assay. Each plasmid was shown to produce strong *lacZ* activity in combination with pDG840, confirming that the full-length fusion proteins do activate the *GAL1*-*lacZ* reporter gene in combination with the lexA-Rad23p bait protein (see Table 6). The plasmid combination pDG649 (pBTM116-*RAD7*) and pJR3 (pACTII-*SIR3*) was used as a positive control as these constructs were previously shown to activate the *lacZ* reporter gene in this assay (Paetkau *et al.*, 1994).

Table 6 *lacZ* Activity Induced by Fusion Constructs in CTY10-5d

Binding Domain Fusion	Activating Domain Fusion	Relative *lacZ* Activity *
pDG649 (*lex*A-Rad7p)	pJR3 ($Gal4_{AD}$-Sir3p)	+++++
pDG840 (*lex*A-Rad23p)	pRK34 ($Gal4_{AD}$-Hmo1p)	++++
pDG840 (*lex*A-Rad23p)	pRK26 ($Gal4_{AD}$-Sap1p)	+++
pDG840 (*lex*A-Rad23p)	pRK36 ($Gal4_{AD}$-Byh1p)	+++
pRK88 (*lex*A-Hmo1p)	pRK34 ($Gal4_{AD}$-Hmo1p)	++
pRK88 (*lex*A-Hmo1p)	pRK36 ($Gal4_{AD}$-Byh1p)	-

* The relative *lacZ* activity is assigned a value on a scale of:

'-'	= white after overnight incubation
'+'	= pale blue after overnight incubation
'++'	= blue color development under 8 hours
'+++'	= blue color development under 4 hours
'++++'	= blue color development under 2 hours
'+++++'	= blue color development under 1 hour

3.4 Mapping of Interaction Domains

The regions of each ORF containing the domains responsible for the interaction with Rad23p in the two-hybrid system were mapped by deletion analysis. Nested deletions from the 3' end of each of the fusion ORFs were constructed and tested in the two-hybrid system with the Rad23p bait plasmid (pDG840). The lack of a positive result in the two-hybrid system was taken to indicate destruction or deletion of the interacting motif. Alternatively, this could suggest destabilization of the protein resulting in its degradation, and, therefore, its absence.

The internal restriction sites *Bsu*36I, *Bcl*I and *Nde*I of *SAP1* were used in conjunction with 3' external *Sma*I sites to delete the defined regions of the *SAP1* ORF in pRK26 (see Figure 8). After digestion with the appropriate enzymes, the large fragment

was isolated and then blunt-end ligated on itself to form the deletion plasmids. Removal of the *Bsu*36I-*Sma*I region resulted in the deletion of the C-terminal 328 aa of Sap1p and created pRK38. Removal of the *Bcl*I-*Sma*I and the *Nde*I-*Sma*I regions resulted in the deletion of the C-terminal 653 and 724 aa, respectively. These deletions created pRK54 and pRK44 respectively.

Each deletion plasmid was co-transformed into CTY10-5d with pDG840 and tested for *lacZ* activity. The deletion constructs of pRK38 and pRK54 continued to activate *lacZ* activity with pDG840 (*lex*A-*RAD23*) while pRK44 did not. These results suggest that the region between the *Nde*I and *Bcl*I sites of the *SAP1* ORF is necessary for the interaction of Sap1p and Rad23p in the two-hybrid system. As indicated by the decrease in interaction strength of pRK38 and pRK54 compared to pRK26, the C-terminal portion of Sap1p also appears to be important, but not necessary, for interaction between Sap1p and Rad23p.

The deletion plasmids for the *HMO1* ORF were constructed using an external *Bam*HI site at the 3' end of the ORF in combination with the unique *Bsi*WI and *Hpa*I sites in pRK34 to create pRK46 and pRK48 respectively (see Figure 9). While the *Bsi*WI-*Bam*HI deletion plasmid continued to show good activation of the *lacZ* reporter in combination with pDG840 (*lex*A-*RAD23*), the *Hpa*I-*Bam*HI deletion plasmid showed only a weak interaction. This suggests that the region between the *Bsi*WI and *Hpa*I sites of the *HMO1* ORF is important for interaction of Hmo1p with Rad23p.

Deletion analysis of the *BYH1* ORF was performed using plasmid pRK36 and digesting with *Eco*RI to remove a 1.0 kb C-terminal fragment of the gene (see Figure 10). This plasmid, pRK50, which contained a C-terminal deletion of 313 aa, failed to show an interaction with the *lex*A-*RAD23* plasmid.

Figure 8 Deletion Mapping Analysis of Sap1p Interacting Domain

The domain of Sap1p which is responsible for interaction with Rad23p was determined by nested deletions of the *SAP1* ORF. The intact portion of the *SAP1* coding region for each construct is shown with numbers to indicate the base pair location of each restriction enzyme site used. The hatched box represents the location of the ATP/GTP binding site motif (see Appendix). A *Sma*I site 3' to the *SAP1* ORF was used in conjunction with the restriction sites shown here to create the deletions. Approximate interaction strength of each construct with Rad23p is shown under *lac*Z activity. The *SAP1* ORF contains 2694 bp.

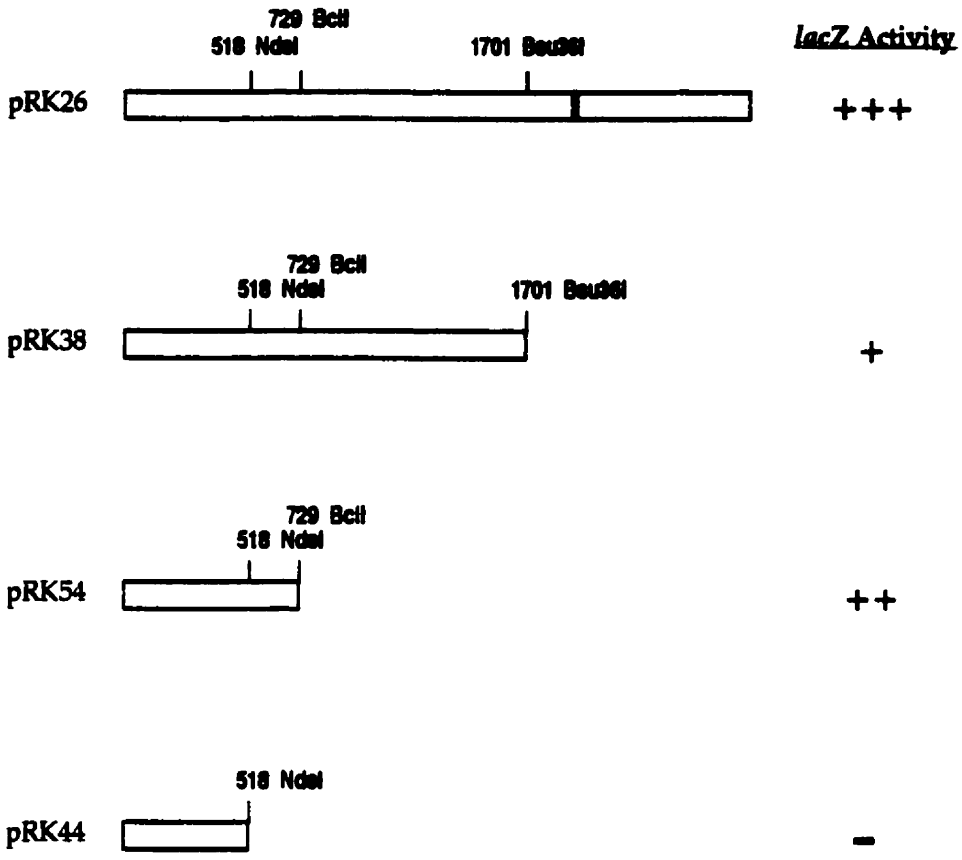
5'
3'
729 BclI
518 NdeI
1701 Bsu36I
lacZ Activity
pRK26
+++
729 BclI
518 NdeI
1701 Bsu36I
pRK38
+
729 BclI
518 NdeI
pRK54
++
518 NdeI
pRK44
-

Figure 9 Deletion Mapping Analysis of Hmo1p Interacting Domain

The domain of Hmo1p which is responsible for interaction with Rad23p was determined by nested deletions of the *HMO1* ORF. The intact portion of the *HMO1* coding region for each construct is shown with numbers to indicate the base pair location of each restriction enzyme site used. The filled box represents the location of the leucine zipper motif (see Appendix). A *Bam*HI site 3' to the *HMO1* ORF was used in conjunction with the restriction sites shown here to create the deletions. Approximate interaction strength of each construct with Rad23p is shown under *lacZ* activity. The *HMO1* ORF contains 741 bp.

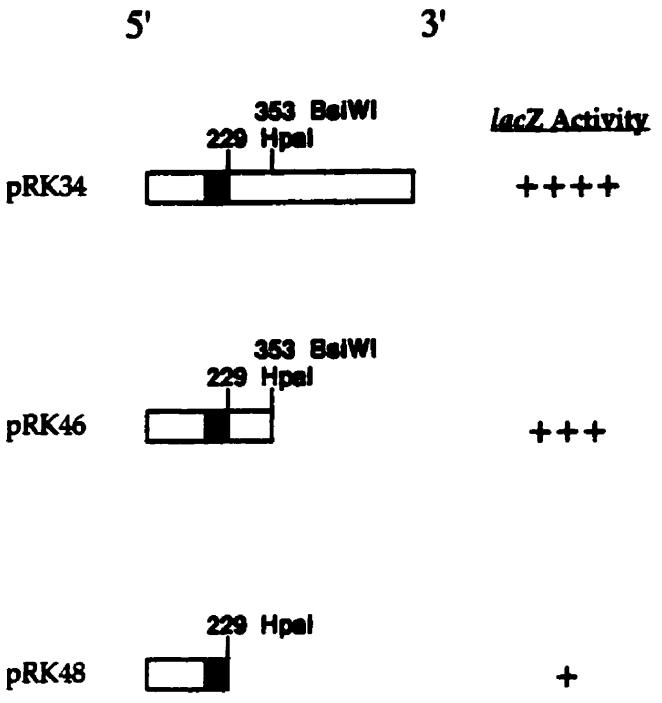
5'
3'
353 BsiWI
229 HpaI
lacZ Activity
pRK34
++++
353 BsiWI
229 HpaI
pRK46
+++
229 HpaI
pRK48
+

Figure 10 Deletion Mapping Analysis of Byh1p Interacting Domain

The domain of Byh1p which is responsible for interaction with Rad23p was determined by nested deletions of the *BYH1* ORF. The intact portion of the *BYH1* coding region for each construct is shown with numbers to indicate the base pair location of each restriction enzyme site used. The filled box represents the location of the leucine zipper motif while the grey box represents the C2H2 zinc finger domain (see Appendix). An *Eco*RI site 3' to the *BYH1* ORF was used in conjunction with the *Eco*RI site shown here to create the deletion. Approximate interaction strength of each construct with Rad23p is shown under *lac*Z activity. The *BYH1* ORF contains 1758 bp.

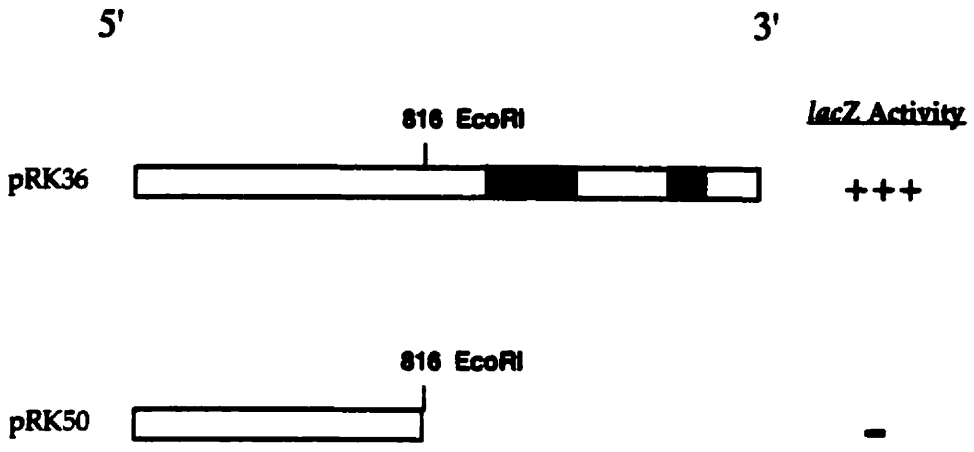
5'
3'
816 EcoRI
lacZ Activity
pRK36
+++
816 EcoRI
pRK50
-

3.4.1 Quantitation of the Rad23p-Sap1p Interaction

The interaction between Sap1p and Rad23p was monitored by liquid ONPG assay to quantitate the strength of the interaction. The *RAD23* bait plasmid pDG840 was transformed into CTY10-5d in combination with the $GAL4_{AD}$-*SAP1* plasmid (pRK26) or the *SAP1* deletion plasmids and assayed as in the Materials and Methods. The column titled "Empty Plasmids" in Figure 11 refers to the units of β-galactosidase activity produced by the plasmids pBTM116 and pGAD424 lacking inserts. This value represents the background level of activity seen in this assay. The plasmid containing the full length Sap1p (pRK26) produced approximately 5 units of β-galactosidase activity in combination with the *RAD23* bait plasmid (pDG840) as shown in Figure 11 "Sap1 (7-897)". The nested deletions produced a similar pattern of interaction with Rad23p as seen during the mapping of interacting domains.

3.4.2 Evidence for Possible *HMO1* Dimerization

The putative leucine zipper pattern found in the Hmo1 protein suggested that it might be able to homodimerize. To test this the *HMO1* ORF was cloned into the plasmid pBTM116 to produce a fusion with the *lex*A protein and yield pRK88. This plasmid was transformed into CTY10-5d with pRK34 ($GAL4_{AD}$-*HMO1*) and tested for β-galactosidase activity by filter lift. This plasmid combination produced good blue color development

Figure 11 Quantitation of the Rad23p-Sap1p Interaction

Plasmid constructs coding for full length or truncated Sap1p were transformed into CTY10-5d with the *lex*A-*RAD23* fusion plasmid pDG840 and tested for *lacZ* activity by liquid culture ONPG assay. The combination of plasmids pGAD424 and pBTM116, lacking inserts, were assayed as negative controls ("Empty Plasmids"). Each plasmid combination was assayed from three separate cultures and each bar represents an average of two assays of the same culture (see Section 2.18.2). Values are expressed in Miller units (Miller, 1972). The Rad7p and Sir3p combination (Paetkau *et al.*, 1994) was used as a positive control yielding 73.6, 78.5, and 121.5 Miller Units. For simplicity, these values are not shown on the graph.

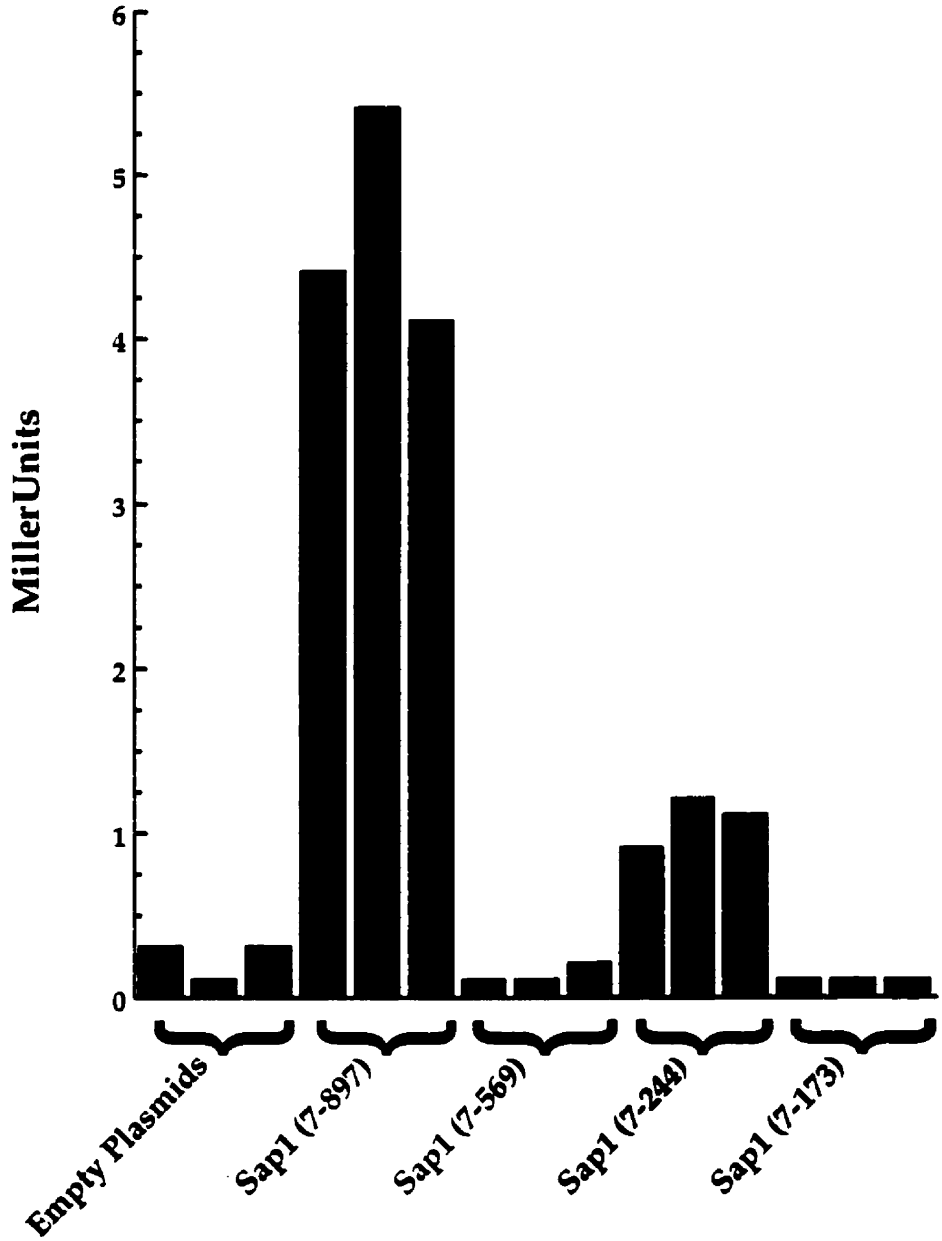
Miller Units
6
5
4
3
2
1
0
Empty Plasmids
Sap1 (7-897)
Sap1 (7-569)
Sap1 (7-244)
Sap1 (7-173)

after approximately 5 hours suggesting that Hmo1p does homodimerize in the two-hybrid system (see Table 6). The *lex*A-*HMO1* plasmid did not activate the reporter gene in the absence of a $Gal4_{AD}$ plasmid. The *BYH1* protein also contains a putative leucine zipper pattern suggesting it might heterodimerize with Hmo1p. The plasmid pRK36 (*GAL4*$_{AD}$-*BYH1*) was tested for β-galactosidase activity in combination with pRK88 (*lex*A-*HMO1*), however these constructs did not activate the *lacZ* reporter gene (see Table 6).

3.5 Construction of Mutant Strains

3.5.1 Construction of Deletion/Disruption Plasmids

Disruption alleles for each of the Rad23p interacting proteins were constructed in order to determine if these gene products were involved in DNA repair. Null alleles of each positive were created by insertion of a nutritional marker (*LEU2* or *URA3*) into the coding region to disrupt the ORF and allow selection of yeast containing disrupted genes. The plasmid pRK1 (pUC19-*SAP1*) was digested with *Bgl*II and *Eco*47III to remove a 2.4 kb region of the *SAP1* ORF (see Figure 5A). The remainder of the plasmid was purified and blunt-end ligated to a 1.6 kb *Bam*HI/*Eco*RI fragment containing the *LEU2* gene isolated from pDG317 (Gietz and Sugino, 1988). The resulting deletion/disruption plasmid was designated pRK15 (see Figure 12A). The *HMO1* gene was disrupted by digesting the plasmid pRK7 (see Figure 5B) with *Bsm*BI. The 1.6 kb *Bam*HI/*Eco*RI fragment containing the *LEU2* gene was blunt-end ligated into this site to form pRK41 (see Figure 12B). The *BYH1* gene was disrupted by *Nco*I digestion of plasmid pRK9 (see Figure 5C) and blunt-end ligation to a 1.2 kb *Hin*dIII *URA3* gene fragment from pRDG98. The resulting disruption plasmid was designated pRK43 (see Figure 12C).

Figure 12 Construction of Null Alleles of *SAP1*, *HMO1* and *BYH1*

Nutritional markers were inserted into the coding region of each ORF to disrupt translation. Solid bars indicate position of putative leucine zipper patterns. The gray box represents the putative C2H2 zinc finger domain of Byh1p.

A. The plasmid pRK1 was digested with *Eco*47III and *Bgl*II to delete a 2.4 kb region of the *SAP1* ORF (see Fig. 5A) and replaced with the 1.6 kb *Eco*RI/*Bam*HI fragment of *LEU2* (Gietz and Sugino, 1988) to create pRK15. Note that the ATP/GTP binding site motif of Sap1p was deleted in the creation of the null allele and is thus not shown. The 2.5 kb *Pst*I fragment from pRK15 is shown here.

B. The 1.6 kb *Eco*RI/*Bam*HI fragment of *LEU2* (Gietz and Sugino, 1988) was inserted into the *Bsm*BI site of the *HMO1* ORF (see Fig. 5B) to disrupt the ORF. The 4.2 kb *Hin*dIII fragment from pRK41 is shown here. The *Hin*dIII fragments were additionally digested with *Bsr*GI before transformation to cleave DNA suspected of harboring an ARS sequence (see Section 3.5.2).

C. The 1.2 kb *Hin*dIII fragment of *URA3* was blunt-end ligated into the *Nco*I site of the *BYH1* ORF (see Fig. 5C) to disrupt the ORF. The 3.4 kb *Cla*I fragment from pRK43 is shown here.

A

sap1Δ::LEU2 **from pRK15** **(2.5 kb)**

B

hmo1Δ::LEU2 **from pRK41** **(4.2 kb)**

C

byh1Δ::URA3 **from pRK43** **(3.4 kb)**

3.5.2 Allele-Replacement by Homologous Recombination

The disruption alleles were used to replace the genomic copies of each gene and create mutant strains. The plasmids pRK15 (*sap1*Δ), pRK41 (*hmo1*Δ) and pRK43 (*byh1*Δ) were digested to completion with *Pst*I, *Hin*dIII and *Cla*I, respectively. This treatment releases the plasmid backbone from the yeast genes and allows efficient replacement of the genomic allele by homologous recombination (Rothstein, 1983). Each digested plasmid sample was transformed into MKP° and the diploid strain RSY185 by the high efficiency method described in the materials and methods. Recombinant yeast colonies were selected by growth on SC-Leu media (*hmo1*Δ and *sap1*Δ) or SC-Ura media (*byh1*Δ). Slow growing colonies were seen in both the *hmo1*Δ*::LEU2* and *sap1*Δ*::LEU2* transformations, suggesting that these genes may be involved in important cellular processes. No such growth defects were seen in the *byh1*Δ*::URA3* transformants.

The *Hin*dIII *hmo1*Δ*::LEU2* allele was suspected to carry an autonomously replicating sequence (ARS) due to the high number of Leu$^+$ transformants resulting from transformation with this fragment. The plasmid was additionally digested with *Bsr*GI before transformation to remove any unnecessary DNA which might contain ARS sequences, while still retaining a significant amount of homology for recombination. The resulting *Hin*dII-*Bsr*GI fragment of the *hmo1*Δ*::LEU2* allele yielded much lower numbers of Leu$^+$ transformants consistent with this type of transformation.

3.5.3 Confirmation of Genotype by Southern Blot Analysis

Southern blot analysis was used to confirm the replacement of genomic alleles with the null allele constructs. Genomic DNA from Leu$^+$ or Ura$^+$ colonies was extracted as

described in the Materials and Methods. This DNA was digested with either *Pst*I (*SAP1*), *Hin*dIII (*HMO1*) or *Cla*I (*BYH1*), electrophoresed and transferred to Zetaprobe® membrane as described in the Materials and Methods. The *PstI* fragment of *SAP1* from pRK1, *Hin*dIII fragment of *HMO1* from pRK7 and *Cla*I fragment of *BYH1* from pRK9 were labeled with ^{32}P-dATP using the random primed Klenow labeling method and used to probe the appropriate membranes as described in the Materials and Methods. A characteristic autoradiograph for the construction of *sap1*Δ strains is shown in Figure 13. In both haploid and diploid strains, the disruption of the *SAP1* gene is indicated by the presence of a 2.5 kb band (Lanes A-D, E, and F). Note that in Lanes A-D, the wild type band (3.2 kb) is present due to the diploid nature of RSY185. It is apparent that in these diploid strains one copy of the *SAP1* ORF has undergone allele replacement while one copy remained intact. Lanes G-J represent colonies which have not undergone allele replacement yet are Leu$^+$. The nature of these colonies was not investigated. Colonies corresponding to Lanes E and F (corresponding to *sap1*Δ) presented the slow-growth phenotype, all others grew at normal rates. The strains containing gene disruptions were retained for further analysis (see Table 7).

Table 7 Mutant Yeast Strains

Mutant Strain	Designation	Mutant Strain	Designation
MKP° *sap1*Δ	RKY2	RSY185 *sap1*Δ	RKY3
MKP° *hmo1*Δ	RKY16	RSY185 *hmo1*Δ	RKY11
MKP° *byh*Δ	RKY5	RSY185 *byh*Δ	RKY7

Figure 13 Confirmation of the *sap1*Δ Genotype by Southern Blot Analysis

Autoradiographs from a Southern blot shows *Pst*I digested genomic DNA probed with the 3.2 kb *Pst*I allele of *SAP1* from pRK1 (see Fig. 5A). Lanes containing DNA from wild type strains are indicated by RSY185 and MKP°. Allele replacement is indicated by loss of the 3.2 kb band (in haploid only) and appearance of the 2.5 kb band. Lanes A-D indicate allele replacement of one copy of *SAP1* in the diploid strain RSY185 thus displaying both the 3.2 kb band and the 2.5 kb band. Lanes E and F show allele replacement in MKP° while lanes G-J represent DNA from Leu$^+$ transformants which did not undergo allele replacement. The probe used for this blot routinely hybridized to the 1.6 kb band of the 1 kb ladder and was used as a reference point.

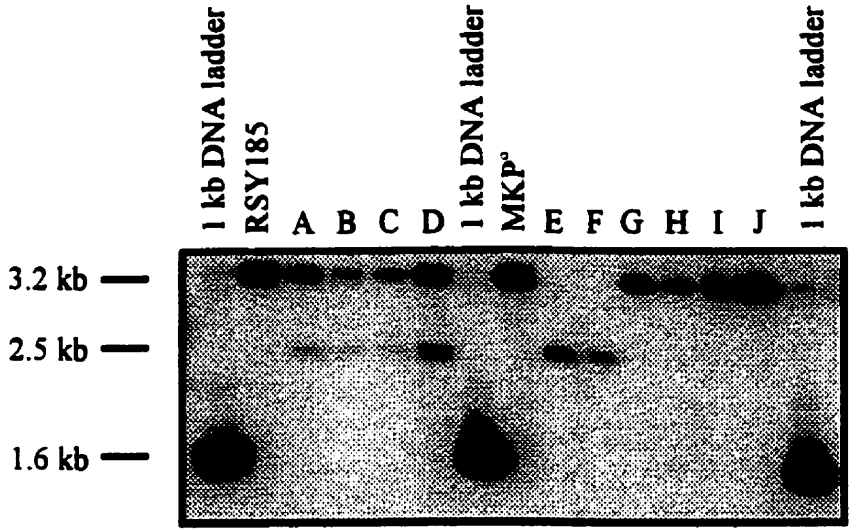
1 kb DNA ladder
RSY185
A
B
C
D
1 kb DNA ladder
MKP°
E
F
G
H
I
J
1 kb DNA ladder
3.2 kb
2.5 kb
1.6 kb

3.5.4 Phenotypic Analysis of Deletion/Disruption Mutants

The MKP° *hmo1*Δ and MKP° *sap1*Δ colonies showing a slow growth phenotype were analyzed to more accurately document the growth defect. Observations of growth on solid medium showed that the growth defect seen in MKP° *hmo1*Δ appears to hinder initial growth such that the mutant colonies do not reach the growth potential of wild-type colonies for at least 5 days, but thrive thereafter. On solid media, MKP° *sap1*Δ also displays a growth defect, however these colonies never obtain the size of wild type colonies. The growth rate of the mutant strains (*sap1*Δ and *hmo1*Δ) was monitored in liquid culture (see Figure 14) for approximately 7-9 hours after innoculation to 1-5 x 10^6 cells/ml. While the *sap1*Δ strain appears to enter into log phase at approximately the same time as wild type (MKP°), it does not show as rapid an increase in cell concentration as wild type. The *hmo1*Δ strain appears to only be starting into log phase after 9 hours while the wild type MKP° in the same experiment entered log phase after only 4.5 hours. From this data and the observations of the growth defect on solid media, it appears that the nature of the two growth defects is quite different. In addition to the growth defect, MKP° *sap1*Δ colonies had an altered colony texture and color. The colonies appear to have a white appearance and "gooey" texture when collected on a toothpick. The knockout strains of *BYH1* did not exhibit any noticeable phenotypic growth defects.

3.5.4.1 Analysis of Sensitivity to UV Light

Proteins that interact with Rad23p might play a role in DNA repair. The sensitivity of each disruption mutant strain to UV light was analyzed. Each strain to be tested was

Figure 14 Growth Rate Analysis of *hmo1*Δ and *sap1*Δ

The *hmo1*Δ mutant strain (RKY16) was inoculated into YPAD media at a starting concentration of approximately 1 x 10^6 cells/ml. The *sap1*Δ mutant strain (RKY2) was inoculated into YPAD media at a starting concentration of approximately 5 x 10^6 cells/ml. Cell concentration was measured every 45 minutes. The isogenic wild-type strain MKP° was used as a control and inoculated to the same starting concentration as each mutant strain. Growth was carried out at 30°C with aeration.

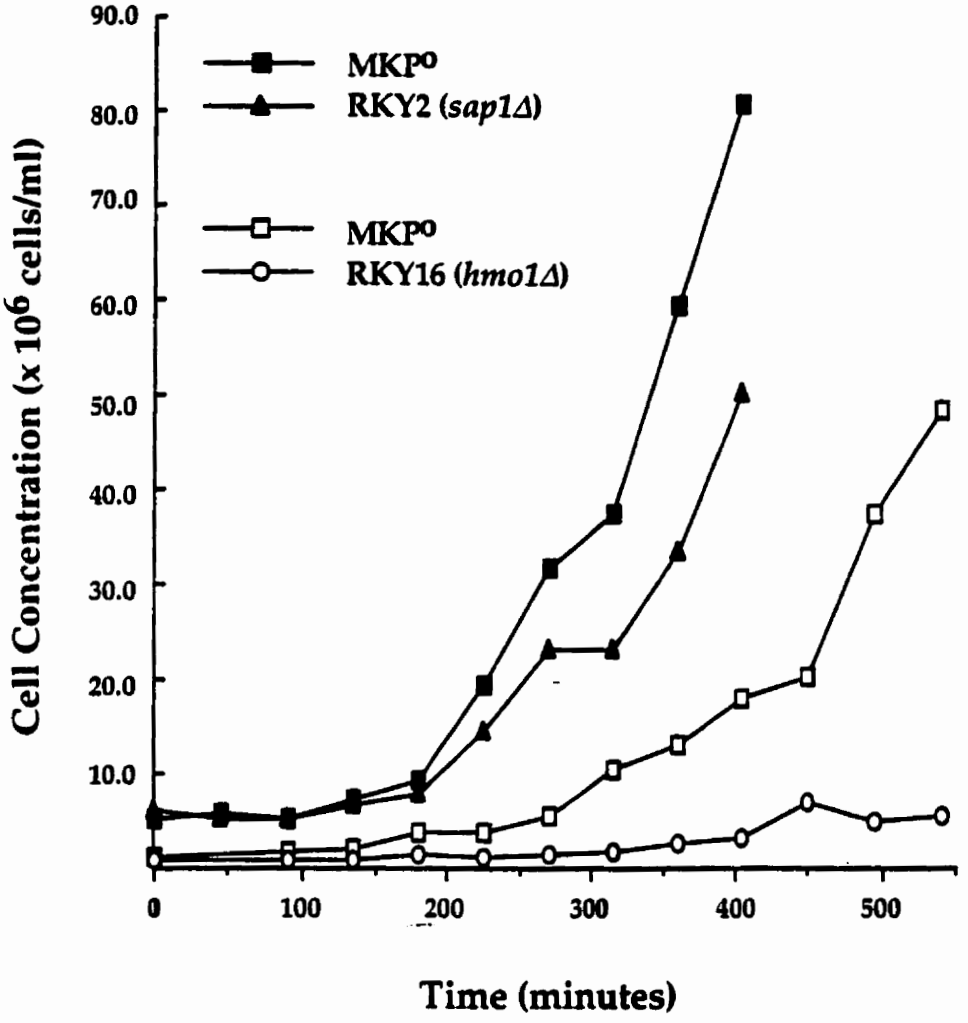
90.0
80.0
70.0
60.0
50.0
40.0
30.0
20.0
10.0
0
100
200
300
400
500
MKP⁰
RKY2 (sap1Δ)
MKP⁰
RKY16 (hmo1Δ)
Cell Concentration (x 10⁶ cells/ml)
Time (minutes)

plated on YPAD media and irradiated at 2 $J/m^2/s$ to achieve the desired dose. The plates were then incubated in darkness to prevent the activation of the photoreactivation repair pathway which may mask repair affects due to NER. Percent survivors were counted after 3 or 4 days and plotted. Figure 15 shows the survival curves for this analysis. These results show that both *sap1*Δ and *byh1*Δ strains have survival curves similar to the MKP° parent strain. Interestingly, the *hmo1*Δ strain appears to exhibit a slight increase in UV survival when compared to MKP° parental strain, however none of the disruption mutants were as UV sensitive as the *rad23*Δ mutant.

3.5.4.2 Phenotypic Analysis of *sap1*Δ

3.5.4.2.1 Analysis of Temperature Sensitivity

The MKP° *sap1*Δ strain was tested for any gross temperature sensitivity at elevated or lowered temperatures from optimal (30°C). Cultures were streaked out on YPAD and incubated at 37°C and 16°C for 2-3 days. In each case, the mutant strain did not appear to behave differently from the controls at higher or lower temperatures.

3.5.4.2.2 Galactose-Utilization Phenotype of *sap1*Δ

During the analysis of the *sap1* mutant, it was found that this strain was unable to grow on galactose media with any vigor. When the strain was streaked from the stock culture at -80°C, directly to galactose media, the growth was hampered relative to growth on dextrose (glucose) media. If the MKP° *sap1*Δ strain was instead streaked from the stock culture at -80°C to dextrose media then transferred to galactose media, the growth was impaired almost completely.

Figure 15 UV Sensitivity Analysis of Deletion Mutants

A. The survival rate of mutant strains was measured after irradiation at various doses of UV light. Colonies were incubated in the dark in order to attribute survival to non-photoreactivation repair. Each point represents an average of duplicate irradiations from the same culture. The UV dose was delivered at a rate of 2 Joules/m^2/sec.

B. The *rad23*Δ survival data was provided by Mrs. Sharon Simon and was obtained by similar methods as described in Materials and Methods. The survival rate of *rad23*Δ is consistent with published results (Watkins *et al.*, 1993).

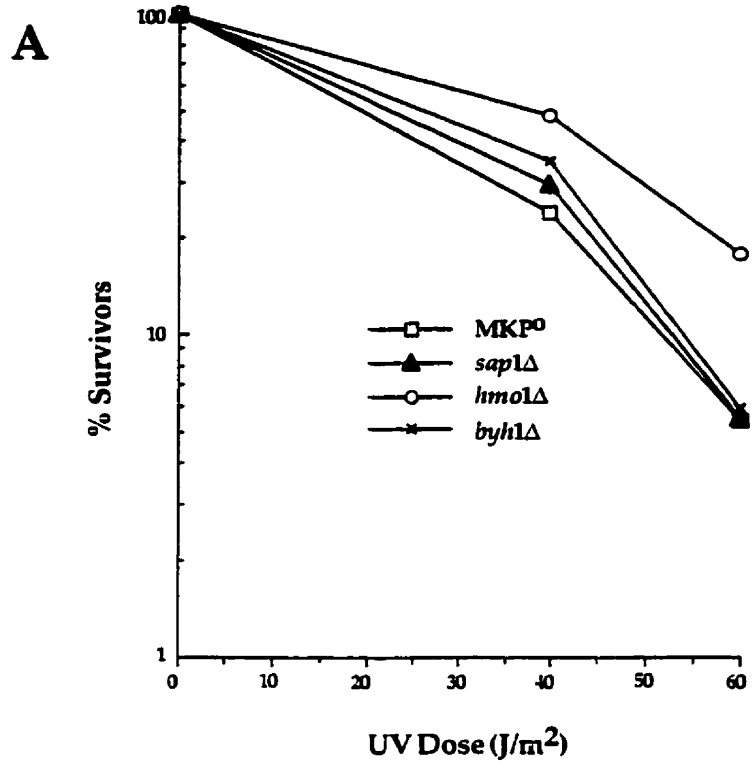
A
100
10
1
% Survivors
MKP°
sap1Δ
lmo1Δ
byh1Δ
0
10
20
30
40
50
60
UV Dose (J/m2)

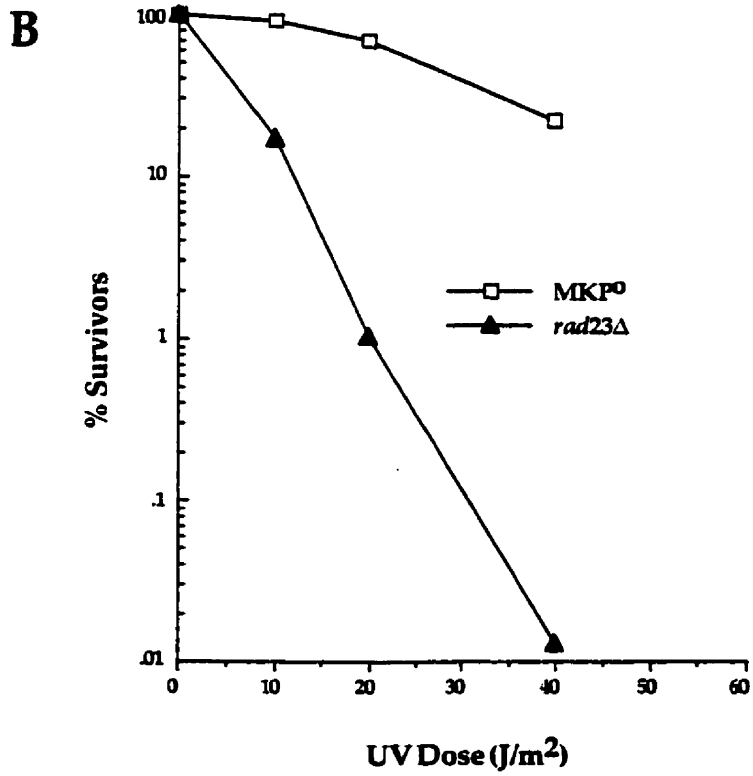
B
100
10
1
.1
.01
% Survivors
MKP°
rad23Δ
0
10
20
30
40
50
60
UV Dose (J/m2)

3.6 Analysis of *in vitro* Interactions With Rad23p

3.6.1 Construction of Plasmids

In order to verify that the result seen in the two-hybrid system was due to protein-protein interaction, the proteins for each gene were expressed in reticulocyte lysate and subjected to coimmunoprecipitation and SDS-PAGE analysis. Antibodies to the proteins were not available, so proteins were made immunoreactive by the addition of the HA-tag which is recognized by the antibody 12CA5 (BAbCo). The HA-tag was incorporated by cloning each gene into the vector pKM1310 (see Figure 16). Genes were then cloned into the expression vector pKG86 with and without the addition of the HA-tag epitope (see Figure 17). The expression vector pKG86 is based on the vector pSP64 with the addition of a Kozak sequence (Kozak, 1990) and β-globin leader sequence (Kozak, 1986) upstream of the initiator ATG, as well as additional cloning sites.

To create gene fusions with the HA-tag, the *Eco*RI/*Sal*I fragment of *RAD23* from pDG840 was blunt-end cloned into the *Sma*I site of pKM1310 to create pRK74. The *Eco*RI fragment of *SAP1* from pRK16 was blunt-end cloned into the *Sma*I site of pKM1310 to create pRK70. The *Bsr*GI fragment of *HMO1* was blunt-end cloned into the *Sma*I site of pKM1310 to create pRK84.

The plasmids to be used in the expression system were created by cloning the gene fragments into pKG86. The *Eco*RI/*Sal*I fragment of *RAD23* from pDG840 was blunt-end ligated into the *Bam*HI site of pKG86 to create pRK92. The *Bsr*GI fragment of *HMO1* from pRK7 was blunt-end ligated into the *Bam*HI site of pKG86 to create pRK81. The *Eco*RI fragment of *SAP1* from pRK16 was blunt-end ligated into the *Bam*HI site of

Figure 16 Fusion of HA-tag Coding Sequence to *HMO1* ORF

The Hmo1 protein was made immunoreactive by addition of the 9 amino acid HA-tag sequence to the N-terminus. The *Bsr*GI fragment of *HMO1* was blunt end ligated into the *Sma*I site of pKM1310 to create pRK84. Rad23p, Sap1p, and Byh1p were also cloned into pKM1310 in a similar fshion.

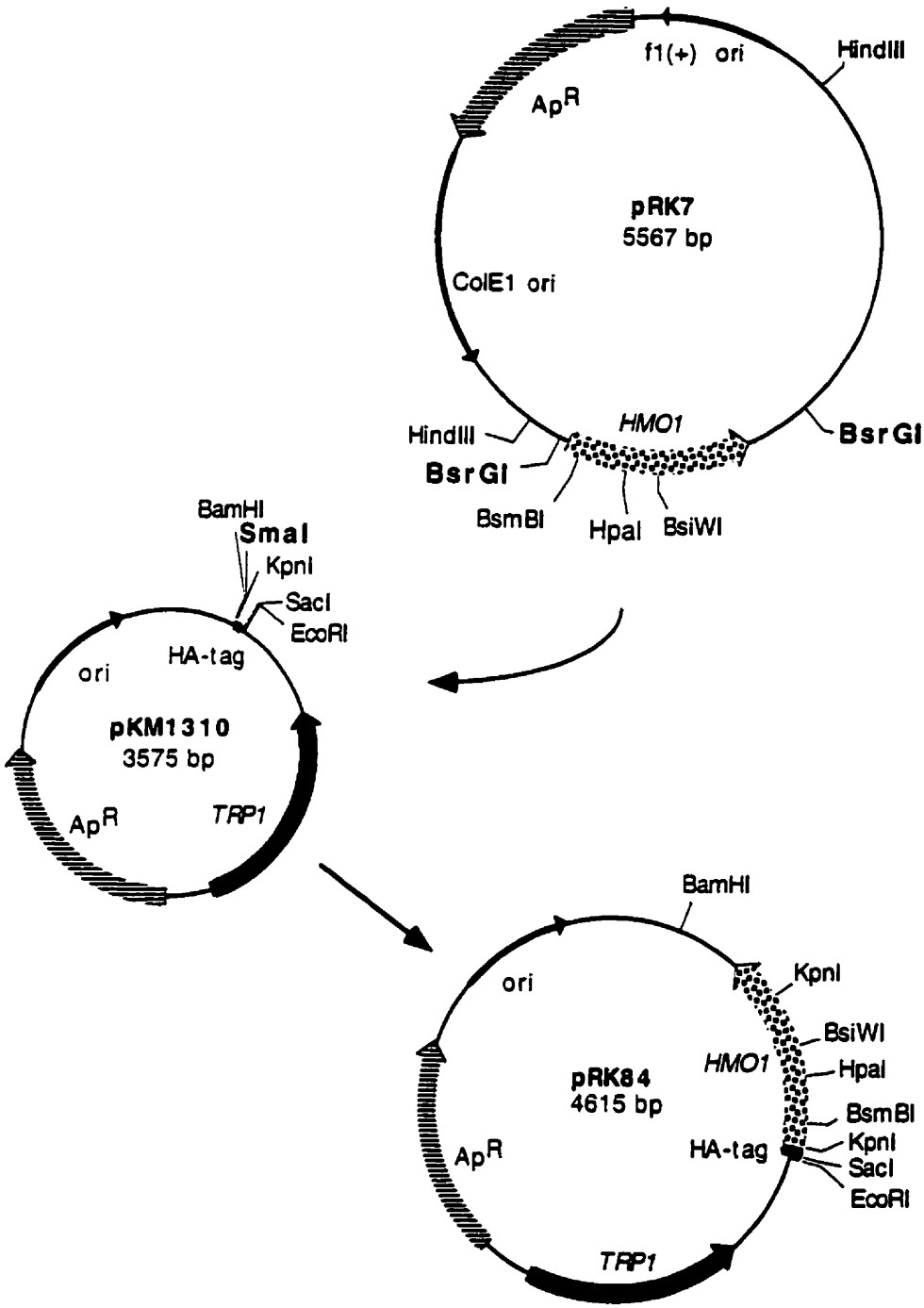
f1(+) ori
HindIII
Ap^R
pRK7
5567 bp
ColE1 ori
HMO1
HindIII
BsrGI
BsrGI
BsmBI
HpaI
BsiWI
BamHI
SmaI
KpnI
SacI
EcoRI
HA-tag
ori
pKM1310
3575 bp
Ap^R
TRP1
BamHI
ori
KpnI
BsiWI
HMO1
HpaI
pRK84
4615 bp
BsmBI
KpnI
SacI
EcoRI
HA-tag
Ap^R
TRP1

Figure 17 Construction of *HMO1 in vitro* Expression Plasmids

The HA-*HMO1* gene was cloned into the vector pKG86 for *in vitro* expression in the TNT™ system. The *Bam*HI-*Eco*RI fragment of HA-*HMO1* from pRK84 was blunt-end ligated into the *Bam*HI site of pKG86 to create pRK108 (pKG86-HA-*HMO1*). The un-tagged *HMO1* gene was cloned into pKG86 in a similar fashion as were *SAP1* and *RAD23* genes.

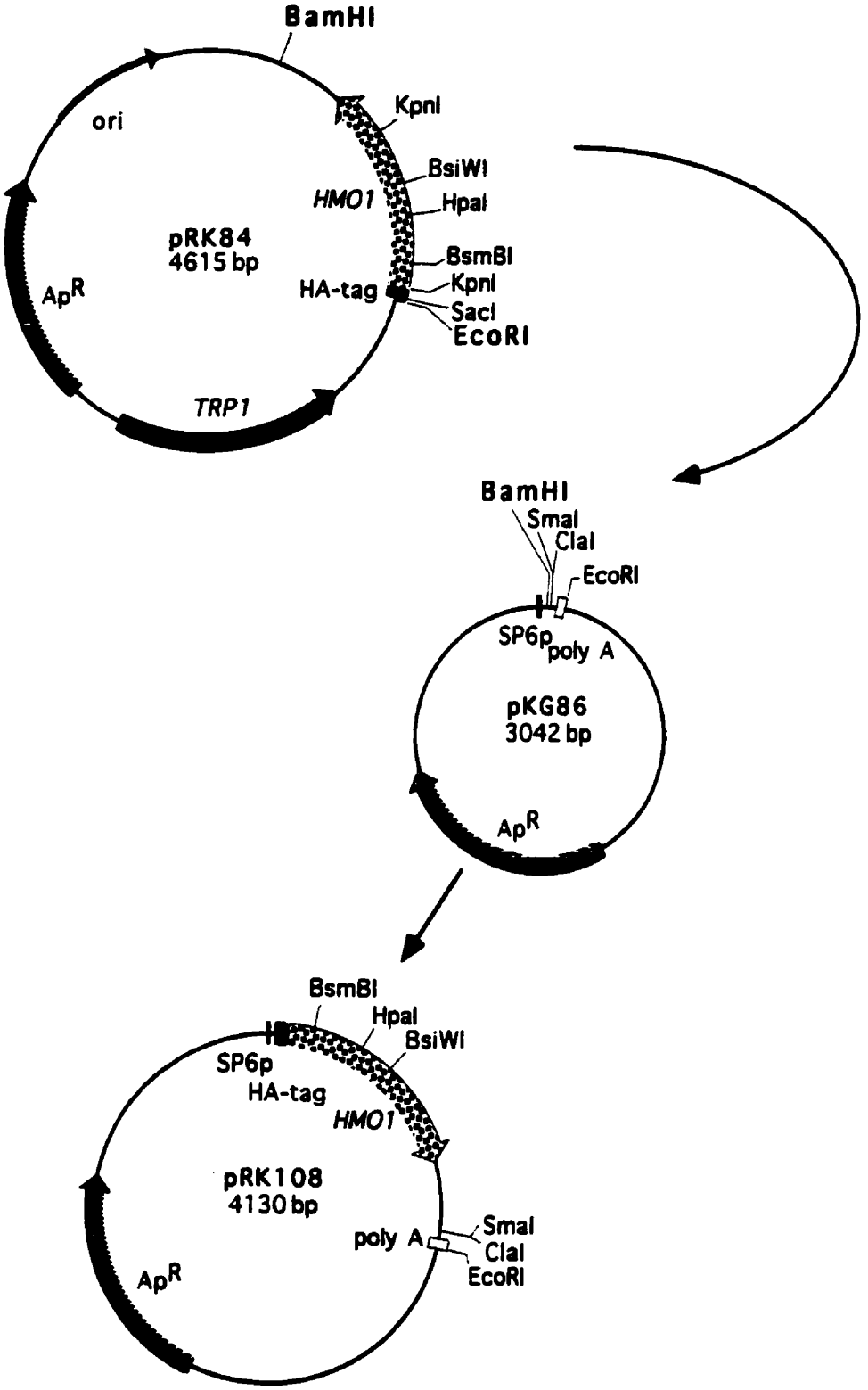
BamHI
ori
KpnI
BsiWI
HMO1
HpaI
pRK84
4615 bp
BsmBI
HA-tag
KpnI
SacI
EcoRI
ApR
TRP1
BamHI
SmaI
ClaI
EcoRI
SP6p
poly A
pKG86
3042 bp
ApR
BsmBI
HpaI
BsiWI
SP6p
HA-tag
HMO1
pRK108
4130 bp
poly A
SmaI
ClaI
EcoRI
ApR

pKG86 to create pRK95. Each of the pRK74 (HA-*RAD23*), pRK70 (HA-*SAP1*) and pRK84 (HA-*HMO1*) plasmids was digested with *Bam*HI and *Eco*RI to release the HA-tag-ORF fusion fragment which was then blunt-end cloned into the *Bam*HI site of pKG86 to create pRK104 (HA-*RAD23*), pRK99 (HA-*SAP1*) and pRK108 (HA-*HMO1*).

3.6.2 Expression of Proteins *in vitro*

The expression of Rad23p, Sap1p and Hmo1p was tested in the TNT™ system. The *SAP1* constructs did not show any significant expression in this system therefore no further analysis could be accomplished. The *RAD23* constructs gave good levels of protein expression while those expressing *HMO1* gave reproducibly low expression levels. The *BYH1* gene was not examined by *in vitro* analysis.

Plasmids coding for each protein were expressed in the TNT™ system as described in Materials and Methods. Protein extracts containing the radiolabeled Hmo1 and Rad23 proteins were combined in various combinations and subjected to co-immunoprecipitation using the 12CA5 antibody as described in Materials and Methods. The results from these experiments are shown in Figure 18. Lane A contains the protein extract from a TNT™ reaction expressing the Rad23 protein (plasmid pRK92) and shows a prominent band at approximately 70 kDa corresponding to the Rad23 protein. Lane B contains the protein extract from an HA-Hmo1p expression reaction (plasmid pRK108) and shows a prominent band at approximately 39 kDa corresponding to the HA-Hmo1 protein. Lane C contains the immunoprecipitate of the Rad23p reaction demonstrating that in the absence of the HA-tag, Rad23p is not immunoprecipitated to an appreciable level. The 70 kDa band that appears in Lane C is likely due to non-specific immunoprecipitation. Lane D contains the immunoprecipitate from the HA-Hmo1p reaction and shows that this recombinant protein is

immunoprecipitated by the 12CA5 antibody. Lane E contains the immunoprecipitate from a combined sample of radiolabeled HA-Hmo1p and Rad23p. Although the HA-Hmo1p was immunoprecipitated efficiently, the amount of Rad23p present is no more significant than seen in Lane C, suggesting that Rad23p was not co-immunoprecipitated with HA-Hmo1p. This suggests that Rad23p and Hmo1p do not interact *in vitro*. The HA-Rad23p was also efficiently immunoprecipitated by the 12CA5 antibody but could not co-immunoprecipitate the Hmo1p to any significant degree (data not shown). The predicted molecular weights of the Rad23p (42.4 kDa) and Hmo1p (27.5 kDa) differ significantly from that seen by SDS-PAGE analysis, however these bands were later shown to correspond to the proteins by use of specific antibodies (data not shown).

Figure 18 Co-Immunoprecipitation Analysis for Hmo1p and Rad23p

Radiolabelled proteins produce in the TnT™ system were separated on a 10% SDS-PAGE gel and flourographed as described in the Materials and Methods. Arrows indicate position of Rad23 and HA-tagged Hmo1 proteins. Note that both proteins migrate at a higher molecular weight than predicted from the aa sequence.

Lane A: Rad23p TnT™ reaction prior to immunoprecipitation

Lane B: HA-Hmo1p TnT™ reaction prior to immunoprecipitation

Lane C: Rad23p TnT™ reaction after immunoprecipitation with 12CA5 antibody

Lane D: HA-Hmo1p TnT™ reaction after immunoprecipitation with 12CA5 antibody

Lane E: mixed TnT™ reaction containing Rad23p and ha-Hmo1p after immunoprecipitation with 12CA5 antibody

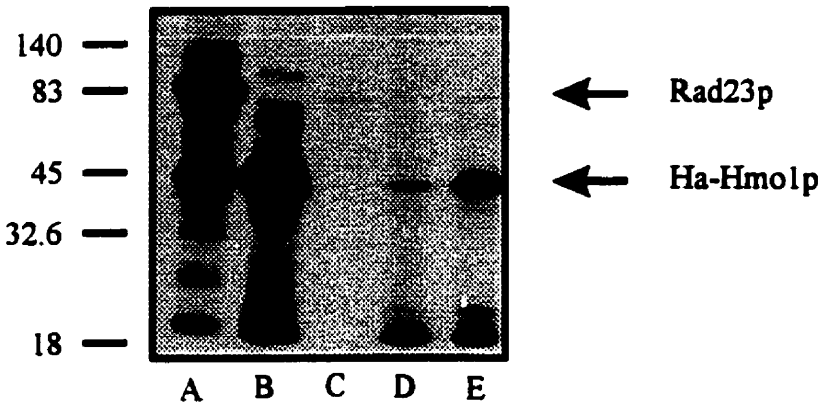
140
83
45
32.6
18
A
B
C
D
E
Rad23p
Ha-Hmo1p

4. DISCUSSION

In this study, three novel genes whose protein products were found to interact with Rad23p in the two-hybrid system were analyzed to determine the significance of these interactions. Null mutants for each gene were constructed and the resulting strains were examined for phenotypes related to DNA repair. Evidence of direct protein-protein interaction was also sought to demonstrate biological significance for the interactions seen in the two-hybrid system.

4.1 The Role of *RAD23* in DNA Repair

The true role of *RAD23* in DNA repair remains unknown. Recent biochemical analysis of NER proteins suggest that Rad23p allows the efficient assembly of the NER machinery (especially TFIIH) at sites of damage (Svejstrup *et al.*, 1995; Guzder *et al.*, 1995a; Guzder *et al.*, 1996). The demonstration that *RAD23* is involved in spindle pole body duplication suggests that *RAD23* plays a role in cell cycle control (Biggins *et al.*, 1996). It is tempting to suggest that these two pathways are connected through *RAD23* in a manner similar to a damage checkpoint (Weinert, 1992) where duplication of the genome is delayed until proper repair can take place. How the Rad23 protein divides its efforts between these two processes remains to be seen. If TFIIH is limiting, then recruitment of TFIIH into a repair role in the absence of DNA damage would adversely affect the cell (You *et al.*, 1998; Svejstrup *et al.*, 1995; Mayne and Lehmann, 1982). However, in the presence of damage, sequestering TFIIH away from a transcription role may be beneficial to delay transcription until the damage is repaired. This implies that the role of Rad23p in

assembly of the NER complex is tightly regulated by an unknown mechanism. How Rad23p is regulated during its role in cell-cycle progression is also unknown, however, Schauber *et al.* (1998) have observed a cell cycle specific degradation of Rad23p. Although Rad23p does not appear to be an essential protein in any one cellular process, it is clearly important in these two pathways.

The *RAD23* homologues in humans present a similar assessment of the function of *RAD23*. RAD23B was found to interact with XPC in a similar fashion to the Rad4p-Rad23p complex (van der Spek *et al.*, 1996). Drapkin *et al.* (1994) found an association of XPC with components of TFIIH, providing an indirect link between RAD23B and TFIIH, similar to that seen in yeast. RAD23A was found to play a role in cell cycle arrest in the presence of the HIV-1 protein Vpr (Withers-Ward *et al.*, 1997), suggesting that this homologue fulfills the role of Rad23p in the cell-cycle progression. Perhaps the dual functions of the yeast Rad23 protein are split between two proteins in higher organisms.

The fact that no human diseases have been attributed to either *RAD23* gene further complicates the assessment of the importance of *RAD23*. This may imply that the genes are so crucial that mutations cannot be tolerated, or more likely, that disease conditions do exist but remain to be identified. As van der Spek *et al.* (1996) have suggested, a *RAD23*-related disease may present an unexpected phenotype which reflects the unique role that these proteins play in the cell.

In order to understand the role of *RAD23*, it will be necessary to define how Rad23p is regulated in its many roles. It will also be very useful to identify additional cellular processes that Rad23p participates in order to understand how important this protein really is. Perhaps one of the strongest clues about Rad23p function will come from understanding the role of its tightly complexed partner, Rad4p. When an interacting protein is found, its biological function will reveal the pathways in which *RAD23*

participates, thus aiding in defining the role of *RAD23* itself. The two-hybrid system allows us to determine which proteins Rad23p interacts with.

4.2 The *RAD23* Two-Hybrid Screen

The *RAD23* two-hybrid screen identified three interacting proteins encoded by the *SAP1*, *HMO1* and *BYH1* genes. The latter two had not previously been linked to DNA repair. It is interesting that the screen did not identify proteins known to interact with Rad23p, suggesting that we identified only a fraction of all Rad23p interacting proteins. For instance, Schauber *et al.* (1998) showed that Rad23p interacts with at least four members of the 26S proteosome (Cim3p, Cim5p, Pup1p, and Pre1p). Guzder *et al.* (1995a) demonstrated interactions between Rad23p and the damage recognition protein Rad14p, as well as with two components of the transcription factor complex TFIIH (Rad25p and Tfb1p). The immunoprecipitation systems used by these authors tested interactions *in vivo* using either recombinant (Schauber *et al.*, 1998) or native (Guzder *et al.*, 1995a) Rad23p protein. Neither of these authors reported finding interactions between Rad23p and the three proteins in this study. The differences in observed interactions may be dependent on the condition used and thus explain our contrasting results.

It is not yet known what effect the fusion of the lexA protein has on the structure of the Rad23 protein, but the addition of this binding domain may conceal interacting domains at the N-terminus and interfere with interactions in this region of Rad23p. This may be especially important for proteins like Rad4p which is known to interact with the N-terminus of Rad23p (Wang *et al.*, 1997). The ubiquitin-like domain may also be inaccessible for interactions with members of the protein degradation family (Hofman and Bucher, 1996).

4.2.1 *SAP1*

The predicted protein sequence of *SAP1* places it in the 'AAA' class of proteins (see Appendix). Members of this class include such proteins as 26S subunits (see Appendix) and transcription factors. While there is no strong physical evidence to assign Sap1p to either of these classes, Liberzon *et al.* (1996) suggested that, based on the predicted isoelectric point of *SAP1*, it most likely belongs to the transcription factor group. If this is true, the interaction between Rad23p and Sap1p provides yet another link between DNA repair and transcription. If however Sap1p proves to be a member of the protein degradation machinery, then the Rad23p-Sap1p interaction may prove to be an additional physical link between DNA repair and the 26S proteosome as seen by Schauber *et al.* (1998).

Determination of the interacting domain of Sap1p with Rad23p revealed that a Sap1 protein lacking the C-terminal 724 aa interacted more strongly with Rad23p than did a Sap1 protein lacking only the C-terminal 328 aa. The removal of the additional 316 aa appears to enhance the Sap1p-Rad23p interaction, suggesting the presence of an inhibitory domain in this region. Another possibility is that the truncated fusion proteins differ in stability which affect their levels in the cell and thus affect their ability to interact with Rad23p.

The reduced ability of *sap1*Δ to utilize galactose as a carbon source could be attributed to a defect in either transcription or protein degradation. Growth of the *sap1*Δ strain on glucose media prior to transfer to galactose media appears to exacerbate the poor growth phenotype suggesting that the mutant strain is unable to efficiently switch carbon sources. The role of *SAP1* in galactose utilization requires further investigation to demonstrate whether this gene is a transcription factor or protein degradation component.

4.2.2 *HMO1*

Chromosomal DNA in the cell is associated with an abundance of histones and other non-histone proteins, including the HMG class of proteins (see Appendix). The processes by which DNA repair systems gain access to DNA in spite of this highly ordered chromatin structure is poorly understood. Paetkau *et al.* (1994) showed an interaction between the DNA repair protein Rad7p and a component of silent chromatin (Sir3p), suggesting that Rad7p may actively participate in the remodeling of chromatin structure at sites of damage. *HMO1* appears to support this general connection by its interaction with *RAD23* in the THS. The observation that Hmo1p may homodimerize in the THS suggests that this dimerization may be important for interaction with Rad23p, possibly explaining why I was unable to observe a direct interaction *in vitro*.

It is interesting to note that in determining the interacting domain of Hmo1p with Rad23p, the region thought to code for a leucine zipper pattern correlates well with the region necessary for interaction. The *HMO1* ORF of pRK48 is truncated such that the potential leucine zipper motif (aa 55-76) is juxtaposed to the resulting C-terminus and possibly causes the disruption of the motif. The deletion analysis fully supports the notion that the leucine zipper pattern of these proteins may be required, directly or indirectly, for interaction with Rad23p. Furthermore, it may be the relative position of this motif within the protein that is crucial for interaction.

How *HMO1* participates in DNA repair is unknown, but some HMG proteins have been shown to bind to damaged DNA, single stranded DNA or DNA in kinked conformation (reviewed in Grosschedl *et al.*, 1994). This may imply that HMG proteins act as specific damage sensors. Homologues of *HMO1* in higher organisms have been proposed to bind linker DNA between histones (Peters *et al.*, 1979). Lu *et al.* (1996) showed that deletion of *HMO1* resulted in DNA that was hypersensitive to DNAseI

suggesting that the chromatin structure in the *hmo1*Δ mutant has a more open conformation. In light of this, it is tempting to think of Hmo1p as an "architectural keystone" and that loss of the protein causes the dissociation of the ordered structure of chromatin. In order for DNA repair to occur in silent chromatin regions, we can hypothesize that a key protein such as this may be targeted to rapidly assemble or disassemble chromatin structure.

4.2.3 *BYH1*

The function of *BYH1* in yeast remains unknown, however the recent work by Li *et al.* (1998) may reveal an important regulatory mechanism for DNA repair. These researchers showed that the human protein BRAP2 binds to the nuclear localization signals (NLS) of the BRCA1 protein, potentially to maintain BRCA1 in the cytoplasm and effectively inactivate it. The Byh1 protein is the proposed homologue of BRAP2 based on sequence homology and similar NLS binding properties (Li *et al.* , 1998). It can be hypothesized that Byh1p may act on Rad23p to regulate the cellular localization of Rad23p. The Rad23 protein, however, may not contain nuclear localization signals (Boulikas, 1997) suggesting that Byh1p may be interacting indirectly with Rad23p through another protein. A likely candidate for this intermediate protein is the tightly complexed Rad4p, a protein with multiple nuclear localization signals (Boulikas, 1997).

The deletion of *BYH1* from yeast does not appear to have a visible affect on the cells. This could mean that the *BYH1* product is not essential or that there is functional redundancy with another protein. To emphasize the unessential nature of *BYH1*, it should be noted that every Ura+ colony examined by Southern blot during the creation of the *byh1*Δ strain was shown to have undergone allele replacement; in contrast, only 2 of 6

haploid colonies in the creation of the *sap1Δ* strain were shown to have undergone allele replacement (see Figure 13).

Deletion analysis of the interacting domain of Byh1p with Rad23p demonstrated that the region containing the putative leucine zipper motif is necessary for this interaction. The explanation for this may be that dimerization of Byh1p is necessary for it to interact with Rad23p. The putative zinc-finger domain of Byh1p implies that this protein may enter the nucleus and interact with DNA, contrary to the cytoplasmic location of its human homologue.

4.3 Conjecture

In order to claim that the interaction of these proteins with Rad23p is of biological significance, it must be established that the proteins interact physically. The problems associated with Sap1 or Hmo1 protein expression in the TNT™ kit suggest that a different approach is necessary to demonstrate interaction. Also, the *in vitro* environment may not reflect the state of the cell which may promote interactions between Rad23p and the three interacting proteins as discussed in section 4.2. It may be necessary to first look at the *in vivo* environment, distinct from the two-hybrid system. If co-immunoprecipitation of these proteins cannot be easily demonstrated in the *in vivo* environment, this may imply an additional level of complexity, such as the requirement of post-translational modification of one or more proteins.

Environmental insults such as UV are known to induce the phosphorylation of key proteins and alter their functions. For example, Stone and Pillus (1996) demonstrated that Sir3p underwent phosphorylation in response to stress, which was a result of activation of a phosphorylation cascade pathway. This phosphorylation resulted in tighter

transcriptional silencing. Based on this, it is possible that Rad23p interacts with different subsets of proteins depending on its state of phosphorylation, or the phosphorylation of its interaction partners. If the cell cycle and DNA repair activities of Rad23p are separable, it may be due to regulation by phosphorylation or other post-translational modifications. Why Rad23p interacts with Sap1p, Hmo1p and Byh1p in the two hybrid system may reflect the nature of the fusion proteins themselves. The addition of the GAL4 activating domain or the lexA protein may affect the structure of the proteins to represent an "induced" state of the protein, mimicking any affect derived from post-translation modification.

The reason for the defective galactose utilization phenotype of *sap1Δ* needs to be elucidated to properly classify this protein as either a transcription factor or as a component of the protein degradation pathway. In addition, the *sap1Δ* strain should be tested to see what effect it has on the stability of known protein degradation targets in pathways other than the N-end rule. This strain should also be examined for effects on general or specific transcription.

The observation that Hmo1p may homodimerize needs to further established. Mutant Hmo1p could be tested in the two-hybrid system to delineate the homodimerization domain and see if it maps to the leucine zipper region. Proteins containing mutant leucine zipper motifs could then be tested for physical interaction by co-immunoprecipitation.

It needs to be established whether Byh1p truly represents the yeast homologue of BRAP2. To do this, the sub-cellular localization of Byh1p must be determined. If Byh1p is found to reside in the cytoplasm and to interact physically with Rad23p or Rad4p, it may play a crucial regulatory role in the localization of Rad23p, and thereby regulate the process of nucleotide excision repair and/or cell cycle.

Mutant strains need to be constructed that are deficient for the *RAD23* product in combination with a deficiency for the product of each interacting gene. These strains could

then be tested for phenotypes such as increased/reduced UV sensitivity, growth alteration, and induced mutagenesis.

Finally, because the N-terminus of Rad23p appears to be so crucial to its function, it would be interesting to perform a two-hybrid screen using a $Gal4_{BD}$ fusion to the C-terminus of Rad23p, thus leaving the N-terminus free for interaction. The fact that S. Simon was unable to identify any of the known Rad23p interacting proteins in the two-hybrid screen suggests that the bait construct used is of limited applicability to understanding the function of *RAD23*.

4.4 Concluding Remarks

One of the most interesting aspects of DNA repair research is the many overlaps and connections with other, seemingly unrelated, cellular processes such as the connection to transcription (Mayne and Lehmann, 1982). The two-hybrid system is proving to be a valuable tool for demonstrating such connections.

I was unable to demonstrate the biological significance of the interactions detected in the two-hybrid system either by supporting the physical interactions or demonstrating genetic interactions. However, due to the failure to properly express the recombinant proteins in the TNT™ system, as well as the complexity of variables in co-immunoprecipitation studies, it would not be wise to rule out the possibility that Rad23p does truly physically interact with any of the three positives. Nor can a genetic interaction be ruled out since the tests used were aimed only at detecting gross changes in UV sensitivity.

The three Rad23p interacting genes investigated in this study require much additional research to discern their roles in the cell and whether or not these roles are

associated with DNA repair. Preliminary results indicate that several genes of the *RAD* group and the *SIR* group interact genetically to influence the rate of induced mutation (Sharon Simon, personal communication) and may be worth investigating further with the three *RAD23* interacting genes.

5. APPENDIX

5.1 HMG Proteins

The HMG proteins comprise a superfamily of related proteins whose cellular functions are poorly understood. In general, the proteins are small (<30 kDa), are capable of binding DNA and influence DNA metabolism (reviewed in Bustin *et al.*, 1990). Three classes of proteins have been identified within the HMG superfamily based on size, amino acid composition and DNA binding characteristics. Members of the HMG-1/2 class, defined by the human HMG1 and HMG2 proteins, contain two copies of a conserved DNA binding domain termed the "HMG box" (Landsman and Bustin, 1993). They also contain a charged C-terminal region of adjacent basic and acidic portions thought to participate in the binding of DNA and histones, respectively. *HMO1* is considered to be a homologue of HMG1 with slight variation in the charged C-terminal region (Lu *et al.*, 1996). The HMG-1/2 class of proteins does not appear to have sequence specificity but rather binds altered forms of DNA including single stranded regions (reviewed in Landsman and Bustin, 1993). HMG-1/2 proteins have been hypothesized to play roles in transcription, replication and DNA repair but to date remain poorly understood.

5.2 The 26S Protease

The 26S protease is a multi-protein complex involved in the regulated degradation of cellular proteins, usually mediated by ubiquitination of targeted proteins (reviewed in Hilt and Wolf, 1996). This complex consists of two distinct multi-protein components

referred to as the 20S 'core' or proteosome and the 19S 'regulatory cap'. The 20S core is composed of multiple subunits arranged in a cylindrical manner and contains at least five different proteolytic activities (reviewed in Hilt and Wolf, 1996). The 19S regulatory cap constituents comprise a highly conserved class of proteins that function to control the entry of proteins into the proteosome. These proteins bestow both recognition and energy-dependence to the 20S core, thus limiting the susbstrates for degradation (reviewed in Dubiel *et al.*, 1995).

5.3 Protein Motifs

5.3.1 Leucine Zipper Patterns

The leucine zipper pattern (Prosite entry # PDOC00029) is identified by the arrangement of leucine residues every 7 amino acids for the length of ~8 helical turns, folded into an alpha-helix (consensus pattern L-x(6)-L-x(6)-L-x(6)-L) (Landschulz *et al.*, 1988). The leucine side chains protrude outwards from one face of the alpha-helix to interact with a similar domain of another protein, thus mediating the interaction between two protein molecules. The interaction between two such zipper motifs forms a coiled coil. These domains are known to be crucial for interactions among many proteins including the proto-oncogenes Jun and Fos (Gentz *et al.*, 1989).

5.3.2 ATP/GTP Binding Site Motif A

The ATP/GTP binding site motif (Prosite entry # PDOC00017), also referred to as a P-loop, is a glycine rich stretch of amino acids that typically adopts a loop structure that

interacts with a phosphate group of the nucleotide (Saraste *et al.*, 1990). The consensus sequence for this motif is [AG]-x(4)-G-K-[ST].

5.3.3 'AAA' Protein Family Signature

The AAA protein family signature (Prosite entry # PDOC00572) is a large conserved domain (~220 aa) that contains an ATP binding site but has no other known function (Confalonieri and Dugeut, 1995). The acronym 'AAA' stands for 'ATPases associated with diverse cellular activities' to emphasize the ubiquitous nature of this domain. In yeast there may be as many as 17 different classes of AAA proteins (Confalonieri and Dugeut, 1995). The ATPase activity of these proteins is quite distinct from other ATPase proteins in that the rate of ATP hydrolysis is low (Confalonieri and Dugeut, 1995).

5.3.4 C2H2 Zinc Finger Domain

The zinc finger domain (Prosite entry # PDOC00028) is composed of 25-30 amino acid residues which fold into a secondary structure that is coordinated by the binding of a zinc atom (reviewed in Klug and Rhodes, 1987). The amino acids that bind to the zinc atom give the structure its classification. A C2H2 zinc finger utilizes two cysteine and two histidine residues to bind the zinc atom. These structures are capable of binding nucleic acid and are commonly found in transcription factors.

5.3.5 UBA Domain

The ubiquitin associated domain (UBA) is roughly 55 aa in length and is thought to code for a protein-protein interaction domain (Hofman and Bucher, 1996). It is proposed that the specificity of the UBA domain is for interactions with other proteins involved in ubiquitin pathway and acts to regulate this process (Hofman and Bucher, 1996).

6. REFERENCES

Aboussekhra, A., M. Biggerstaff, M.K.K. Shivji, J.A. Vilpo, V. Moncollin, V.N. Podust, M. Protic, U. Hübscher, J.-M. Egly, and R.D. Wood. 1995. Mammalian DNA nucleotide excision repair reconstituted with purified protein components. *Cell.* **80**: 859-868.

Agatep, R., R.D. Kirkpatrick, D.L. Parchaliuk, R.A. Woods and R.D. Gietz. 1998. Transformation of *Saccharomyces cerevisiae* by the lithium acetate/single-stranded carrier DNA/polyethylene glycol protocol. *Technical Tips Online.* (http://tto.trends.com).

Altschul, S.F., W. Gish, W. Miller, E.W. Myers, and D.J. Lipman. 1990. Basic local alignment search tool. *J. Mol. Biol.* **215**: 403-410.

Bachmair, A., D. Finley, and A. Varshavsky. 1986. In vivo half-life of a protein is a function of its amino-terminal residue. *Science.* **234**: 179-186.

Bartel, P., C. Chien, R. Sternglanz, and S. Fields. 1993. Using the two-hybrid system to detect protein-protein interactions. In Hartley D.A. (ed): *Cellular Interactions in Development, A Practical Approach.* Oxford: IRL Press. pp. 153-179.

Biggins, S. I., Ivanovska, and M.D. Rose. 1996. Yeast ubiquitin-like genes are involved in duplication of the microtubule organizing center. *J. Cell Bio.* **133**: 1331-1346.

Birnboim, H.C. and J. Doly. 1979. A rapid alkaline extraction procedure for screening recombinant plasmid DNA. *Nucl. Acids Res.* **7**: 1513-1517.

Breeden, L., and K. Nasmyth. 1985. Regulation of the yeast HO gene. *Cold Spring Harb. Symp. Quant. Biol.* **50**: 643-650.

Bohr, V.A. 1991. Gene specific DNA repair. *Carcinogenesis.* **12**: 1983-1992.

Botstein, D., S.A. Chervitz, and J.M. Cherry. Yeast as a model organism. *Science.* **277**: 1259-1260.

Boulikas, T. 1997. Nuclear import of DNA repair proteins. *Anticancer Res.* **17**: 843-864.

Bregman, D.B., R. Halaban, A.J. van Gool, K.A. Henning, E.C. Friedberg, and S.L. Warren. 1996. UV-induced ubiquitination of RNA polymerase II: a novel modification deficient in Cockayne syndrome cells. *Proc. Natl. Acad. Sci. USA.* **93**: 11586-11590.

Burns, J.L., S.N. Guzder, P. Sung, S. Prakash, and L. Prakash. 1996. An affinity of human pelication protein A for ultraviolet-damaged DNA. Implications for damage recognition in nucleotide excision repair. *J. Biol. Chem.* **271**: 11607-11610.

Bustin, M., D.A. Lehn, and D. Landsman. 1990. Structural features of the HMG chromosomal proteins and their genes. *Biochim. Biophys. Acta.* **1049**: 231-243.

Chamberlain, J.P. 1979. Flourographic detection of radioactivity in polyacrylamide gels with the water-soluble flour, sodium salicylate. *Anal. Biochem.* **98**: 132-135.

Chu, G., and L. Mayne. 1996. Xeroderma pigmentosum, Cockayne syndrome and trichothiodystrophy: do the genes explain the diseases? *Trends Genet.* **12**: 187-192.

Cleaver, J.E. 1968. Defective repair replication in Xeroderma Pigmentosum. *Nature.* **218**: 652-656.

Cleaver, J.E. 1994. It was a very good year for DNA repair. *Cell.* **76**: 1-4.

Cleaver, J.E., and C. States. 1997. The DNA damage-recognition problem in human and other eukaryotic cells: the XPA damage binding protein. *Biochem. J.* **328**: 1-12.

Confalonieri, F., and M. Duguet. 1995. A 200-amino acid ATPase module in search of a basic function. *BioEssays.* **17**: 639-650.

De Laat, W.L., E. Appledoorn, K. Sugasawa, E. Weterings, N.G.J. Jaspers, and J.H.J. Hoeijmakers. 1998. DNA-binding polarity of human replication protein A positions nucleases in nucleotide excision repair. *Genes & Dev.* **12**: 2598-2609.

Dower, W.J., J.F. Miller, and C.W. Ragsdale. 1988. High efficiency transformation of *E. coli* by high voltage electroporation. *Nucl. Acids Res.* **16**: 6127-6144.

Drapkin, R., A. Sancar, and D. Reinberg. 1994. Where transcription meets repair. *Cell.* **77**: 9-12.

Dubiel, W., K. Ferrel, and M. Rechsteiner. 1995. Subunits of the regulatory complex of the 26S protease. *Mol. Bio. Reports.* **21**: 27-34.

Evans, E., J.G. Moggs, J.R. Hwang, J.-M. Egly, and R.D. Wood. 1997. Mechanism of open complex and dual incision formation by human nucleotide excision repair factors. *EMBO J.* **16**: 6559-6573.

Feaver, W.J., N.L. Henry, Z. Wang, X. Wu, J.Q. Svejstrup, D.A. Bushnell, E.C. Friedberg, and R.D. Kornberg. 1997. Genes for Tfb2, Tfb3, and Tfb4 subunits of yeast transcription/repair factor IIH. *J. Biol. Chem.* **272**: 19319-19327.

Feinberg, A.P., and B. Vogelstein. 1984. "A technique for radiolabeling DNA restriction endonuclease fragments to high specific activity". Addendum. *Anal. Biochem.* **137**: 266-267.

Fields, S., and O. Song. 1989. A novel system to detect protein-protein interactions. *Nature.* **340**: 245-246.

Friedberg, E.C. 1985. *DNA Repair.* W.H. Freeman, New York.

Gentz, R., F.J. Rauscher III, C. Abate, and T. Curran. 1989. Parallel association of Fos and Jun leucine zippers juxtaposes DNA binding domains. *Science.* **243**: 1695-1699.

Gietz, R.D., and A. Sugino. 1988. New yeast-*Escherichia coli* shuttle vectors constructed with *in vitro* mutagenized yeast genes lacking six-base pair restriction sites. *Gene* **74**: 527-534.

Gietz, R.D., B. Triggs-Raine, A. Robbins, K.C. Graham, and R.A. Woods. 1997. Identification of proteins that interact with a protein of interest: Applications of the yeast two-hybrid system. *Mol. Cell Biochem.* **172**: 67-79.

Girvitz, S.C., S. Bacchetti, A.J. Rainbow, and F.L. Graham. 1980. A rapid and efficient procedure for the purification of DNA from agarose gels. *Anal. Biochem.* **106**: 492-496.

Grosschedl, R., K. Giese, and J. Pagel. 1994. HMG domain protein: architectural elements in the assembly of nucleoprotein structures. *TIGS.* **10**: 94-100.

Gunz, D., M.T. Hess, and H. Naegeli. 1996. Recognition of DNA adducts by human nucleotide excision repair. Evidence for a thermodynamic probing mechanism. *J. Biol. Chem.* **271**: 25089-25098.

Guzder, S.N., V. Bailly, P. Sung, L. Prakash, and S. Prakash. 1995a. Yeast DNA repair protein *RAD23* promotes complex formation between transcription factor TFIIH and DNA damage recognition factor *RAD14*. *J. Biol. Chem.* **270**: 8385-8388.

Guzder, S.N., Y. Habraken, P. Sung, L. Prakash, and S. Prakash. 1995b. Reconstitution of yeast nucleotide excision repair with purified Rad proteins, replication protein A, and transcription factor TFIIH. *J. Biol. Chem.* **270**: 12973-12976.

Guzder, S.N., P. Sung, L. Prakash, and S. Prakash. 1993. Yeast DNA-repair gene *RAD14* encodes a zinc metalloprotein with affinity for ultraviolet-damaged DNA. *Proc. Natl. Acad. Sci. USA.* **90**: 5433-5437.

Guzder, S.N., P. Sung, L. Prakash, and S. Prakash. 1996. Nucleotide excision repair in yeast is mediated by the sequential assembly of repair factors and not by a pre-assembled repairosome. *J. Biol. Chem.* **271**: 8903-8910.

Guzder, S.N., P. Sung, L. Prakash, and S. Prakash. 1998. DNA-dependent ATPase activity of yeast nucleotide excision repair factor 4 and its role in DNA damage recognition. *J. Biol. Chem.* **273**: 6292-6296.

Habraken, Y., P. Sung, S. Prakash, and L. Prakash. 1996. Transcription factor TFIIH and DNA endonuclease Rad2 constitute yeast nucleotide excision repair factor 3: implications for nucleotide excision repair and Cockayne syndrome. *Proc. Natl. Acad. Sci. USA.* **93**: 10718-10722.

He, Z., L.A. Henricksen, M.S. Wold, and C.J. Ingles. 1995. RPA involvement in the damage-recognition and incision steps of nucleotide excision repair. *Nature.* **374**: 566-569.

He, Z., J.M.S. Wong, H.S. Maniar, S.J. Brill, and C.J. Ingles. 1996. Assessing the requirements for nucleotide excision repair proteins of *Saccharomyces cerevisiae* in an *in vitro* system. *J. Biol. Chem.* **271**: 28243-28249.

Henning, K.A., L. Li, N. Iyer, L.D. McDaniel, M.S. Reagan, R. Legerski, R.A. Schultz, M. Stefanini, A.R. Lehmann, L.V. Mayne, and E.C. Friedberg. 1995. The Cockayne syndrome group A gene encodes a WD repeat protein that interacts with CSB protein and a subunit of RNA polymerase II TFIIH. *Cell.* **82**:555-564.

Hill, R.F. 1958. A radiation-sensitive mutant of Escherichia coli. *Biochim. Biophys. Acta.* **30**: 636-637.

Hilt, W., and D.H. Wolf. 1996. Proteosomes: destruction as a program. *TIBS* **21**: 96-102.

Hoffman, C.S., and F. Winston. 1987. A ten-minute preparation from yeast efficiently releases autonomous plasmids for transformation of *Escherichia coli*. *Gene.* **57**: 267-272.

Hofman, K., and P. Bucher. 1996. The UBA domain: a sequence motif present in multiple enzyme classes of the ubiquitination pathway. *TIBS* :172-173.

Huang, J.-C., D.S. Hsu, A. Kazantsev, and A. Sancar. 1994. Substrate spectrum of human excinuclease: repair of abasic sites, methylated bases, mismatches, and bulky adducts. *Proc. Natl. Acad. Sci. USA.* **91**: 12213-12217.

James, P., J. Halladay, and E.A. Craig. 1996. Genomic libraries and a host designed for highly efficient two-hybrid selection in yeast. *Genetics.* **144**: 1425-1436.

Jansen, L.E.T., R.A. Verhage, and J. Brouwer. 1998. Preferential binding of yeast Rad4•Rad23 complex to damaged DNA. *J. Biol. Chem.* **273**: 33111-33114.

Jones, C.J., and R.D. Wood. 1993. Preferential binding of the xeroderma pigmentosum group A complementing protein to damaged DNA. *Biochemistry.* **32**: 12096-12104.

Kim, C., R.O. Snyder, and M.S. Wold. 1992. Binding properties of replication protein A from human and yeast cells. *Mol. Cell Biol.* **12**: 3050-3059.

Klug, A., and D. Rhodes. 1987. 'Zinc fingers': a novel protein motif for nucleic acid recognition. *TIBS.* **12**: 464-469.

Kolodner, R.D. 1995. Mismatch repair: mechanisms and relationship to cancer susceptibility. *TIBS.* **20**: 397-401.

Kozak, M. 1986. Point mutations define a sequence flanking the AUG initiator codon that modulates translation by eukaryotic ribosomes. *Cell.* **44**: 283-292.

Kozak, M. 1990. Evaluation of the fidelityof initiation of translation in reticulocyte lysates from commercial sources. *Nucl. Acids Res.* **18**: 2828.

Landschulz, W.H., P.F. Johnson, and S.L. McKnight. 1988. The leucine zipper: a hypothetical structure common to a new class of DNA binding proteins. *Science.* **240**: 1759-1763.

Landsman, D., and M. Bustin. 1993. A signature for the HMG-1 box DNA-binding proteins. *BioEssays.* **15**: 539-546.

Li, S., C.-Y. Ku, A.A. Farmer, Y.-S. Cong, C.-F. Chen, and W.-H. Lee. 1998. Identification of a novel cytoplasmic protein that specifically binds to nuclear localization signal motifs. *J. Biol. Chem.* **273**: 6183-6189.

Liberzon, A., S. Shpungin, H. Bangio, E. Yona, and D.J. Katcoff. 1996. Association of yeast *SAP1*, a novel member of the 'AAA' ATPase family of proteins, with the chromatin protein *SIN1*. *FEBS Letts.* **388**: 5-10.

Lindahl, T., P. Karran, and R.D. Wood. 1997. DNA excision repair pathways. *Curr. Opin. Genet. Dev.* **7**: 158-169.

Lu, J., R. Kobayashi and S.J. Brill. 1996. Characterization of a high mobility group 1/2 homolog in yeast. *J. Biol. Chem.* **271**: 33678-33685.

Masutani, C., K. Sugasawa, J. Yanagisawa, T. Sonoyama, M. Ui, T. Enomoto, K. Takio, K. Tanaka, P.J. van der Spek, D. Bootsma, J.H.J. Hoeijmakers, and F. Hanaoka. 1994. Purification and cloning of a nucleotide excision repair complex involving the xeroderma pigmentosum group C protein and a human homologue of yeast RAD23. *EMBO J.* **13**: 1831-1843.

Matsunaga, T., C.-H. Park, T. Bessho, D. Mu, and A. Sancar. 1996. Replication protein A confers structure-specific endonuclease activities to the XPF-ERCC1 and XPG subunits of human DNA repair excision nuclease. *J. Biol. Chem.* **271**: 11047-11050.

Mayne, L.V., and A.R. Lehmann. 1982. Failure of RNA synthesis to recover after UV irradiation: an early defect in cells from individuals with Cockayne's syndrome and xeroderma pigmentosum. *Cancer Res.* **42**: 1473-1478.

McKnight, G.L., T.S. Cardillo, and F. Sherman. 1981. An extensive deletion causing overproduction of yeast iso-2-cytochrome c. *Cell.* **25**: 409-419.

Melnick, L., and F. Sherman. 1993. The gene clusters ARC and COR on chromosomes 5 and 10, respectively, of *Saccharomyces cerevisiae* share a common ancestry. *J. Mol. Bio.* **233**: 372-388.

Miller, R.D., L. Prakash, and S. Prakash. 1982. Defective excision of pyrimidine dimers and interstrand DNA crosslinks in *rad7* and *rad23* mutants of *Saccharomyces cerevisiae*. *Mol. Gen. Genet.* **188**: 235-239.

Mitra, S., and B. Kaina. 1993. Regulation of repair of alkylation damage in mammalian genomes. *Prog. Nucleic Acid Res. Mol. Biol.* **44**: 109-142.

Modrich, P., and R. Lahue. 1996. Mismatch repair in replication fidelity, genetic recombination, and cancer biology. *Annu. Rev. Biochem.* **65**: 101-133.

Mu, D., and A. Sancar. 1997. Model for XPC-independent transcription-coupled repair of pyrimidine dimers in humans. *J. Biol. Chem.* **272**: 7570-7573.

Mu, D., D.S. Hsu, and A. Sancar. 1996. Reaction mechanism of human DNA repair excision nuclease. *J. Biol. Chem.* **271**: 8285-8294.

Mueller, J.P., and M.J. Smerdon. 1996. Rad23 is required for transcription-coupled repair and efficient overall repair in *Saccharomyces cerevisiae*. *Mol. Cell. Bio.***16**: 2361-2368.

Nakai, S., and S. Matsumoto. 1967. Two types of radiation-sensitive mutant in yeast. *Mutat. Res.* **4**: 129-136.

Norrander, J., T. Kempe, and J. Messing. 1983. Construction of improved M13 vectors using oligodeoxynucleotide-directed mutagenesis. *Gene.* **26**: 101-106.

Paetkau, D.W., J.A. Riese, W.S. MacMorran, R.A. Woods, and R.D. Gietz. 1994. Interaction of the yeast *RAD7* and *SIR3* proteins: implications for DNA repair and chromatin structure. *Genes & Dev.* **8**: 2035-2045.

Park, C.-H., and A. Sancar. 1994. Formation of a ternary complex by human XPA, ERCC1 and ERCC4 (XPF) excision repair proteins. *Proc. Natl. Acad. Sci. USA.* **91**: 5017-5021.

Peters, E.H., B. Levy-Wilson, and G.H. Dixon. 1979. Evidence for the location of high mobility group protein T in the internucleosomal linker regions of trout testis chromatin. *J. Biol. Chem.* **254**: 3358-3361.

Pierce, M.K., C.N. Giroux and B.A. Kunz. 1987. Development of a yeast system to assay mutational specificity. *Mutat. Res.* **182**: 65-74.

Reed, K.C., and D.A. Mann. 1985. Rapid transfer of DNA from agarose gels to nylon membranes. *Nucl. Acids Res.* **13**: 7207-7221.

Rothstein, R.J. 1983. One-step gene disruption in yeast. *Meth. Enzymology.* **101**:202-211.

Sambrook, J., E.F. Fritsch, and T. Maniatis. 1989. *Molecular Cloning: A Labroratory Manual.* 2nd Edition. Cold Spring Harbor Press, Cold Spring Harbor, N.Y.

Sancar, A. 1996a. DNA excision repair. *Annu. Rev. Biochem.* **65**: 43-81.

Sancar, A. 1996b. No "end of history" for photolyases. *Science.* **272**: 48-49.

Sanger, F., S. Nicklen, and A.R. Coulson. 1977. DNA sequencing with chain-terminating inhibitors. *Proc. Natl. Acad. Sci. USA.* **74**: 5463-5467.

Saraste, M., P.R. Sibbald, and A. Wittinghofer. 1990. The P-loop - a common motif in ATP- and GTP-binding proteins. *TIBS*. **15**: 430-434.

Schauber, C., L. Chen, P. Tongaonker, I. Vega, D. Lamberston, W. Potts, and K. Madura. 1998. Rad23 links DNA repair to the ubiquitin/proteosome pathway. *Nature*. **391**: 715-718.

Schultz, T.F., and R.S. Quatrano. 1997. Characterization and expression of a rice RAD23 gene. *Plant Mol. Biol.* **34**: 557-562.

Selby, C.P., and A. Sancar. 1990. Transcription preferentially inhibits nucleotide excision repair of the template strand *in vitro*. *J. Biol. Chem.* **265**: 21330-21336.

Selby, C.P., and A. Sancar. 1993. Molecular mechanism of transcription-repair coupling. *Science*. **260**: 53-57.

Selby, C.P., and A. Sancar. 1994. Mechanisms of transcription-repair coupling and mutation frequency decline. *Microbiol. Rev.* **58**: 317-329.

Shinohara, A., and T. Ogawa. 1995. Homologous recombination and the roles of double-strand breaks. *TIBS*. **20**: 387-391.

Stone, E.M., and L. Pillus. 1996. Activation of an MAP kinase cascade leads to Sir3p hyperphosphorylation and strengthens transcriptional silencing. *J. Cell Biol.* **135**: 571-583.

Sturm, A., and S. Lienhard. 1998. Two isoforms of plant RAD23 complement a UV-sensitive rad23 mutant in yeast. *Plant J.* **13**: 815-821.

Sugasawa, K., C. Masutani, A. Uchida, T. Maekawa, P.J. van der Spek, D. Bootsma, J.H.J. Hoeijmakers, and F. Hanaoka. 1996. HHR23B, a human Rad23 homolog, stimulates XPC protein in nucleotide excision repair *in Vitro*. *Mol. Cell. Bio.* **16**: 4852-4861.

Svejstrup, J.Q., Z. Wang, W.J. Feaver, X. Wu, D.A. Bushnell, T.F. Donahue, E.C. Friedberg, and R.D. Kornberg. 1995. Different forms of TFIIH for transcription and DNA repair: holo-TFIIH and a nucleotide excision repairosome. *Cell*. **80**: 21-28.

Svoboda, D.L., J.-S. Taylor, J.E. Hearst, and A. Sancar. 1993. DNA repair by eukaryotic excision nuclease. Removal of thymine dimer and psoralen monoadduct by HeLa cell-free extract and of thymine dimer by *Xenopus laevis* oocytes. *J. Biol. Chem.* **268**: 1931-1936.

Tijsterman, M., R.A. Verhage, P. van de Putte, J.G. Tasseron-de Jong, and J. Brouwer. 1997. Transitions in the coupling of transcription and nucleotide excision repair within RNA polymerase II-transcribed genes of *Saccharomyces cerevisiae*. *Proc. Natl. Acad. Sci. USA*. **94**: 8027-8032.

Van der Spek, P.J., C.E. Visser, F. Hanaoka, B. Smit, A. Hagemeijer, D. Bootsma, and J.H.J. Hoeijmakers. 1996. Cloning, comparative mapping, and RNA expression of the

mouse homologues of the *Saccharomyces cerevisiae* nucleotide excision repair gene *RAD23*. *Genomics*. **31**: 20-27.

Van Gool, A.J., R. Verhage, S.M.A. Swagemakers, P. van de Putte, J. Brouwer, C. Troelstra, D. Bootsma, and J.H.J. Hoeijmakers. 1994. RAD26, the functional *S. cerevisiae* homolog of the Cockayne syndrome B gene *ERCC6*. *EMBO J.* **13**: 5361-5369.

Van Gool, A.J., E. Citterio, S. Rademakers, R. van Os, W. Vermeulen, A. Constantinou, J.-M. Egly, D. Bootsma, and J.H.J. Hoeijmakers. 1997. The Cockayne syndrome B protein, involved in transcription-coupled DNA repair, resides in an RNA polymerase II-containing complex. *EMBO J.* **19**: 5955-5965.

Verhage, R., A.-M. Zeeman, N. de Groot, F. Gleig, D.D. Bang, P. van de Putte, and J. Brouwer. 1994. The *RAD7* and *RAD16* genes, which are essential for pyrimidine dimer removal from the silent mating type loci, are also required for repair of the nontranscribed strand of an active gene in *Saccharomyces cerevisiae*. *Mol. Cell. Biol.* **14**: 6135-6142.

Walker, G.C. 1995. SOS-regulated proteins in translesion DNA synthesis and mutagenesis. *TIBS*. **20**: 416-420.

Wang, Z., S. Wei, S.H. Reed, X. Wu, J.Q. Svejstrup, W.J. Feaver, R.D. Kornberg, and E.C. Friedberg. 1997. The *RAD7*, *RAD16*, and *RAD23* genes of *Saccharomyces cerevisiae*: requirement for transcription-independant nucleotide excision repair *in Vitro* and interactions between the gene products. *Mol. Cell. Bio.* **17**: 635-643.

Watkins, J.F., P. Sung, L. Prakash, and S. Prakash. 1993. The *Saccharomyces cerevisiae* DNA repair gene *RAD23* encodes a nuclear protein containing a ubiquitin-like domain required for biological function. *Mol. Cell. Bio.* **13**: 7757-7765.

Weinert, T. 1992. Dual cell cycle checkpoints sensitive to chromosome replication and DNA damage in the budding yeast *Saccharomyces cerevisiae*: *Radiat. Res.* **132**: 141-143.

Westneat, D.F., W.A. Noon, H.K. Reeve, and C.F. Aquadro. 1988. Improved hybridization conditions for DNA 'fingerprints' probed with M13. *Nucl. Acids Res.* **16**: 4161.

Withers-Ward, E.S., J.B.M. Jowett, S.A. Stewart, Y.-M. Xie, A. Garfinkel, Y. Shibagaki, S.A. Chow, N. Shah, F. Hanaoka, D.G. Sawitz, R.W. Armstrong, L.M. Souza, and I.S.Y. Chen. 1997. Human immunodeficiency virus type 1 Vpr interacts with HHR23A, a cellular protein implicated in nucleotide excision DNA repair. *J. Virol.* **71**: 9732-9742.

Yanisch-Perron, C., J. Vieira, and J. Messing. 1985. Improved M13 phage cloning vectors and host strains: nucleotide sequences of the M13mp18 and pUC19 vectors. *Gene*. **33**: 103-119.

You, Z., W.J. Feaver, and E.C. Friedberg. 1998. Yeast RNA polymerase II transcription in vitro is inhibited in the presence of nucleotide excision repair: complementation of inhibition by holo-TFIIH and requirement for *RAD26*. *Mol. Cell Bio.* **18**: 2668-2676.

7. SOLUTIONS

TE (1x)

10 mM Tris-HCl
1 mM EDTA
pH 8.0

Resuspension Buffer

50 mM glucose
25 mM Tris-HCl (pH 8.0)
10 mM EDTA (pH 8.0)

Potassium Acetate Solution

5 M potassium acetate	60.0 ml
glacial acetic acid	11.5 ml
ddH_2O	to 100.0 ml

This solution is 3 M with respect to the potassium and 5 M with respect to the acetate

Band elution buffer (BEB)

50 mM Tris-HCl (pH7.5)
200 mM NaCl
0.1% SDS
1 mM EDTA

SM Media

100 mM NaCl
80 mM $MgSO_4 \cdot 7H_2O$
50 mM Tris-HCl (pH 7.5)
0.01 % Gelatin

Lysis Solution

0.2 N NaOH
1% SDS

TAE (1x)

40 mM Tris-acetate
1 mM EDTA

Loading dye
50% glycerol
1 mg/ml xylene cyanol FF
1 mg/ml bromophenol blue

Dephosphorylation buffer (10 x)

500 mM Tris-HCl
1 mM EDTA pH (8.5)

Bacteriophage T4 DNA ligase buffer (10x)

500 mM Tris-HCl (pH 7.8)
100 mM $MgCl_2$
100 mM DTT
10 mM ATP
250 μg/ml BSA

Blunt-end ligation buffer (10x)

500 mM Tris-HCl (pH 7.2)
100 mM $MgCl_2$
10 mM DTT
500 μg/ml BSA

dNTP solution (pH 7.0)

2 mM dATP
2 mM dCTP
2 mM dGTP
2 mM dTTP

Yeast lysis buffer

2% Triton X-100
1% SDS
100 mM NaCl
20 mM Tris-HCl (pH 8.0)
10 mM EDTA

TBE buffer (1x)

90 mM Tris-borate
1 mM EDTA

Developer solution

21.8% Kodak GBX developer and replenisher

Stop solution

2% acetic acid

Fix solution

24.9% Kodak rapid fixer solution A
2.7% Kodak rapid fixer solution B

Z Buffer

60 mM $Na_2HPO_4 \cdot 7H_2O$
40 mM $NaH_2PO_4 \cdot H_2O$
10 mM KCl
1 mM $MgSO_4 \cdot 7H_2O$

ONPG Solution

4 mg/ml in Z buffer

SSC (2x)

300 mM NaCl
30 mM Na_3Citrate

dNTP mix (2 mM)

Diluted in ddH_2O from 100 mM stocks in 3 mM Tris-HCl (pH 7), 0.2 mM EDTA (Feinberg and Vogelstein, 1984)

Klenow Buffer (10x)

500 mM Tris-HCl (pH 7.6)
100 mM $MgCl_2$

Westneat Hybridization Buffer (Westneat *et al.*, 1988)

7% SDS
1mM EDTA (pH 8.0)
263 mM Na_2HPO_4 (pH 7.2)
1% BSA

Buffer B

20 mM HEPES (pH 7.2)
75 mM KCl
4 mM $MgCl_2$
5 mM sodium bisulfite
0.5 mM EDTA
0.5 mM DTT
0.1% Tween20
12.5% glycerol
0.5 μg/ml leupeptin
0.7 μg/ml pepstatinA
0.1 mM PMSF

Stacking gel buffer (4x)

500 mM Tris-HCl
0.1% SDS
pH 6.8

SDS running buffer (1x)

25 mM Tris-HCl
192 mM glycine
0.1% SDS

SDS sample buffer

20% glycerol
2.4% SDS
25 μg/ml bromophenol blue
720 mM β-ME
37.5 mM Tris-HCl

Phosphate Buffered Saline (PBS)

137 mM NaCl
2.7 mM KCl
10.4 mM Na_2HPO_4
1.8 mM KH_2PO_4
pH 7.4

Separating gel buffer (4x)

1.5 M Tris-HCl
0.1% SDS
pH 8.8